Magnetoresistive (MR) And Giant-Magnetoresistive (GMR) Head Technology

By

Dr. Nader Mahvan
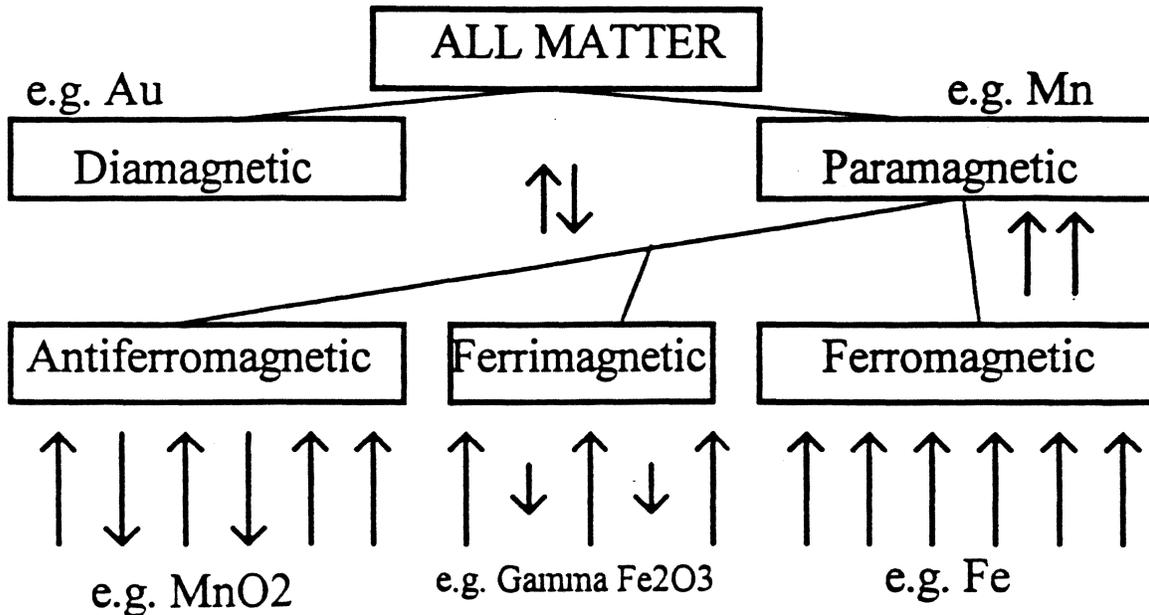
Professional Development Course

MR and GMR Head Technology

MR Head Introduction
Comparison between MR and Inductive Heads
Magnetic Phenomenon as Related to MR Heads
Giant Magnetoresistive Heads (GMR) and Spin-Valve Technology
MR Head Construction
MR Biasing Schemes
MR Signal Output
MR Heads Design and Performance Considerations
Thermal Asperity Problems and Solutions
Mechanical Issues in MR Heads
MR Head manufacturing Concerns
Media for MR heads
AMR Head and GMR Head Similarities and Differences
PRML and MR Heads
Collossal MR Heads

Sponsored by:
The Institute for Information Storage Technology

Magnetism

Intrinsic Magnetization

```
                        ┌─────────────────┐
                        │   ALL MATTER    │
                        └─────────────────┘
e.g. Au                                            e.g. Mn
┌─────────────────┐                        ┌─────────────────┐
│   Diamagnetic   │          ↑↓            │   Paramagnetic  │
└─────────────────┘                        └─────────────────┘
                                                        ↑↑
┌─────────────────┐  ┌───────────────┐  ┌─────────────────┐
│ Antiferromagnetic│ │ Ferrimagnetic │  │  Ferromagnetic  │
└─────────────────┘  └───────────────┘  └─────────────────┘

  ↑↓↑↓↑↑              ↑↓↑↓↑              ↑↑↑↑↑↑

   e.g. MnO2         e.g. Gamma Fe2O3      e.g. Fe
```

I) In empty space, $\chi = 0$ since there is no matter present, and $\mu = 1$.

II) In diamagnetic materials χ is small and negative, $\mu <_{slightly} 1$.

III) In para- and antiferromagnetic materials, χ is small and positive, $\mu >_{slightly} 1$.

IV) In ferro- and ferrimagnetic materials, χ, and, μ are large and positive.

There are two kinds of magnetic moment μ for electrons)
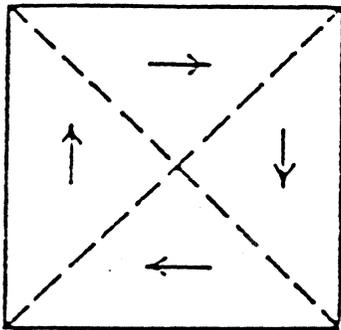
$$I) Orbital \Rightarrow \mu_{orb} = \frac{eh}{4\pi mc}$$

and

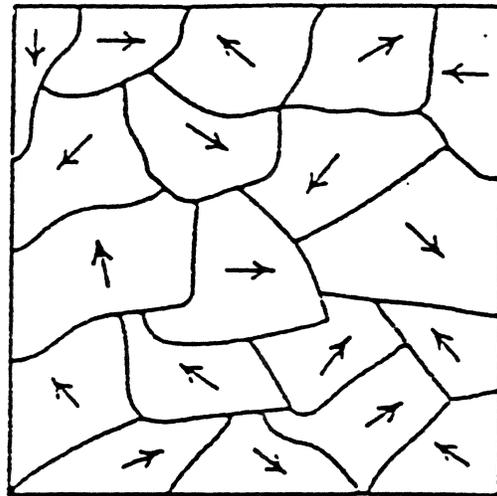$$II) Spin \Rightarrow \mu_{spin} \frac{eh}{4\pi mc}$$

1

Domains

There is $\therefore$ a large internal field $(\approx 10^7 \, Oe)$. Then **why is a piece of iron not necessarily a strong magnet?**
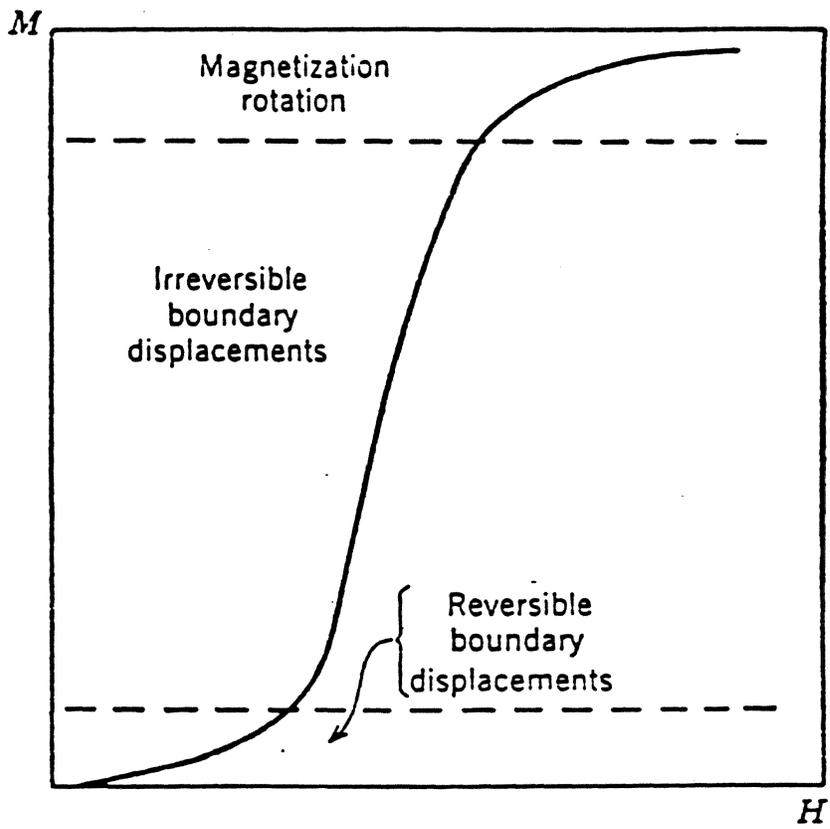
Weiss => " A ferromagnet in demagnetized state is devided into *"domains"*. When one magnetizes a piece of iron we covert it from <u>multi-domain to single-domain</u>."
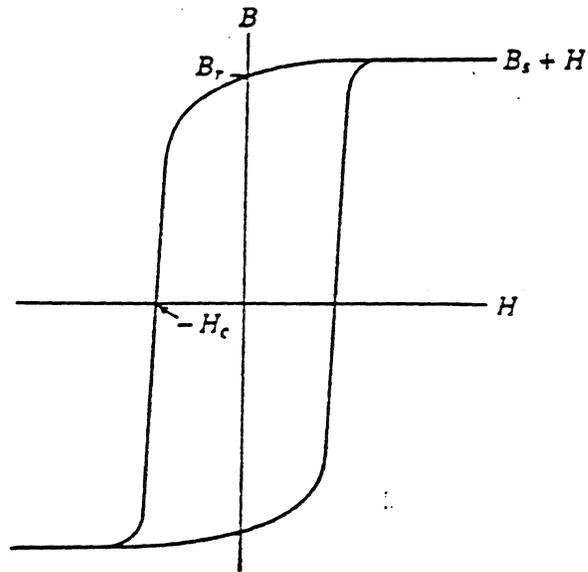

(a) Single crystal   (b) Polycrystal

The magnetization process.

The domain structure of a ferromagnetic material closely affects the major properties such as permeability, coercivity.

By suppressing the possibility of boundary displacement we may achieve a high coercivity.

4

Origin of Domains

Domain structure is a natural consequence of the various contributions to the energy:

a) Exchange

b) Anisotropy

c) Magnetic

Exchange energy and its origin has already been discussed.

Magnetic Anisotropy

a) Magnetocrystalline anisotropy

b) Shape anisotropy

c) Stress anisotropy

d) Anisotropy induced by:
i) Magnetic annealing

ii) Plastic deformation

iii) Irradiation

e) Exchange anisotropy

a) Magnetocrystalline anisotropy

The origin of this anisotropy lies in the spin-orbit coupling.

Apart from the strong spin-spin and orbit-lattice interactions, there is a weak spin-orbit interaction. But the orbit is coupled to the lattice, $\therefore$ the energy required to overcome the *spin-orbit coupling = anisotropy energy*.

Because an applied field must do work to turn the magnetization vector from the *"easy-axis"*, there must be energy stored in a crystal in which direction of $\bar{M}$ is not easy direction.

We $\therefore$ define **easy and hard** direction of magnetization.

For a cubic crystal:

$$E = K_0 + K_1(\alpha_1^2\alpha_2^2 + \alpha_2^2\alpha_3^2 + \alpha_3^2\alpha_1^2) + K_2(\alpha_1^2\alpha_2^2\alpha_3^2) + \cdots$$

$K_0, K_1, K_2 \ldots\ldots$ are constants for a particular material, and $\alpha_1, \alpha_2, \alpha_3$ are the cosines of the angles that M_S makes with crystal axes.
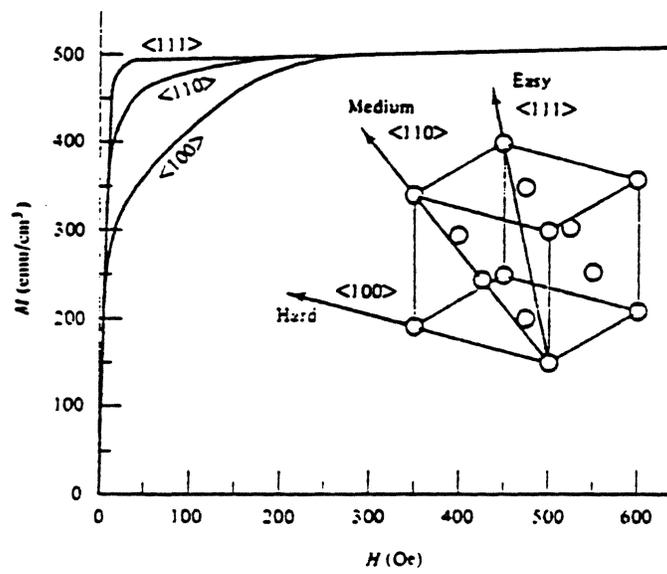
K_0 is independent of angle and is ignored (interested only in energy change as M_S rotates.). K_2 is very small. The direction of easy magnetization is determined with the sign of K_1.

$For + K_1 \Rightarrow E_{100} < E_{110} < E_{111}, and < 100 >= easy-direction, i.e. Iron$

$For - K_1 \Rightarrow E_{111} < E_{110} < E_{100}, and < 100 >= easy-direction, i.e. Nickel$
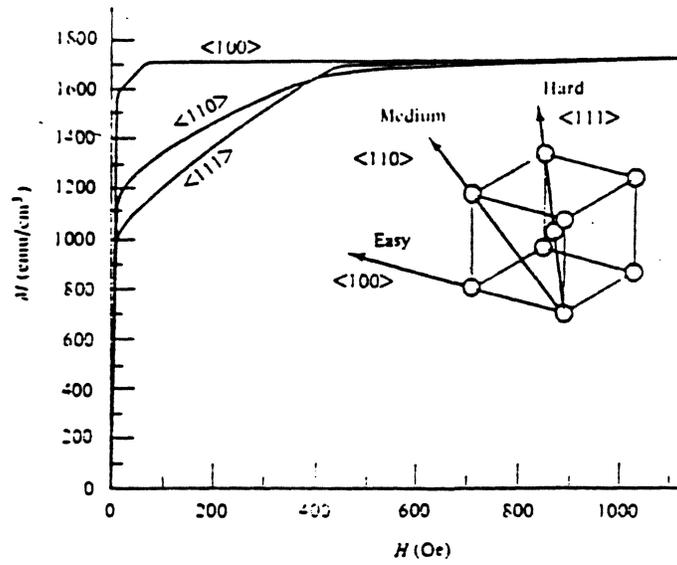
(a)

(b)

Magnetization curves for single crystal of (a) iron and (b) nickel

(culity)

7

Domains growth in fcc crystals:

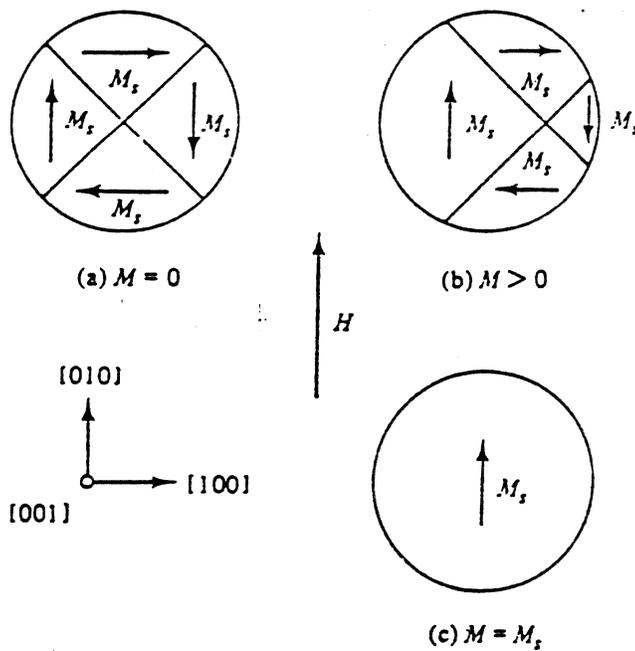Only a small field is required to grow the domains when field is applied in easy direction.

(a) $M = 0$

(b) $M > 0$

H

[010]

[001] → [100]

(c) $M = M_s$

Fig. 7.3 Changes in the domain structure of a crystal of iron (schematic). H is in direction [010]. *(Cullity)*

However, when the external field is in a hard direction, domain wall motion in low field will occur until there is only two domains. Any further increase in magnetization will then take place by *domain rotation*.
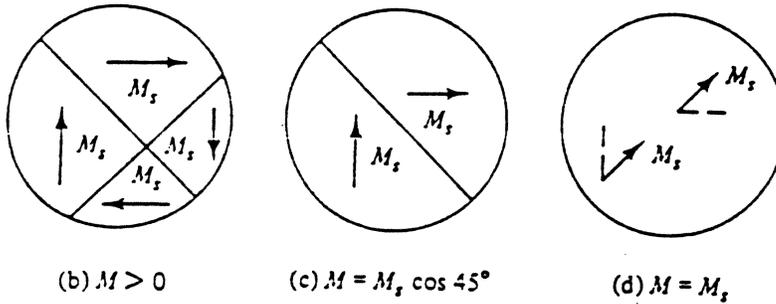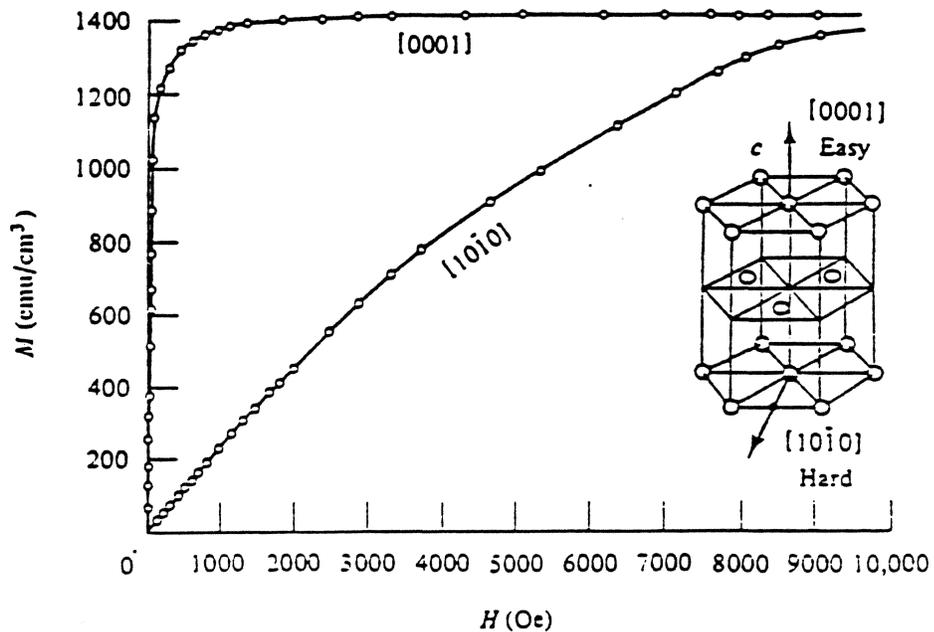
[010] [110]
[001] [100]

(a) M = 0

(b) M > 0   (c) M = M_s cos 45°   (d) M = M_s
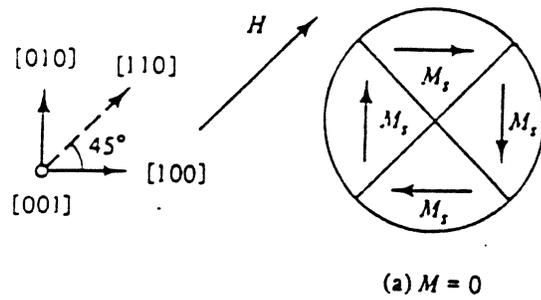
Fig. 7.4 Changes in the domain structure of a crystal of iron (schematic). H is in direction [110]. (Cullity)

For hexagonal crystals:

Here, the hexagonal c axis is the direction of easy magnetization.

M (emu/cm³)

[0001]

[10ĩ0]

[0001]
c Easy

[10ĩ0]
Hard

H (Oe)

∴ the anisotropy energy depends only on a single angle.

$$ E = K_0' + K_1' \cos^2 \theta + K_2' \cos^4 \theta + \ldots \ldots $$

9

It is customary to write E in terms of powers of $\sin \theta$.

$$\cos^2 \theta = 1 - \sin^2 \theta$$
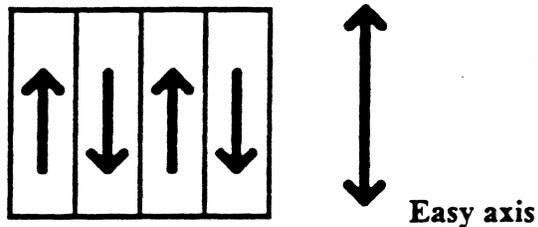
$$E = K_0 + K_1 \sin^2 \theta + K_2 \sin^4 \theta \ldots \ldots$$

$$When, K_1 = +, and, K_2 > -K_1,$$

$$E = MINIMUM, for, \theta = 0$$

and the *c* axis is one of easy magnetization, e.g. *Cobalt*.

A crystal with a single easy axis is called *uniaxial crystal*.

It has a simple domain structure.

Easy axis

Shape (magnetostatic) anisotropy

Consider a polycrystalline specimen with no preferred grain orientation (and ∴ crystal anisotropy).

      If it is spherical, the same field will magnetize it equally in any direction.

      If it is non spherical, it will be easier to magnetize it along a long axis.

If a body is magnetized and the field is removed, a demagnetizing field acting on it decreasing the magnetization.
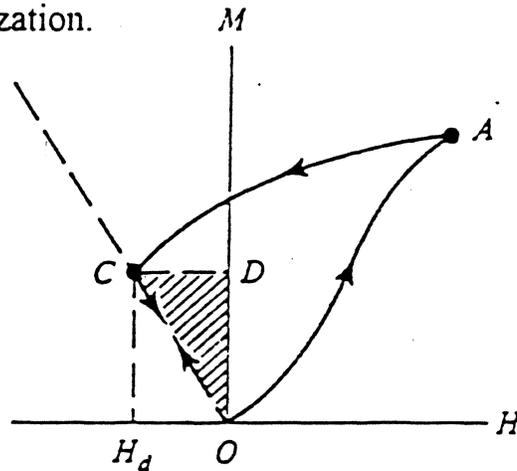
Magnetostatic energy of a magnetized body in zero applied field. *(Cullity)*
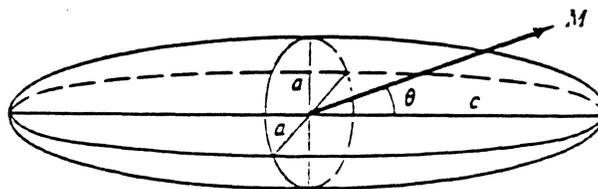
It $\therefore$ contains magnetostatic energy.

In the absence of an external field:

$$E_{ms} = \frac{1}{2} H_d M$$

$$put, H_d = N_d M$$

$$E_{ms} = \frac{1}{2} N_d M^2$$

For a specimen in the shape of a prolate spheroid:

11

If it is magnetized to a level M at an angle θ.

$$E_{ms} = \frac{1}{2}[(M\cos\theta)^2 N_c + (M\sin\theta)^2 N_a]$$

$$\cos^2\theta = 1 - \sin^2\theta$$

$$E_{ms} = \frac{1}{2}M^2 N_c + \frac{1}{2}(N_a - N_c)M^2 \sin^2\theta$$

Note that there is an angle dependent term exactly like the magnetocrystalline anisotropy:

We define the *shape-anisotropy constant*

$$K_S = \frac{1}{2}(N_a - N_c)M^2$$

The above equ's show that the strength of shape anisotropy depends both on *c/a* (from which (Na-Nc) can be calculated) and the extent of the magnetization. It has been calculated that a value of c/a=3.5 would show the same crystal anisotropy as a spherical cobalt with uniaxial anisotropy.
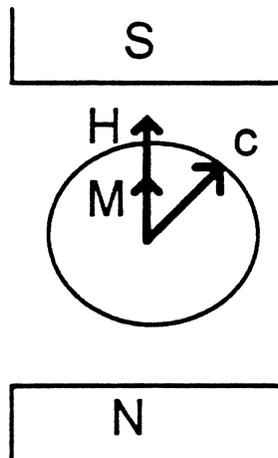
Measurement of magnetic anisotropy

Torque Curves

We measure the torque required to rotate $\bar{M}$ away from the easy direction as a function of angle of rotation.

Let us consider a simple case of a uniaxial crystal cut with c-axis inplane.

If the sample is suspended by torsion wires:

turning the wire will rotate c away from field direction by the angle θ

$$E = K_1 \sin^2 \theta$$

$$torque, L = -\frac{dE}{d\theta}$$

$$L = -K_1 \sin\theta\cos\theta = -K_1 \sin 2\theta$$

K_1 is found from the amplitude of torque curve.

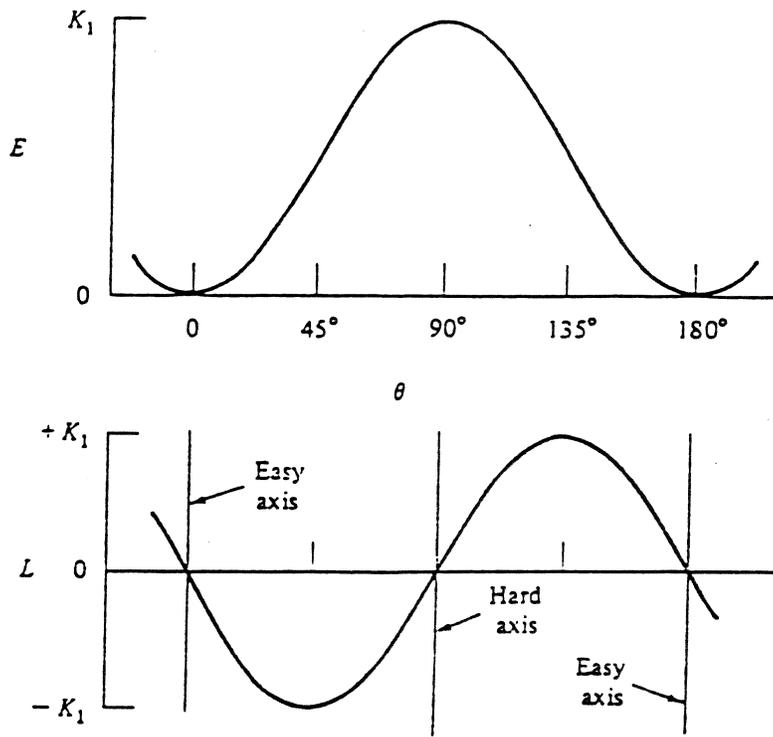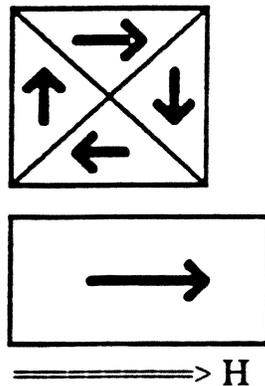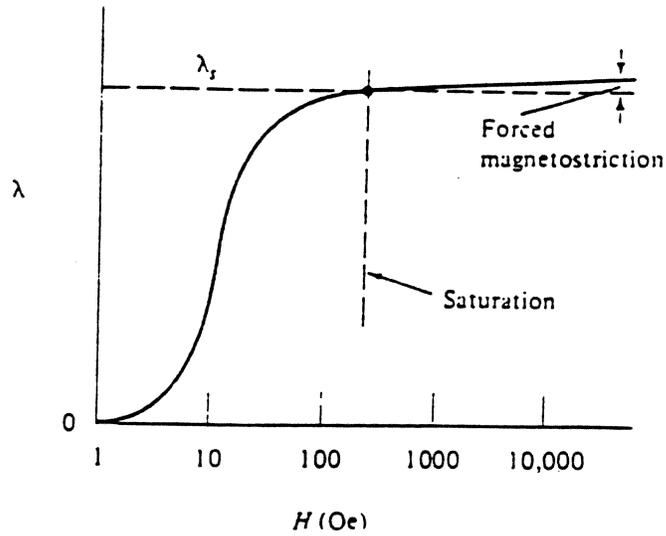Fig. 7.9 Variation with θ of the anisotropy energy E and the torque L $(= -dE/d\theta)$ for a uniaxial crystal. θ is the angle between M_s and the easy axis.

Magnetostriction (magnetoelastic)Energy

When a substance is exposed to a magnetic field, its dimensions change, this is *magnetostriction*.

$$Saturation - Magnetostriction = \lambda_s = \frac{\Delta l}{l}$$

14

This phenomenon too has its origins in spin-orbit coupling:

Subjecting a ferromagnetic crystal to an external stress, the magnetocrystalline anisotropy will change by an amount depending on the strain. an unconstrained crystal in order to reduce its magnetocrystalline anisotropy energy will exhibit a spontaneous strain, which depends on the direction of M relative to the crystal axis.
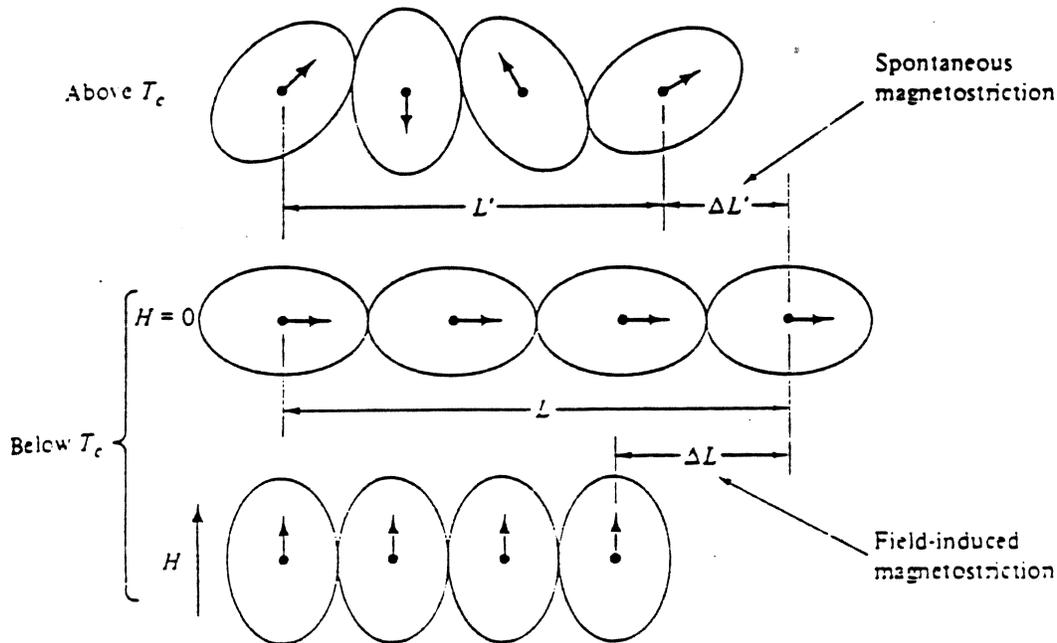
Mechanism of magnetostriction. (Cullity)

15

The expression for magnetostriction (magnetoelastic) energy :

When magnetostriction is isotropic
(for derivation see Cullity p 270)

$$E_{me} = \frac{3}{2}\lambda_s\sigma\sin^2\theta$$

$\therefore$ when stress, whether tensile or compressive, is present, stress anisotropy must be considered:-

$$E_{me} = K_\sigma\sin^2\theta$$
$$where$$
$$K_\sigma => \frac{3}{2}\lambda_s$$

16

Lets now consider domain wall energy and thickness.

Domain Walls Energy

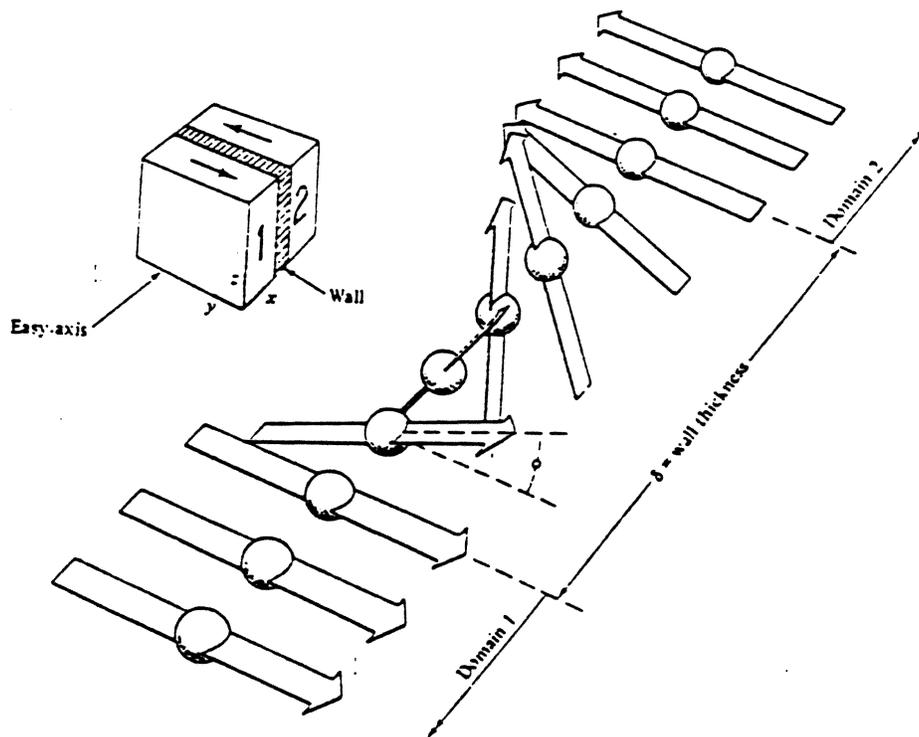Domain walls separate the regions in which the spontaneous magnetization has different directions:

Illustration of a "Bloch" wall (as occurs in bulk materials) *(Cullity)*

This change cannot be abrupt. But results in **large exchange energy** (antiparallel spins).

Reduce this energy by allowing the *180° change to take place gradually.*
∴ <u>this tries to make the wall as wide as possible.</u>

But, since the spins are pointing away from the easy direction, There is *magnetocrystalline energy* involved. This is reduced by reducing the number of spins pointing towards non-easy direction.

$\therefore$ **this tries to make the wall as thin as possible.**

MMathematically expressed

$$E_{ex} = -2JS^2 \cos\phi$$

$$\cos\phi = 1 - \frac{\phi^2}{2} + \frac{\phi^4}{24} - \cdots$$

$$dropping, \phi^4 \, (\phi - small)$$
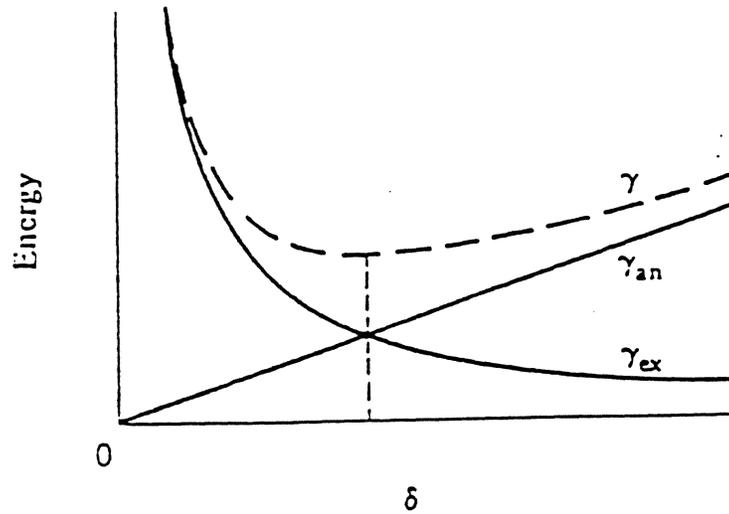
$$E_{ex} = JS^2\phi^2 - 2JS^2$$

The extra energy is the angle dependent first term.

If the wall is **N** atoms thick, and there are $1/a^2$ rows of **N** atoms, where a unit cell edge of a cubic crystal, the extra energy *per unit area of wall:*

$$\gamma_{ex} = (JS^2\phi^2)(N)(1/a^2)$$

$$\phi = \pi/N$$

$$\gamma_{ex} = \frac{JS^2\pi^2}{Na^2}$$

Dependence of wall energy on wall thickness.(Cullity)

Now, **the anisotropy energy = anisotropy constant x wall volume**

$$\gamma_{an} = KNa$$

$$\therefore total - wall - energy / unit - volume$$

$$\gamma = \gamma_{ex} + \gamma_{an} = \frac{JS^2\pi^2}{\delta a} + Ka$$

$$where, wall - thickness = \delta = Na$$

This energy has a minimum given by

$$\frac{d\gamma}{d\delta} = -\frac{JS^2\pi^2}{\delta^2 a} + K$$

$$\delta = \sqrt{\frac{JS^2\pi^2}{Ka}}$$

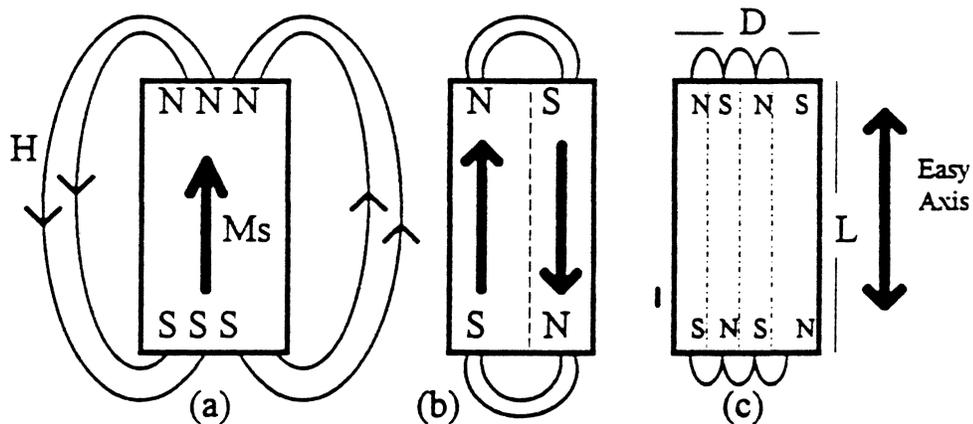$\delta \Rightarrow inversely \sim K$

replacing

$$\gamma = \sqrt{\frac{JS^2\pi^2 K}{a}} + \sqrt{\frac{JS^2\pi^2 K}{a}} = 2K\delta$$

i.e., the minimum in total energy occurs when **exchange energy = anisotropy energy (as shown above)**

We turn now to an examination of the <u>reasons for domain formation</u>.
Magnetostatic energy plays a very important part.

a) Uniaxial Crystal

Consider a single crystal of uniaxial substance

(a)   (b)   (c)

If it is one domain, as in **(a)**, free poles form on the end leading to *large magnetostatic energy.*

$$E_{ms} = N_d M_s^2 / 2 \cdots\cdots\cdots (1)$$
$$N_d here \sim 2\pi$$
$$\therefore = 2\pi M_s^2 L$$

This energy can be halved if the crystal splits into two domains **(b)**. This is because north and south poles are brought closer together, decreasing the spatial extent of **H** field.

The crystal can further split **(c)**,

but each extra wall formed will require energy $= E_{wall} = \gamma L / D$

It can be shown (Chikazumi & Charap, "Physics of Magnetism") that magnetostatic energy for multi-domain **(c)**, provided **D** is smaller than **L**, is given by-

$$E_{ms}(multi-domain) = 1.7\,M_s^2 D$$

The total energy-

$$E = E_{ms} + E_{wall}$$
$$E = 1.7\,M_s^2 D + \gamma L / D \ldots\ldots\ldots\ldots(2)$$

where L/D is the wall area/unit area of the top surface of crystal.

The minimum energy occurs when-

$$\frac{dE}{dD} = 1.7 M_s^2 - \frac{\gamma L}{D^2}$$

$$D = \sqrt{\frac{\gamma L}{1.7 M_s^2}}$$

$replace-in, equ.(2)$

$$E = 2\sqrt{1.7 M_s^2 \gamma L} \dots\dots\dots\dots\dots(3)$$

$For-cobalt, \gamma = 7.6 ergs/cm^2, and$

$if, L = 1cm$

$$D = \sqrt{\frac{(7.6)(1)}{(1.7)(1422)^2}} = 1.5 \times 10^{-3} cm$$

$\therefore very-small$

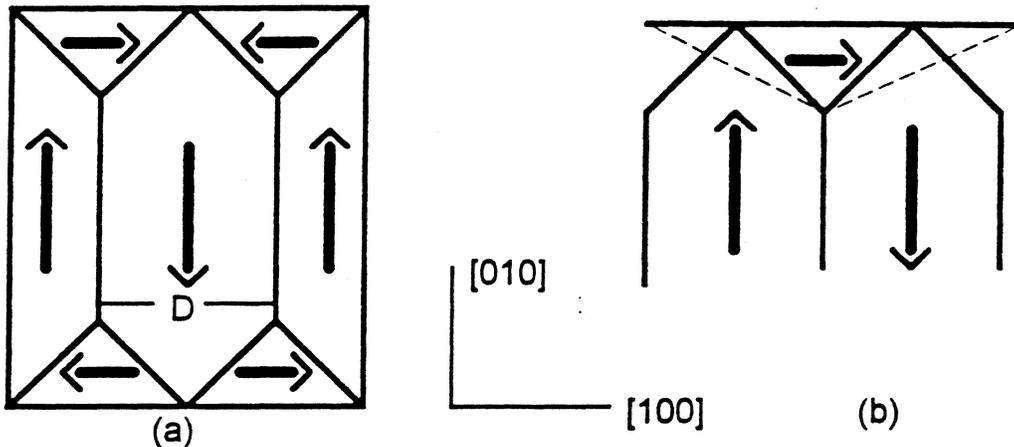$$\frac{E(single-domain)}{E(multi-domain)} = \frac{2\pi M_s^2 L}{2\sqrt{1.7 M_s^2 \gamma L}}$$

$$= 2.4\sqrt{\frac{M_s^2 L}{\gamma}} = 2.4\sqrt{\frac{(1422)^2(1)}{7.6}} = 1200$$

♣ ∴ there is over 1000 times energy advantage in domain creation

Domain structure for cubic crystals:

Here, depending on the sign of K_1 we can have 3 or 4 easy axes-

Thus, it is possible for the flux to close within the crystal, reducing E_{ms} to zero.

Closure domains in cubic crystal with <100> easy axis.

Triangular closure domains are formed are formed as a path for flux closure.

If there are flux closure, then why aren't domains bigger? (since wall energy is the only energy now)

This is because of *magnetoelastic energy*.

For **iron** with its **positive** λ_{100}, [100] closure domains would strain magnetostrictively to the dotted line (above figure), if not kept in check by [010] domains in either side.
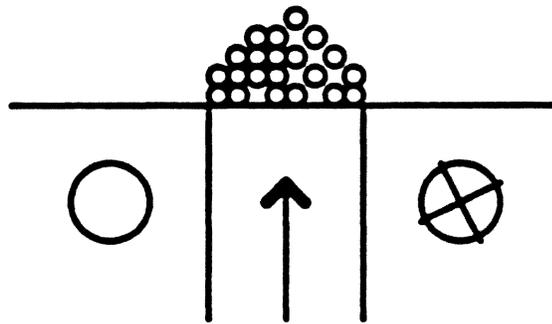
Thus, **the stored magnetoelastic energy ~ volume**

It is, therefore, advantageous for the crystal to split into smaller domains **until the sum of magnetoelastic and wall energies become minimum.**

24

Domain Wall Observation

1) Bitter Method

This involves delineating the boundaries with very fine particles-

(These are more commonly aqueous suspension of colloidal particles of magnetite. Fe_3O_4)

Thus the domains become observable. (microscopes or electron-microscopes)

2) Magnetooptical Methods

a) Faraday Effect

When plane polarized light is passed through a magnetic film, the plane of polarization is rotated by an angle ($\sim 1/3$)° which is proportional to the
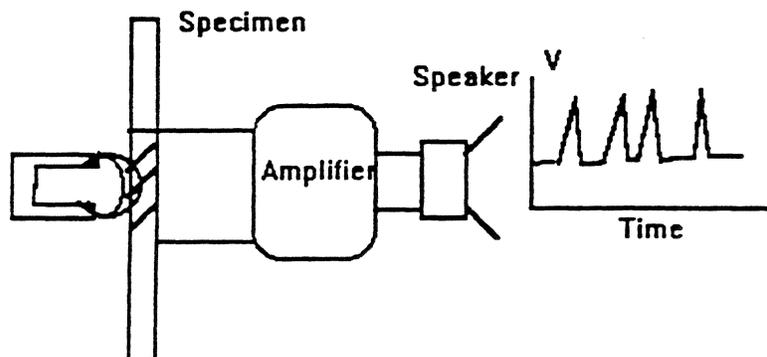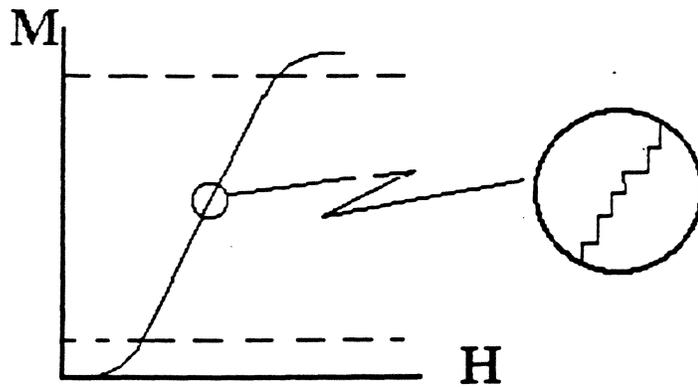
Magnetization Process
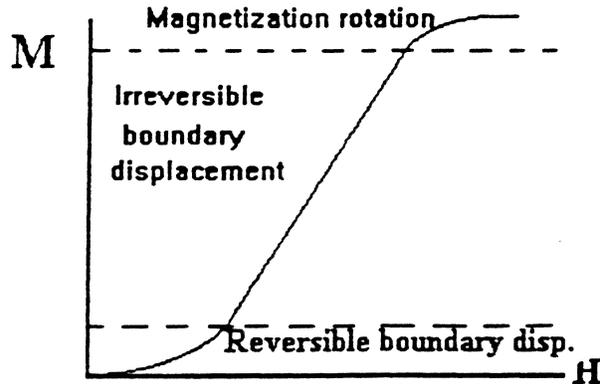
a) Domain Wall Motion

Barkhausen effect

Domain walls move in response to an applied field.

Irregular spikes are detected when a smoothly increasing field is applied to a ferromagnetic specimen around which a "search coil" is placed.
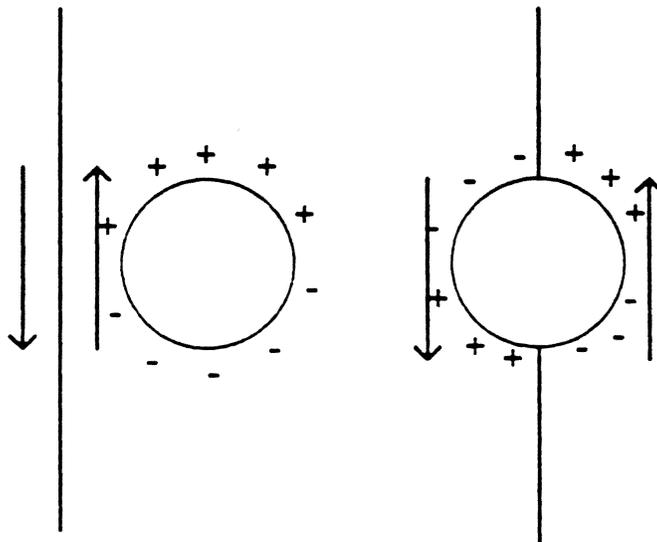
When magnetizing a polycrystalline ferromagnetic material, *"wall motion"* in the main process of change in magnetization. "Domain rotation" will predominate at higher fields.

Hindrances to wall motion

Real materials contain crystal imperfections in the form of *"inclusions"* and *"residual microstresses"*(e.g., lattice dislocations).

A domain wall passing through an inclusion would lead to redistribution of free poles, lowering the magnetostatic energy. The inclusion will "anchor" the wall (*Domain wall pinned*).

If we plot the energy associated with a wall with respect to its position, several minima in energy are observed.
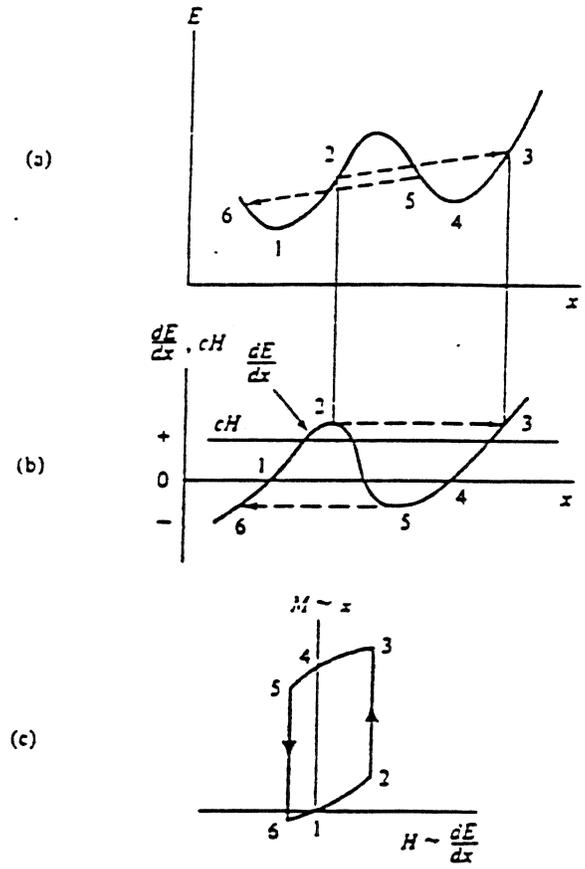
Reversible and irreversible wall motion (Cullity)

$$dE \, / \, dX = restoring - force$$

Note:
$$dE \, / \, dX, at\,"2" = dE \, / \, dX, at\,"3"$$

The movement of the wall from position "1" to "2" is "reversible".

However, the movement from "1" to "3" is irreversible (Barkhausen jump).

If the field is now reduced to zero, the wall will not go back to its previous energy minimum. We have ∴ "remanence and hysteresis".

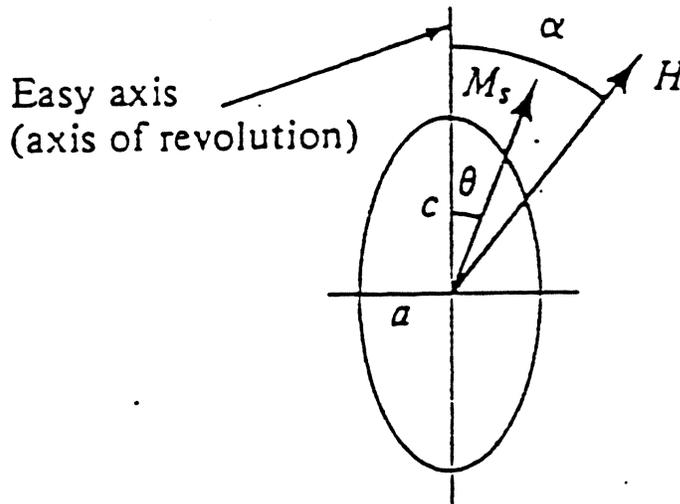# b) Magnetization by (coherent) Rotation

For simplicity,

      a) consider a single domain particles (thus, no walls present).

      b) the particle is in the shape of an ellipsoid.

The rotation will take place against one kind of anisotropy.

      c) Let the rotation takes place against shape anisotropy

The anisotropy energy is given by-

$$E_a = K_u \sin^2 \theta$$

(the uniaxial anisotropy constants for an ellipsoid can easily be calculated, since demag.

constant. are known $K_u = \frac{1}{2}(N_a - N_c)M^2$)

The potential energy of the particle in a magnetic field:

$$E_P = -HM_S \cos(\alpha - \theta)$$

$\therefore total-energy,$

$$\Rightarrow E = E_a + E_p = K_u \sin^2 \theta - HM_S \cos(\alpha - \theta)$$

The equilibrium position of *Ms* (where net torque vanishes) is given by:

$$\frac{dE}{d\theta} = 2K_u \sin\theta \cos\theta - HM_s \sin(\alpha - \theta) = 0$$

If the field is normal to easy axis $(i.e.\, \alpha = 90°)$:

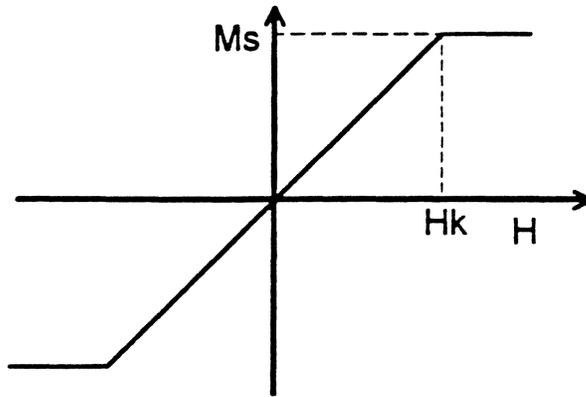$$2K_u \sin\theta \cos\theta = HM_s \cos\theta$$

and

$$M = M_s \sin\theta$$

$i.e.$

$$2K_u(M/M_s) = HM_s$$

$let, m = M/M_s = reduced-magnetization$

$$\Rightarrow m = H\left(\frac{M_s}{2K_u}\right)$$

i.e., *magnetization has no hysteresis* (because it is linear with **H**)

Note the reversible nature of this case.

Saturation is achieved when

$$H = H_K = \frac{2K_u}{M_s} = \text{" } Anisotropy - Field\text{"}$$

If the field is along the easy axis, $(i.e., \alpha = 0)$, then let H be reduced to zero and then increased in negative direction, $(\alpha = 180°)$, although there is no torque involved, the magnetization becomes unstable at $\theta = 0$, and flips over to $\theta = 180°$.

Irreversible
(Barkausen jump)
analogus to domain-wall motion
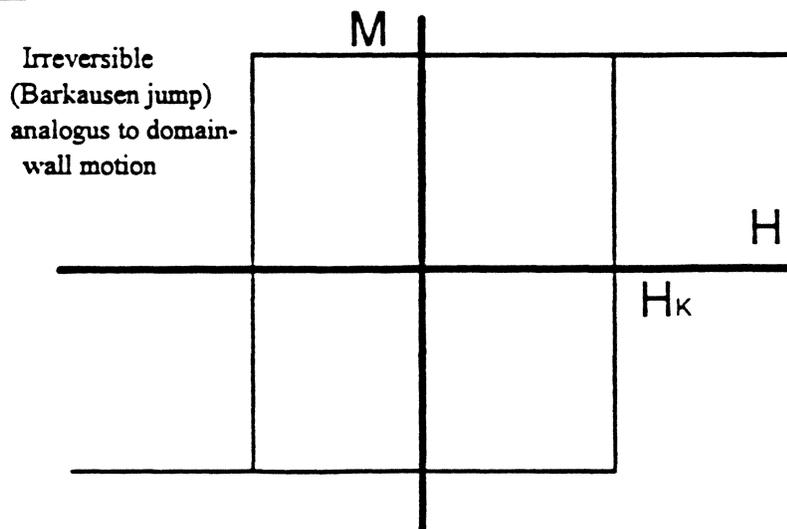
HEADS

RECORDING HEADS

Heads are mostly based on the inductive coil wound on a magnetic core.
Their functions are:
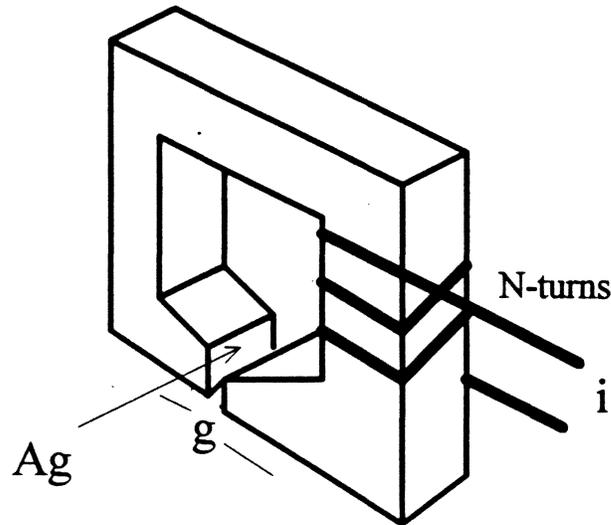
A typical "ring head"

i) Recording

normally, the optimum writing head gap is slightly less ... higher ... recording ...

High permeability, high Ms, they are driven hard by write currents.
Wide gap, to write deep-wider track

ii) Reproducing (reading)

Low flux, ... head efficiency important.

✗ High permeability (low signals) *AT low flux values, uncontrolled domain in the core add noise, especially when small.*

✗ Narrow gap for high resolution, narrow track.

✗ Use maximum No. of Turns

iii) Erasing

Wide gap, wide track.
dc or ac fields

The Reproduction Process

The basis is Reciprocity relationship:
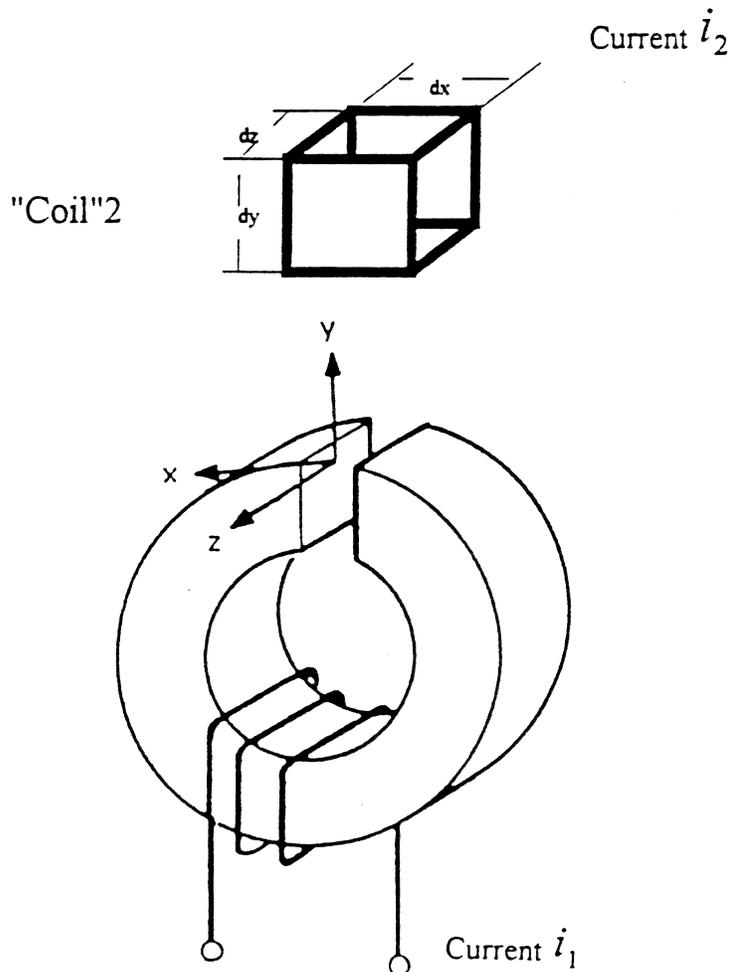
$$\frac{\Phi_2}{i_1} = L_m = \frac{\Phi_1}{i_2}$$

$i_1 =$ Current in coil 1

$\Phi_2 =$ Flux in "coil"2

$i_2 =$ Current in "coil"2

$\Phi_1 =$ Flux in coil 1

Let coil 1 be the head coil

33

Considering only "x" components of the head field, the flux:-
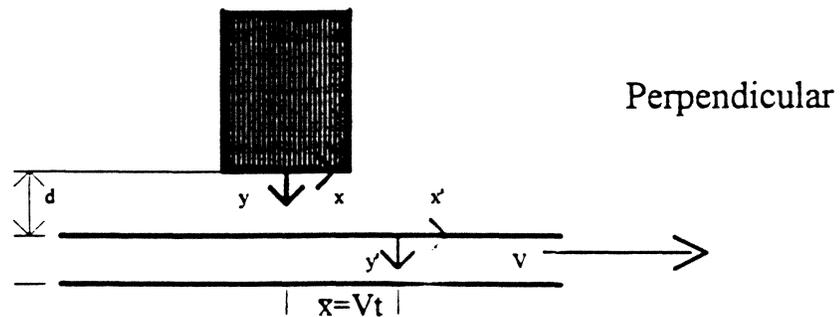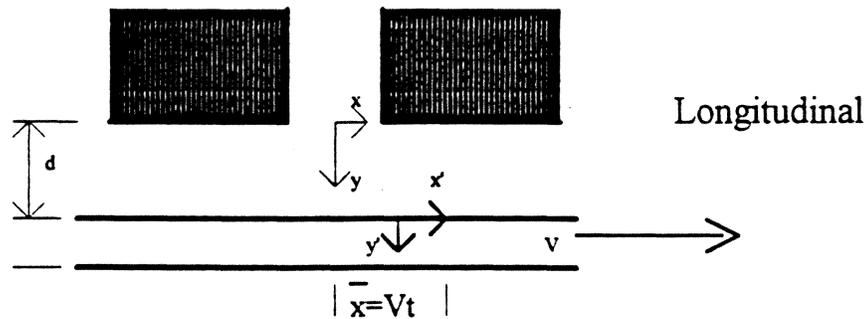
$$\Phi_2 = \mu_0 H_x(x, y) dy dz$$

where dydz is the area enclosed by "coil"2.

The current in the "coil"2 is the current that produces the equivalent to the magnetization M_x (x') at the point x',

$$\frac{i_2}{dx} = M_x(x')$$

and at the point $\overline{x}$ = vt, a point in the medium.

$$\frac{i_2}{dx} = M_x(x - \overline{x})$$

Longitudinal

Perpendicular

Definition of symbols and dimensions employed in this analysis.

Now, solve for Φ_1 and integrate over the volume of the medium leads to the total flux:

$$\Phi = \mu_0 \int\limits_{-\infty}^{\infty} \int\limits_{d}^{d+\delta} \int\limits_{-\infty}^{\infty} M_x(x-\bar{x}) \frac{H_x(x,y)}{i} \, dxdydz$$

"d"- is equivalent to the head-medium spacing, $\delta \equiv$ media thickness

Consider only a track of width, W

$$\Phi = \mu_0 W \int\limits_{-\infty}^{\infty} \int\limits_{d}^{d+\delta} M_x(x-\bar{x}) \frac{H_x(x,y)}{i} \, dxdy$$

Now, $signal \equiv e_x = -\dfrac{d\Phi}{dt}$

$$e_x = -\mu_0 W v \int\limits_{-\infty}^{\infty} \int\limits_{d}^{d+\delta} \frac{dM_x(x-\bar{x})}{d\bar{x}} \frac{H_x(x,y)}{i} \, dxdy$$

where quantity $H_x(x,y)/i_2$ is the head field per unit current in the head winding when it is energized.

Similarly:

$$e_y = -\mu_0 W v \int\limits_{-\infty}^{\infty} \int\limits_{d}^{d+\delta} \frac{dM_y(x - \bar{x})}{d\bar{x}} \frac{H_y(x,y)}{i} \, dx \, dy$$

These are the **"reciprocity formulas"** or **"head sensitivity functions"**.

What the head senses are the derivitives of magnetization, i.e., where the Hex and He are high.
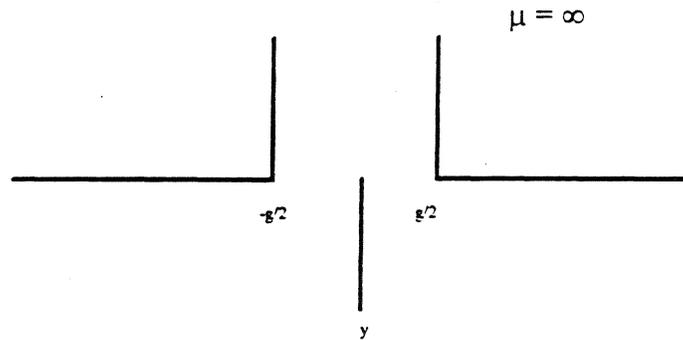
dm/dx corresponds to magnetic charges or **"poles"**.

∴ through reciprocity relationship read back pulses can be calculated if distributions of magnetization and head fields are known or assumed.

The Head Field Function

The next step is to consider the fields generated by the recording head.

Karlqvist treatment.

The solution for the exact fields of head is complex problem involving numerical analysis.

To simplify the problem he had to make several assumptions.

    a) Infinite permeability (i.e., all the field appears across the gap)

    b) since the head is excited by a current source, a vector potential solution is strictly required which may be obtained by integral or differential approach. However, if the region of current source can be isolated and replaced by an equivalent magnetic source then a scalar potential solution is applicable.

$$H = -\nabla U$$

    (The infinite permeability assumption → above the head where the medium passes the potential solution can be approximated to that of a scalar. In simple language, infinite permeability implies constant potential).

c)that the potential across the gap varies linearly both in the x and y directions.
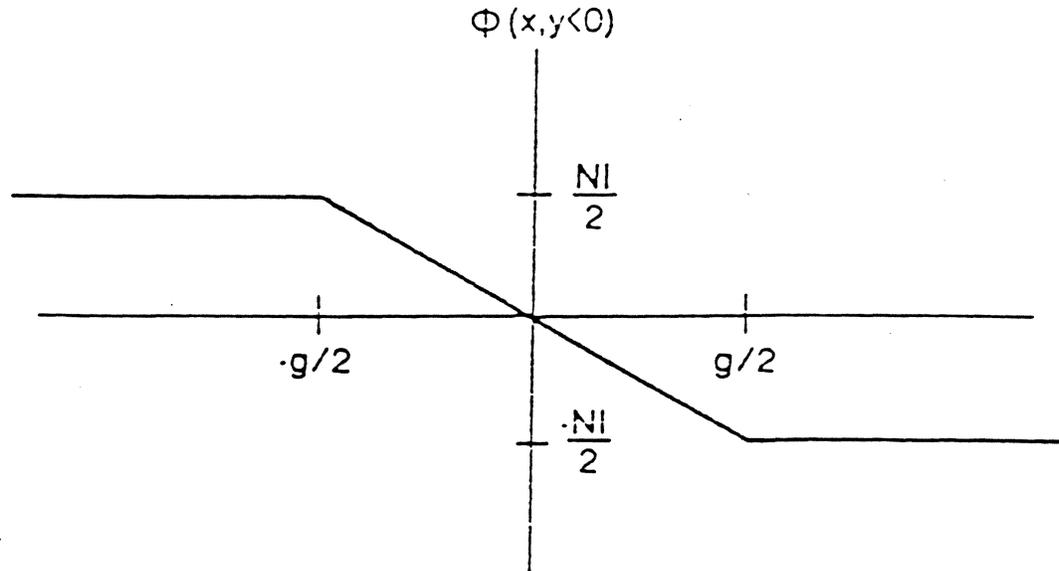
Thus the boundaries are well defined.

Further assumptions:-

d) that the pole-tip lengths are large compared to the gap (reasonable),
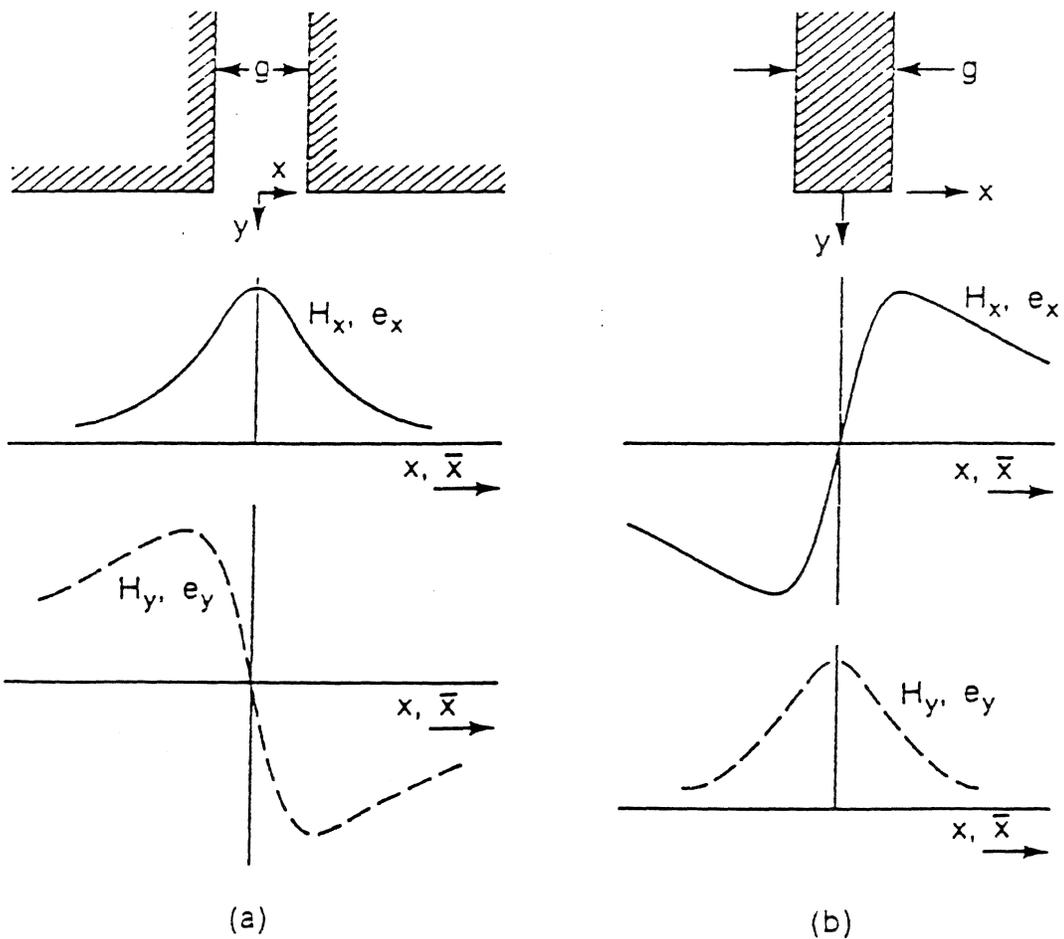∴   reduce to two dimensional problem.

e) ∴ constant head core surface potential.

with H = -∇U the problem is one of potential theory.

$$U(x,y) = \frac{1}{\pi} \int_{-\infty}^{\infty} \frac{U(x',0)y}{(x-x')^2 + y}dx'$$

$$H_x = \frac{H_\xi}{\pi} \left(\arctan \frac{g/2 + x}{y} + \arctan \frac{g/2 - x}{y} \right)$$

$$H_y = \frac{-H_g}{2\pi} \ln \frac{(g/2 + x)^2 + y^2}{(g/2 - x)^2 + y^2}$$

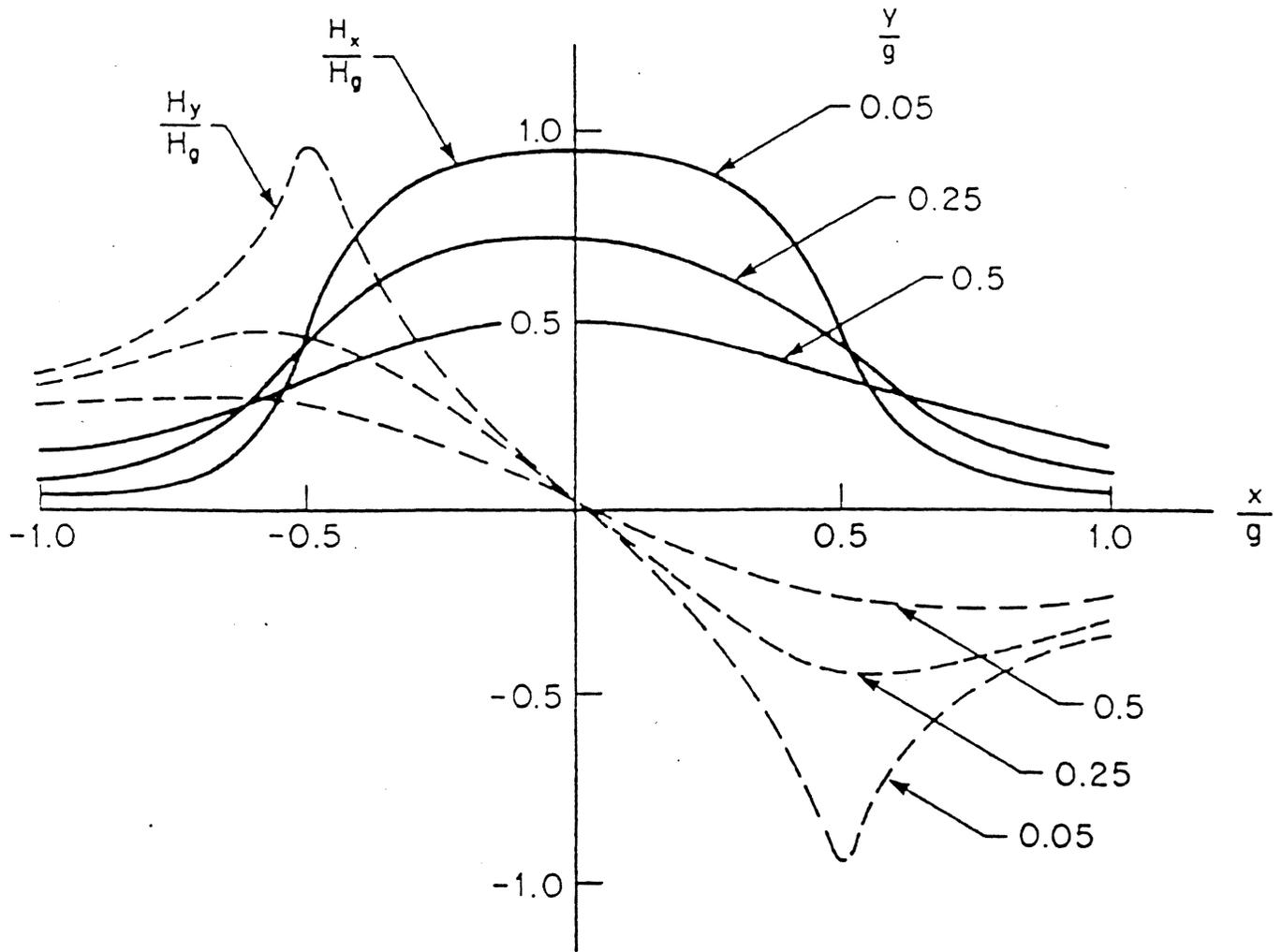General form of field distribution for (a) ring head and (b) single pole head.

34

Fig (4): Field distribution for a ring head derived using Karlqvist's expressions.

Here
$$H_g = NI / g$$

is the *"deep gap field"* and can be easily calculated.

We shall later see that an efficiency factor η should be included in the above equation to represent the finite head permeability, such that:

$$H_g = NI\eta / g$$

34·1

Now that we know the head field, we can calculate the output voltage.

We had:

$$e_x = -\mu_0 Wv \int\limits_{-\infty}^{\infty} \int\limits_{d}^{d+\delta} \frac{dM_x(x-\bar{x})}{d\bar{x}} \frac{H_x(x,y)}{i} \, dxdy$$

We still have to find the form of magnetization M_x.

In the ideal case, the magnetization would undergo a step change (It will be seen that this yields maximum density).

For an infinitely sharp "*delta function*" transition.

$$\frac{dM_x(x-\bar{x})}{d\bar{x}} dx = 2\,M_r \quad \text{at} \quad x = \bar{x}$$
$$= 0 \text{ at } x \neq 0$$

Substituting:

$$e_x = -2\mu_0 WvM_r \int\limits_{d}^{d+\delta} \frac{H_x(x,y)}{i} \, dy$$

For a very thin media:

$$e_x = -2\mu_0 WvM_r \delta \frac{H_x(x,d)}{i}$$

Thin Medium Limit

Consider:

$$e_x(\overline{x}) = -\mu_0 VW \int\limits_{-\infty}^{\infty} \int\limits_{d}^{d+\delta} \frac{dM_x(x-\overline{x})}{dx} \frac{H_x(x,y)}{i} dxdy$$

For a thin media:

$$e_x(\overline{x}) = -\mu_0 VW \,\delta \int\limits_{-\infty}^{\infty} \frac{dM_x(x-\overline{x})}{dx} \frac{H_x(x,d)}{i} dx$$

For the case where $\dfrac{H_x(x,y)}{i}$ is a delta function

$$e_x(\overline{x}) \sim \frac{dM_x(\overline{x})}{dx}$$

$\therefore$ Response is media limited

(a)
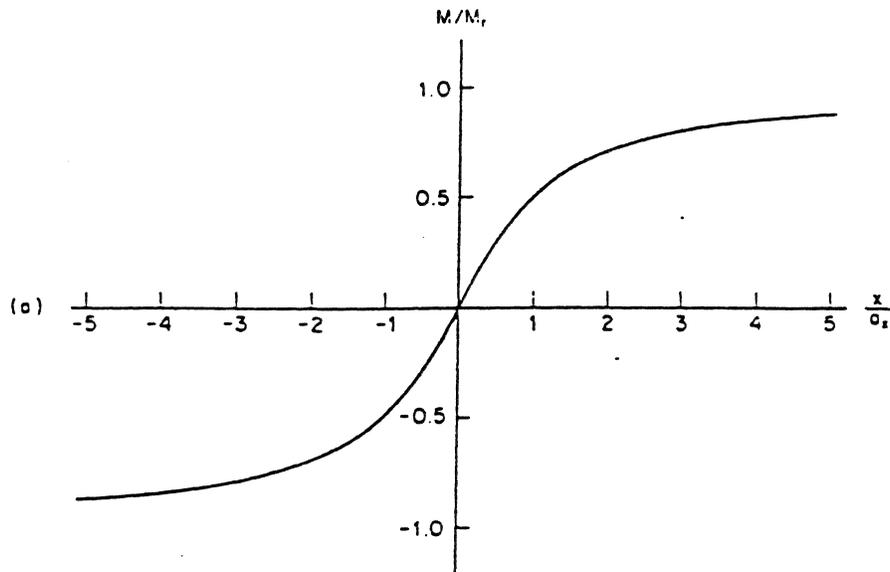
Sine-wave recording.

Consider the magnetization given by:

$$M_x(x) = M_s \sin kx$$

From reciprocity:

$$e_x(\overline{x}) = -\mu_0 VW \int\limits_{-\infty}^{\infty} \int\limits_{d}^{d+\delta} \frac{dM_x(x-\overline{x})}{dx} H_x(x,y) dxdy$$

$$e_x(\overline{x}) = (const.) \int\limits_{-\infty}^{\infty} \int\limits_{d}^{d+\delta} \frac{dM_x(x-\overline{x})}{dx} H_x(x,y) dxdy$$

$$e_x(\overline{x}) = Kk \int\limits_{-\infty}^{\infty} \int\limits_{d}^{d+\delta} \cos k(x-\overline{x}) H_x(x,y) dxdy$$

34·4

In the small gap limit (to facilitate integration):

$$H_x = \frac{1}{\pi} \frac{y}{x^2 + y^2}$$

and

$$\cos k(x - \bar{x}) = \underbrace{\cos kx \cos k\bar{x}}_{even} + \underbrace{\sin kx \sin k\bar{x}}_{odd}$$

Keeping the even function of x, and replacing :-

$$\int_{-\infty}^{\infty} \frac{d(x/y)\cos kx}{1 + (x/Y)^2} = \pi e^{-kx}$$

$$e(x) = \left\{ \frac{Kk}{\pi} \int_{d}^{d+\delta} y\,dy \int_{-\infty}^{\infty} \frac{dx\cos kx}{x^2 + y^2} \right\} \cos k\bar{x}$$

$$= Kk \int_{d}^{d+\delta} e^{-kx} dy$$

$$= K\left\{ e^{-kd} \right\}\left\{ 1 - e^{-k\delta} \right\}$$

$$= K(k\delta)\left\{ e^{-kd} \right\}\left\{ \frac{1 - e^{-k\delta}}{k\delta} \right\}$$

$$\text{"Spacing Loss"} \equiv e^{-kd} = \underline{L}_d$$

$$\text{"Thickness Loss"} \equiv \left\{ \frac{1 - e^{-k\delta}}{k\delta} \right\} = \underline{L}_\delta$$
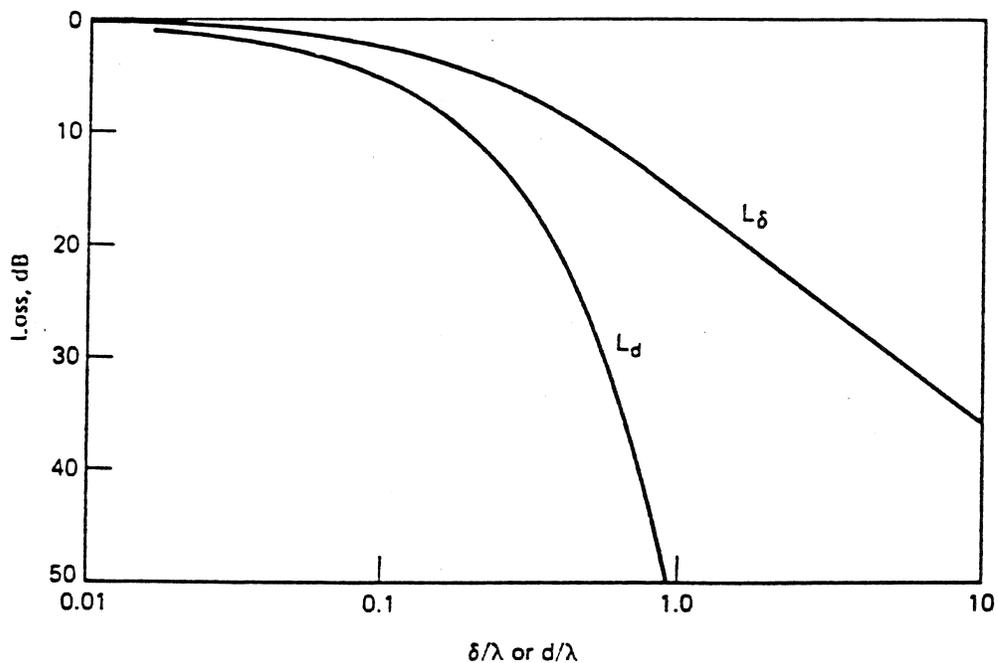

Figure 2.7 Thickness loss L_δ and separation loss L_d as functions of reduced thickness or reduced spacing.

As is seen in the above figure of thickness and spacing loss VS reduced thickness and reduced spacing, **the spacing loss is much more severe**.

34·6

Now, *when not considering small gap limit* (this is done through Fourier analysis and will not be discussed here), the solution of the reciprocity expression for $e_x(\overline{x})$ will involve an extra loss factor, called the **_gap loss._**

$$\underline{\text{Gap - loss term}} \equiv \frac{\sin(kg/2)}{kg/2}$$

Why this expression?

Consider a zero spacing Karlqvist head

Sensitivity function, Hx

Hx
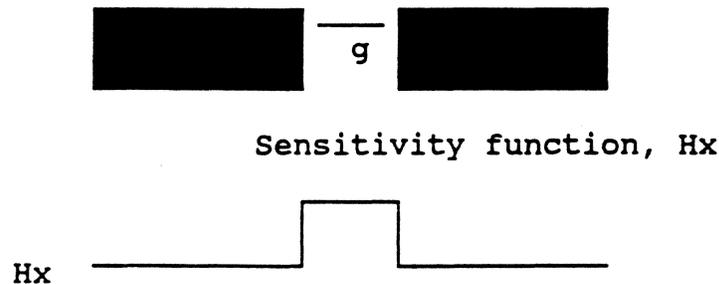
The boundary condition is that the field must vanish at the head surface but is approximately rectangular above the gap.

$$e_x(x) \propto \int_{-g/2}^{g/2} \cos k(x - \overline{x})dx$$

$$\propto \frac{\sin(kg/2)}{Kg/2} \propto \sin\frac{x}{x} \Rightarrow \text{ "Rectangular Sampling Function"}$$

[The exact solution for H_x in fact yield fields that *peak near the gap edges*]

34

Our final expression :-

$$e_x(\bar{x}) = -\mu_0 VWM_0 \frac{H_g g}{i} k\delta\{e^{-kd}\}\left\{\frac{1-e^{-k\delta}}{k\delta}\right\}\left\{\frac{\sin(kg/2)}{kg/2}\right\}\cos k\bar{x}$$
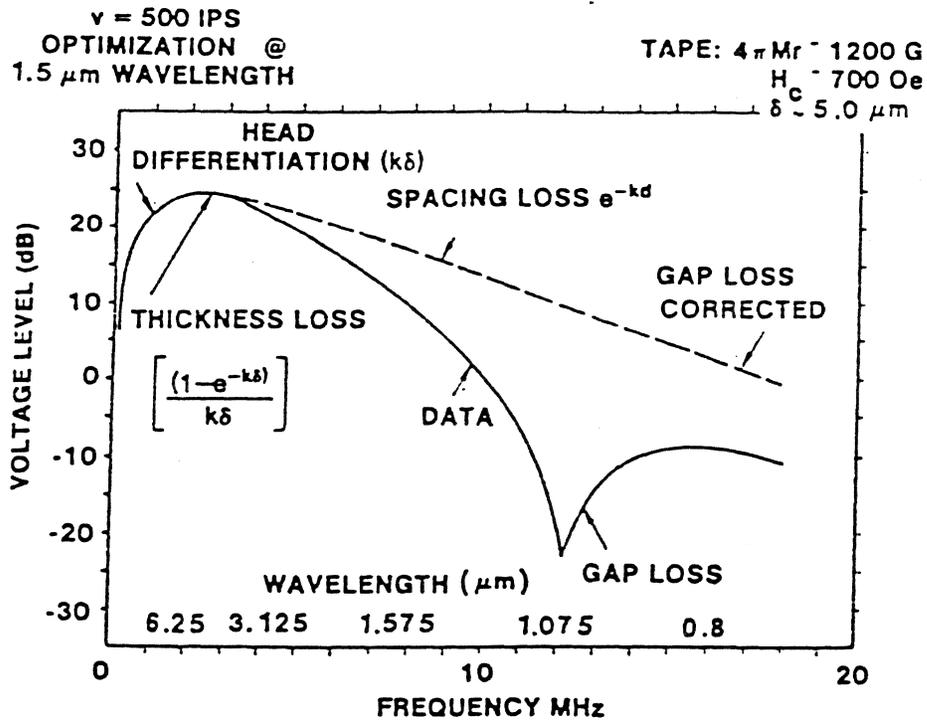
Above figure shows an <u>experimental</u> spectral curve (N. Bertram). The reproduce gap length ~ 0.875 micro-meter.

- It is seen from the above formula that at low frequencies the dominant term is the head *differentiation term,* $k\delta$. ∴, the voltage varies initially as the wave number k .
- As the wave-number increases, the factor representing the thickness loss

$$\left\{\frac{1-e^{-k\delta}}{k\delta}\right\} = L_\delta$$

begins to decrease from unity at wave length $\lambda \cong 2\pi\delta$.

• At wave-numbers $k\delta > 1$ the exponential loss term is such that the reproduce head does not *"see"* the back of the coating.

• At even shorter wavelength the spacing loss e^{-kd} becomes significant, so that voltage decreases with wave number.

• At a wave length approaching the reproduce gap length the voltage decreases rapidly due to sinx/x gap loss term.

Comparing the experimental with the theoretical plots in the above figure, Bertram calculated a spacing loss of $\sim 0.4\mu m$, too large for **contact tape recording!**

The Explanation?

     That the assumption of sharp magnetization transition is incorrect. We have a **"finite transition length".**

MR Heads

Advantages of MR heads

* **Flux-sensing elements are compact** (no turns required). Good for high track density.

* **Higher output voltages.** (an inductive reproduce head would need ~4000 turns to provide the same signal at 100 KFCI and 100 000 at 10 KFCI !)

* **low impedance** (10-100Ω). The *inductive reproduce* heads tend to resonate due to their inductance.

* thin-films $\therefore$ **read and write elements can be placed next to each other.**

* **Higher S/N ratio.** (Since signal is so high)

* **Independent of speed** (Although signal advantages decrease as media speed increases, self resonance which sets a limit on the inductive head signal at high speed does not occur).

Magnetoresistance
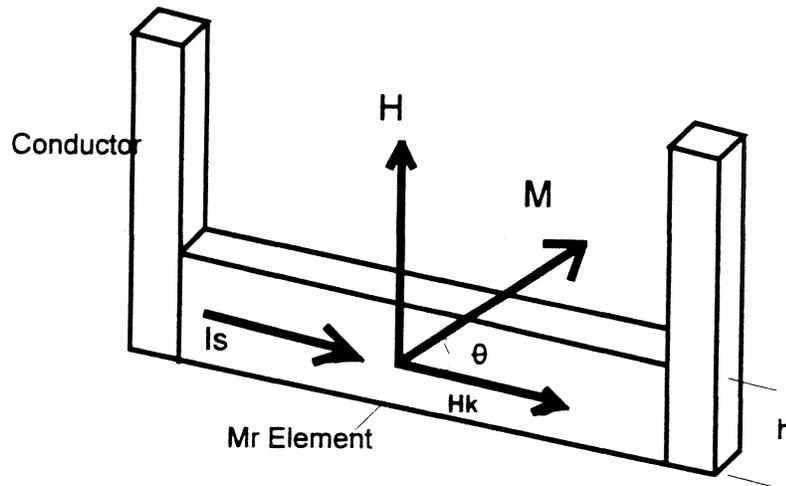
Fig: Magnetoresistive element.

The resistivity changes in response to rotation of the film demagnetization vector as:

$$\rho = \rho_\circ + \Delta\rho \ \cos^2 \theta$$

where θ is the angle between the current and magnetization of the film, $\rho_\circ$ is the **isotropic resistivity**, and $\Delta\rho$ is the **magnetoresistivity**.

• The anisotropy field, H_k (~3-10 Oe), is "induced" through **depositing the element in magnetic field**.

• This field exerts a torque which **acts to keep $\theta=0$ (Easy axis)**.

• The sensor carries a constant **"sense current"** I_S.

• Afield from the medium **rotates the moment, changing the resistance**, which <u>varies the voltage across the MR element</u> **producing signal**.
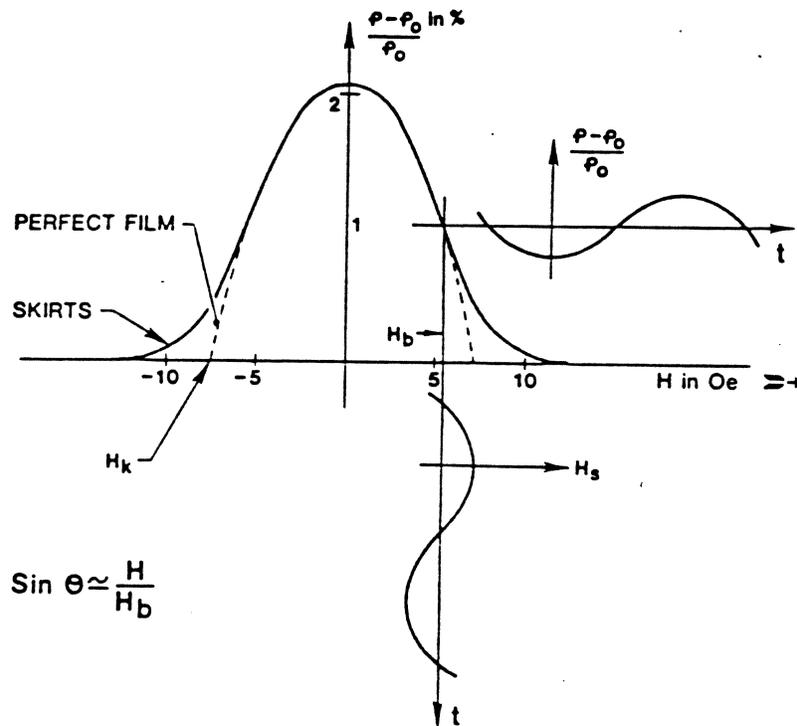
Figure: A sketch of $(\rho - \rho_0)/\rho_0$ versus H.(F. Jeffers)

- The **"skirts"** in the curve are due to <u>minor local deviations in the direction</u> <u>and magnitude of the anisotropy field</u> H_K and any (non uniform) demagnetization that may exist.

- The dotted curve shows how a **"perfect"** MR element would behave.

- In order to get the maximum signal and minimum second harmonic distortion, a constant "bias-field" H_b is applied to the element to move the operating point of the element to the inflection point in the curve $(\sim45° - 55°)$

- For permalloy $\Delta\rho/\rho_o \cong 2.5$ percent.

- For a 50 μm element there is 10 mV due to nonlinearities (e.g. in the *skirt*) and a maximum signal ~25 mV → still very high signal.

Magnetoresistive Heads

These are flux-sensing heads.

The figure shows the Mr Element with labels: Conductor, Is, Mr Element, H, M, Hk, 0, Signal Field, h, and the equation $\rho = \rho_0 + \Delta\rho \cos^2\theta$.
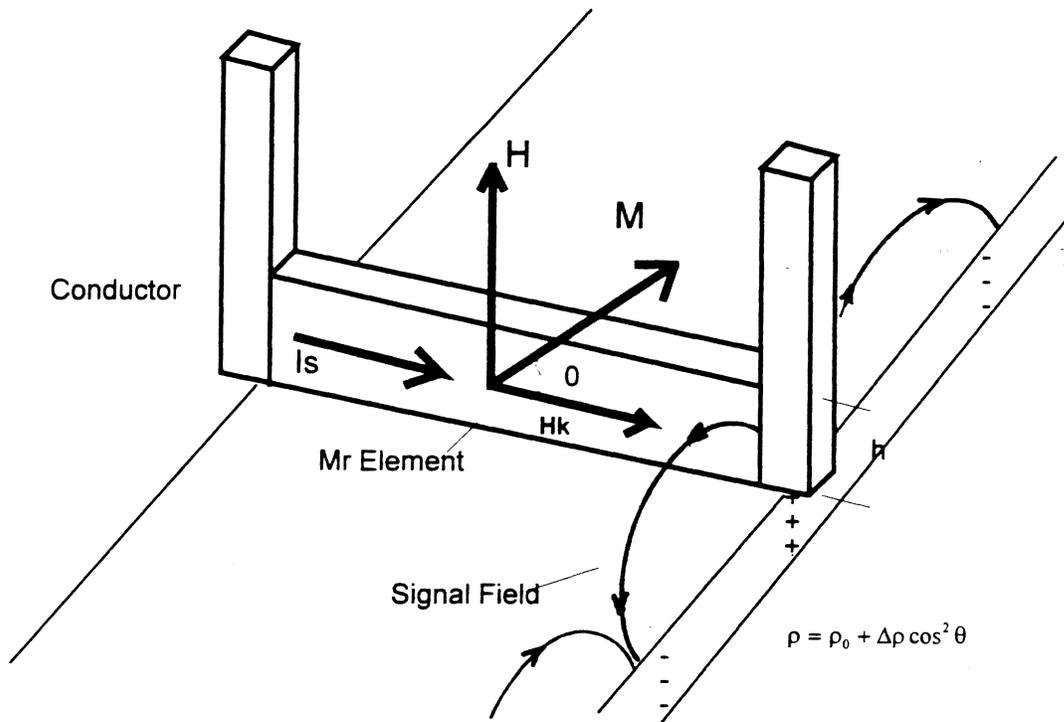
Figure shows an unshielded magnetoresistive head (**Hunt Head**)

- It responds to the vertical field above the media averaged over element height, **h**.

- Because of wear considerations, the element height must be ~ 4-5 μm.

- I_s is constant, ∴ change of resistance → change in voltage across the element.

large area single-domain
ferromagnetic film

$$J$$
$$M$$
$$H_k$$

easy axis

**ZERO EXTERNAL
FIELD**

$$M$$
$$\theta$$
$$J$$
$$H_k$$

easy axis

**EXTERNAL
APPLIED FIELD H**

resistivity
change
$$\rho - \rho_o$$

$$\rho = \rho_o + \Delta\rho \left[1 - \left(\frac{H}{H_k}\right)^2 \right]$$

applied
field

$$H_k \sim 5 \text{ Oe}$$
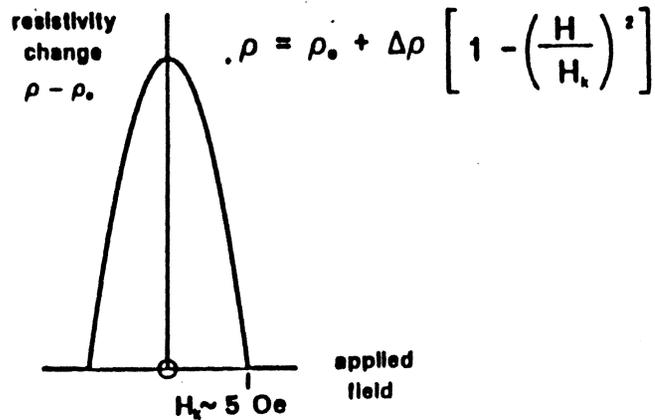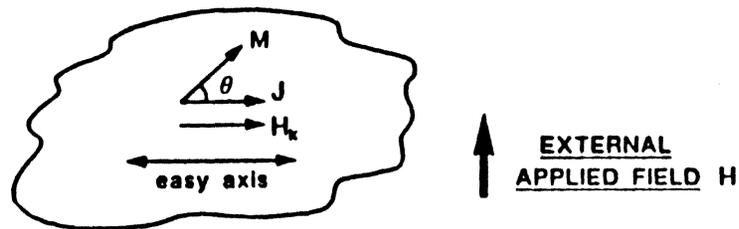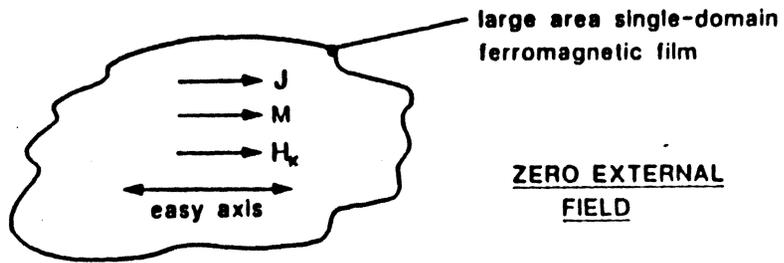
Figure 1.   The magnetoresistance effect.

high conductivity
lead

$$\downarrow I$$ $$\uparrow I$$

$$\rightarrow I$$

nonuniform
M

easy axis

$$h \approx 5\ \mu m$$

APPLIED FIELD (H)

patterned
ferromagnetic
film

High demag
~100 Oe
higher at
edges
∴ Center saturates
first.

$$\frac{\rho - \rho_o}{\rho_o}$$

$$\approx 2.5\%$$

**SENSOR
RESPONSE**

sensor
output

"bias" field ≈ 100 Oe

H

applied
field
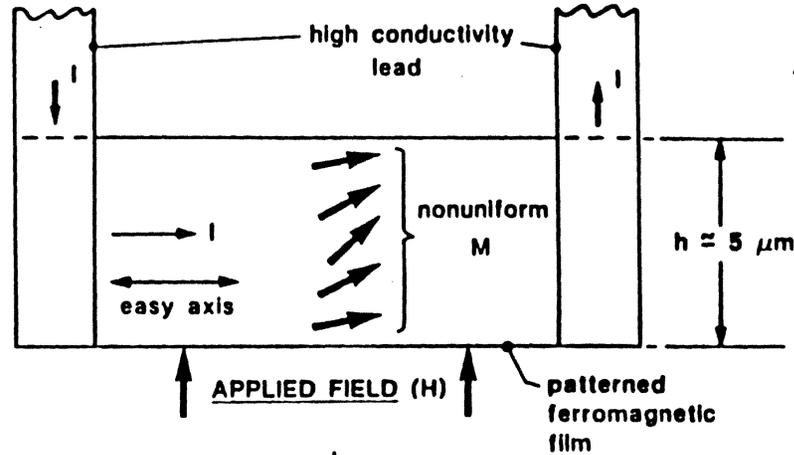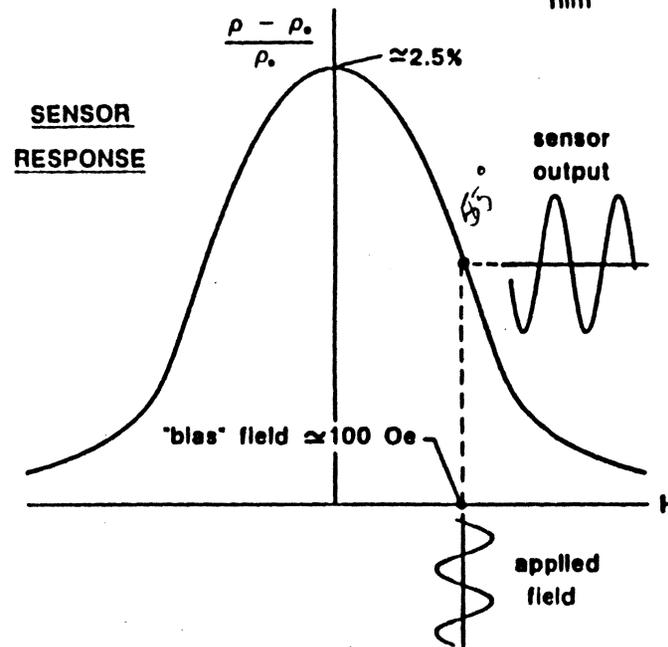
Figure 2.   The magnetoresistive field sensor.

* This is addition of 5 Oe field in easy axis to
eliminate Barkhausen

5

$$\rho = \rho_0 + \Delta\rho \cos^2\theta$$
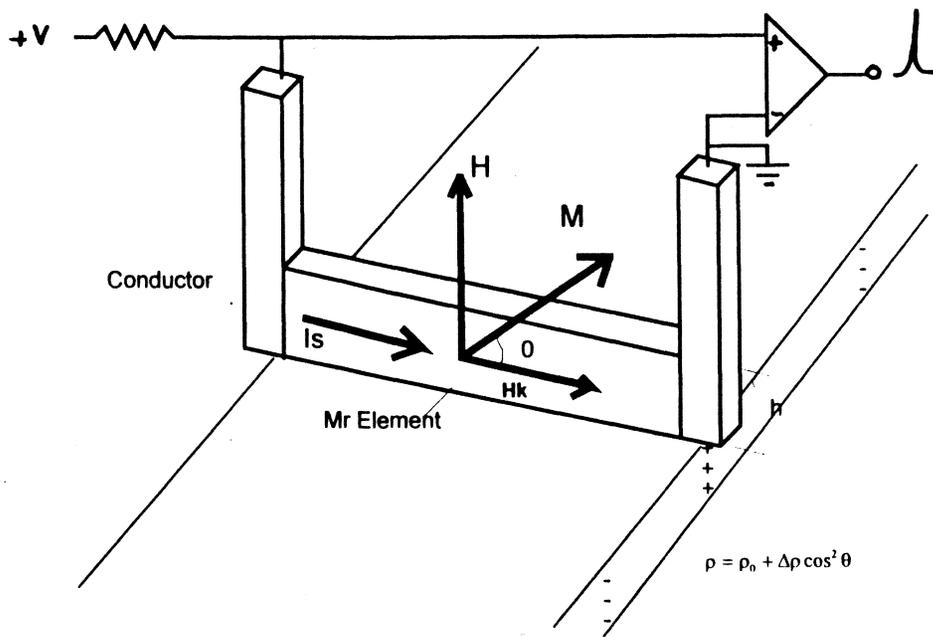
Figure 3. The unshielded MR sensor for magnetic recording applications.

MR Current Density = 6.4×10^6 A/cm^2

Tape Speed = 1 m/sec
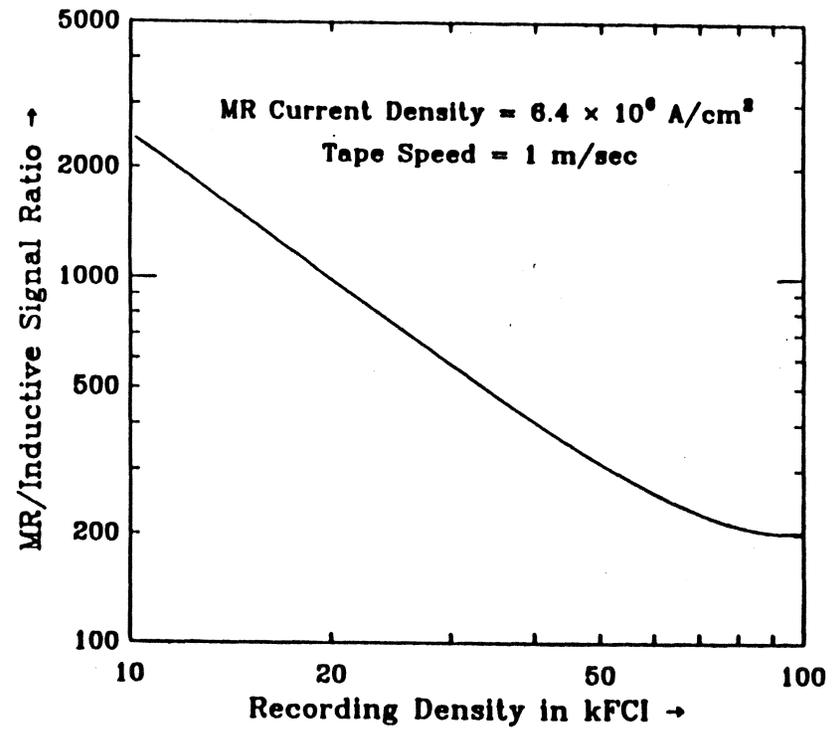
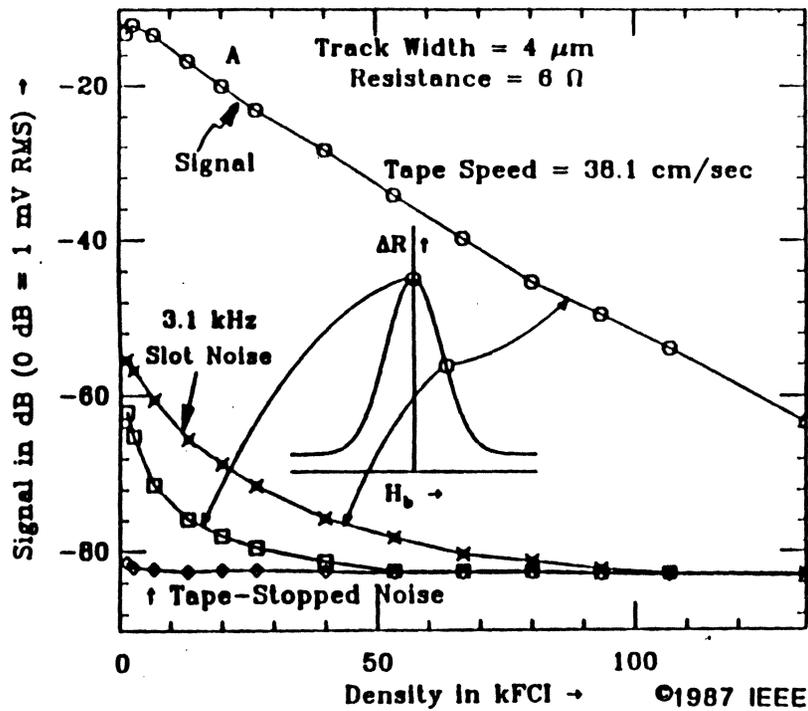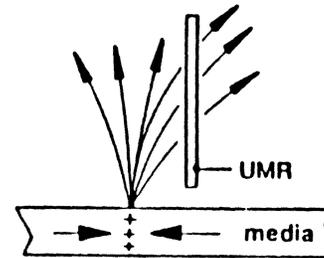Figure 4. Comparison of UMR and inductive signal levels as a function of recording density.

Courtesy of F. Jeffers

Figure 5. Signal and noise performance of a 4 μm trackwidth UMR.

- UMR responds to flux from transition over its entire height
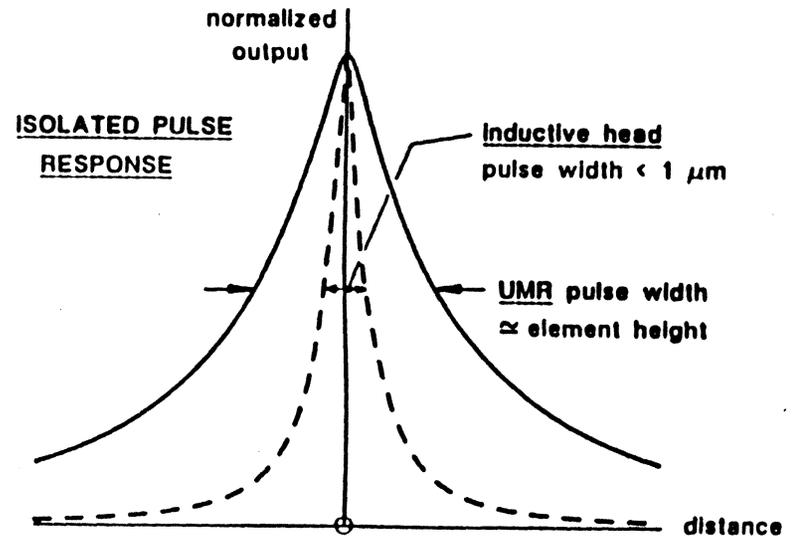 → broad isolated pulse
  → poor resolution

Figure 6. Linear resolution of the UMR.
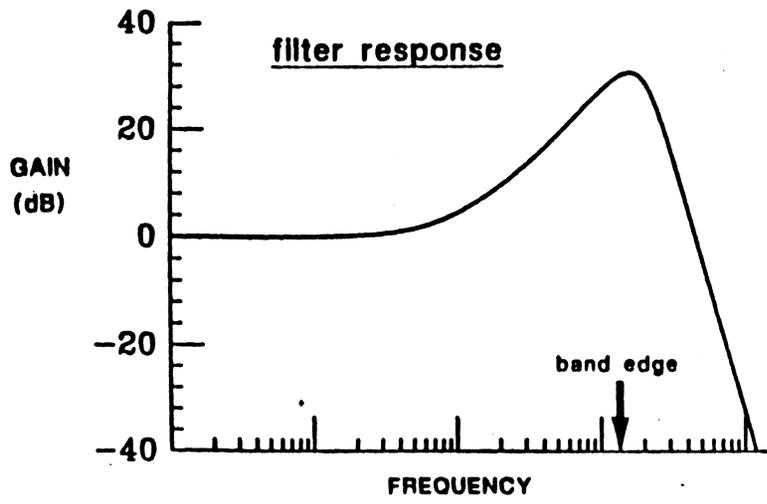
Figure 7.   Linear resolution improvement
by electronic filtering.
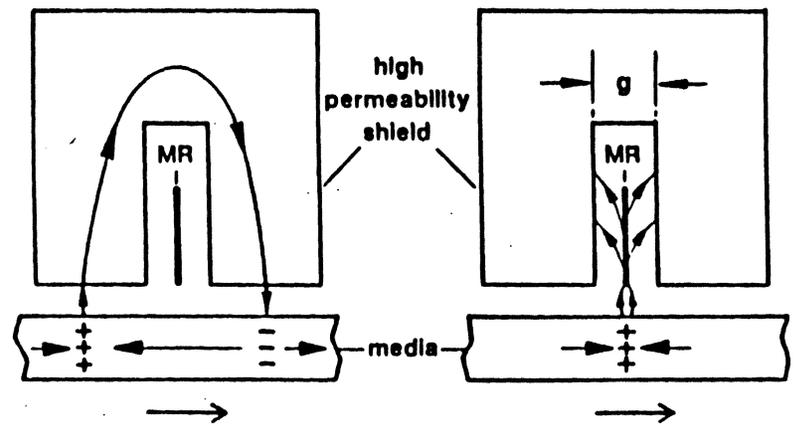
• Shields shunt long-range flux away from MR
→ slims isolated pulse

Figure 8.   Linear resolution improvement by shielding.

43

Why is 45° the best bias?

$$\Delta\rho = \Delta\rho_{max} \cos^2 \theta$$

$$\frac{d(\Delta\rho)}{d\theta} = -\Delta\rho_{max} \sin 2\theta \qquad => \text{Max for } \theta=45$$

What does sensitivity function depend on?

Apply a vertical field

$$H_a = H_{bias} + H_{sig}$$

Total Energy

$$E = -\overline{M} \bullet \overline{H} + \frac{1}{2} M_s H_k \sin^2 \theta + \frac{1}{2} M_s H_D \sin^2 \theta$$

$$= M_s H_a \sin \theta + \frac{1}{2} M_s (H_k + H_d) \sin^2 \theta$$

Find Equilibrium $\frac{\partial E}{\partial \theta}$, and $= 0$

we find $\sin \theta = \dfrac{H_a}{H_k + H_D}$

expanding equ. 1

$$\Delta\rho = \Delta\rho_{max}(1 - \sin^2 \theta)$$

It follows that $\qquad \Delta\rho = \dfrac{\Delta\rho_{max}}{2} - 2\Delta\rho_{max} \dfrac{H_b}{(H_K + H_D)^2} H_s$

it can be shown that $\dfrac{d(\Delta\rho)}{dH_s} = -\dfrac{2H_b}{(H_K + H_D)^2}\Delta\rho_{max}$

for permalloy, $H_K \cong 5Oe$

$$H_D \approx 4\pi M_s \frac{thickness}{height} = \frac{200A}{2\mu m} = 100 Oe$$
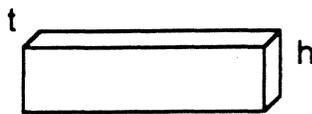
$\therefore$ Mr head sensitivity is largely dominated by demag field!

Reciprocity Theorem As Applied to Shielded MR Heads

Imagine that the MR head is wrapped around with a coil. Then the field produced is the superposition of two inductive heads:
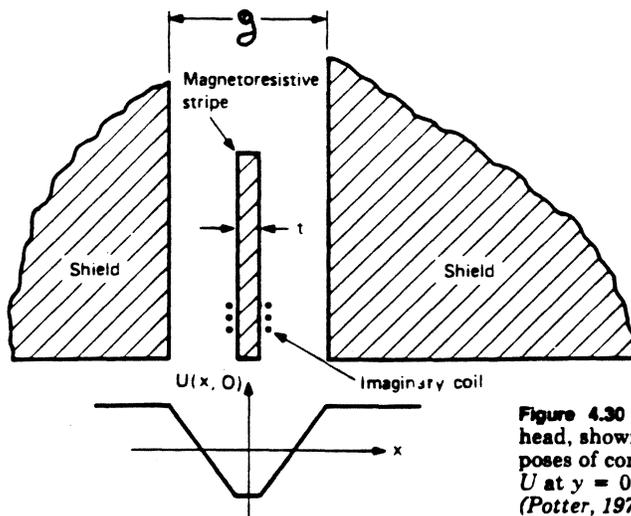

Figure 4.30 Cross section of a shielded magnetoresistive head, showing the coil that is imagined to exist for the purposes of computing the sensitivity function. Scalar potential U at $y = 0$ corresponding to Potter's model is shown below (Potter, 1974).

$$H_x(x,y) = H_x^*(x + \frac{g+t}{2}, y) - H_x^*(x - \frac{g+t}{2}, y)$$

where H_x^* is "Karlquist Field"

45

The magnetic flux into the MR head is

$$\phi(x) = \frac{\mu_0 W}{i} \; dx \; dy \overline{M}(x - \overline{x}, y) \bullet \overline{H}(x.y)$$

$$= \phi^*(\overline{x} + \frac{g+t}{2}) - \phi^*(\overline{x} - \frac{g+t}{2})$$

where

$$\phi^*(x) = \frac{\mu_0 W}{i} \; dx \; dy \overline{M}(x - \overline{x}, y) \bullet \overline{H^*}(x.y)$$

For sinusoidal magnetic transition $\qquad M_x = M_0 \sin kx$

We have for Karlquist recording head

$$e_x^* = -\mu_0 W V M_0 \frac{H_g g}{i} k \delta e^{-kd} \frac{1 - e^{-k\delta}}{k\delta} \frac{\sin(kg/2)}{kg/2} \cos k\overline{x}$$

- -

$$= V.K$$

$$= V.K \cos k\overline{x} = \frac{d\phi^*(\overline{x})}{dt} = \frac{d\phi^*(\overline{x})}{d\overline{x}} V$$

$$\phi^{(\lambda)} = e^*(\overline{x}) \sin \frac{k(g+t)}{2} \times \frac{2}{kV}$$

Note that $\phi(\overline{x})$ is independent of velocity V.

What is the MR voltage output?

We had $\quad \Delta\rho = \dfrac{\Delta\rho_{max}}{2} - 2\Delta\rho_{max}\dfrac{H_b}{(H_K + H_D)^2}H_s$

Signal Flux ϕ within the stripe
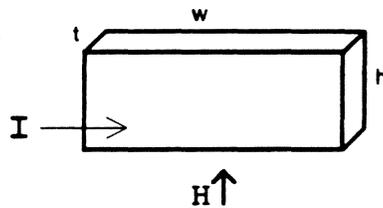
$$\phi = B \cdot tw = \mu\mu_0 H_s \cdot tw$$

$$= \frac{M_S}{H_K + H_D} \cdot \mu_0 H_S \cdot tw$$

$$= \frac{M_S}{H_K + H_D} \cdot \mu_0 H_S \cdot tw, \text{ (since } \mu = \frac{M_S}{H_{Keff}} = \frac{M_S}{H_K + H_D})$$

$$\Delta\rho = \frac{\Delta\rho_{max}}{2} - \sqrt{2}\Delta\rho_{max}\frac{\overline{\phi(x)}}{\mu_0 M_S tw}$$

Now, ϕ is nonuniform, but $<\phi>_{avg} = \dfrac{1}{2}\overline{\phi(x)}$ if MR sensor h is small, and $\overline{\phi(x)}$ is the flux entering the MR stripe

$$<\Delta\rho>_{avg} = \frac{\Delta\rho_{max}}{\sqrt{2}}\frac{\overline{\phi(x)}}{\mu_0 M_S tw} \quad \text{(neglect const. term)}$$

MR voltage output is then

$$e(\bar{x}) = I\Delta R(\bar{x}) = j.t.h. <\Delta\rho> \frac{w}{ht} = Jw <\Delta\rho>$$

$$= J\frac{\Delta\rho_{max}}{\sqrt{2}} \frac{\phi(\bar{x})}{\mu_0 M_S t}$$

$$= J\frac{\Delta\rho_{max}}{\sqrt{2}} \frac{1}{\mu_0 M_S t} \cdot e^*(\bar{x}) \sin\frac{k(g+t)}{2} \cdot \frac{2}{kV}$$

What is the MR/Inductive advantage?

$$\frac{e_{MR}}{e_{IND}} = \frac{e(\bar{x})}{e^*(\bar{x})} = \frac{J\Delta\rho_{max}}{\sqrt{2}} \frac{1}{\mu_0 M_S t} \sin\frac{k(g+t)}{2} \frac{2}{kV}$$

$$\approx \frac{J\Delta\rho_{max}}{\sqrt{2}\mu_0 M_S t} \cdot \frac{g+t}{V} \qquad (\text{since, } \sin\frac{k(g+t)}{2} \approx \frac{k(g+t)}{2}$$

Example:

$$J = 5\times10^{10} A/m^2, \Delta\rho = 2.5\%, \rho_0 = 7\times10^{-9}\Omega m$$

$$t = 200 A, g = 2000 A, \mu_0 M_S = 1T, V = 5m/s$$

$$\frac{e_{MR}}{e_{IND}} \cong 500!$$

MR HEAD EFFICIENCY

$$E = \frac{<\phi>}{\phi_{top}}$$

$$E = \frac{\tanh(D/2l)}{D/l}, \text{ where}$$

$l = $ 'Characteristic (or decay) length'- The distance required for the side

likage to the shields to reduce the MR element flux to $1/e$ of ϕ_{top}. $l = \sqrt{\dfrac{\pi M_s G t}{H_k}} \sim 60\mu"$

$G = $ gap length

$t = $ Strip thickness

- Low MR element reluctance and poor side leakage increases E.
- MR element height should be comparable to the decay length.
- Large values for characteristic length are desired:
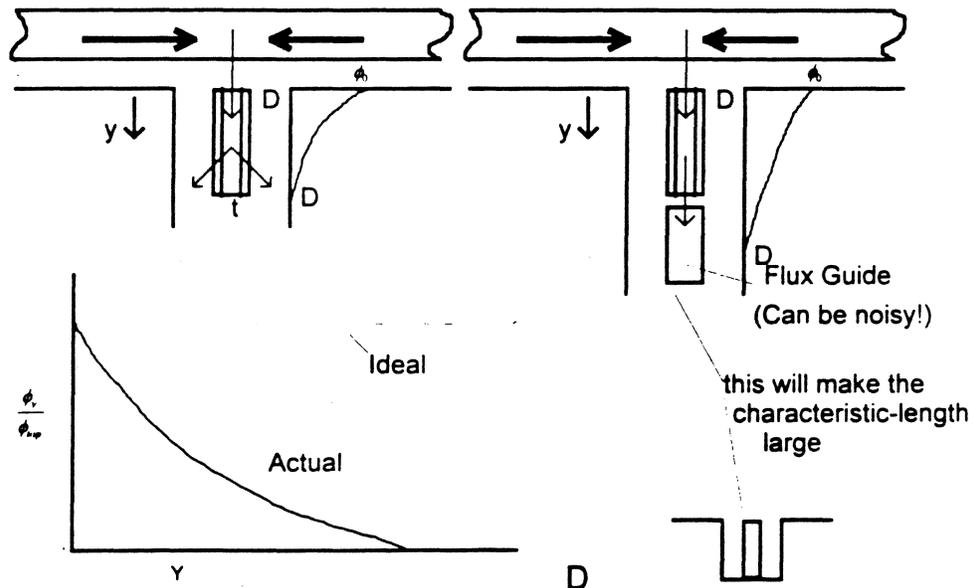
- For a MRH with $\dfrac{D}{l}$ small, $\tanh\dfrac{D}{2l} = \dfrac{D}{2l}$, then $E = 1/2 = 50\%$.
- SAL can shunt some field, ∴ MR thickness has to <u>be cut by two</u>.
- In an <u>unshielded MR</u> head, the spacing loss is the only source of magnetic field decay.

Biasing Schemes of M-R heads

The output of MR head is a function of:

      a) local fields in the stripe arising from the media.
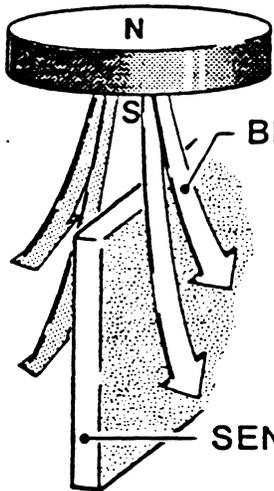   b) biasing field.
      c) shield effects.

Biasing is applied to provide maximum possible linear output (45° to current).
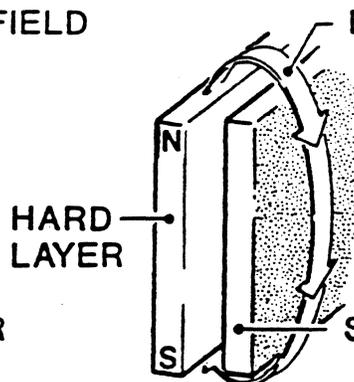However the method of application may vary.

① EXTERNAL MAGNET   ② HARD LAYER   ③ SOFT LAYER   ⑧ CANTED EASY AXIS
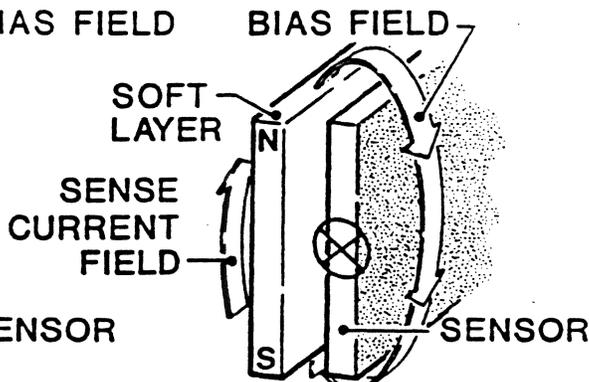
④ SHUNT CURRENT   ⑤ PLACEMENT IN GAP

⑥ BARBER POLE   ⑦ PAIRED SENSORS (2nd harmonic and thermal noise cancellation)   ⑨ EXCHANGE COUPLING

The above figure (F. Jeffers) shows various biasing technique that can be employed.

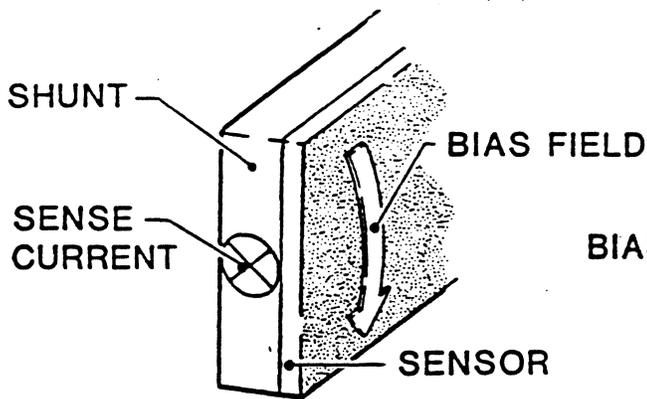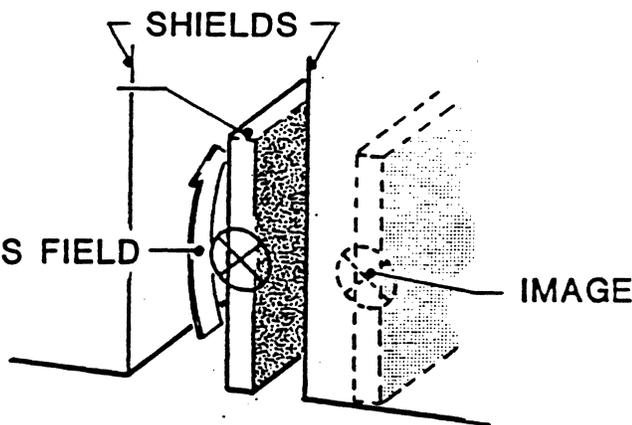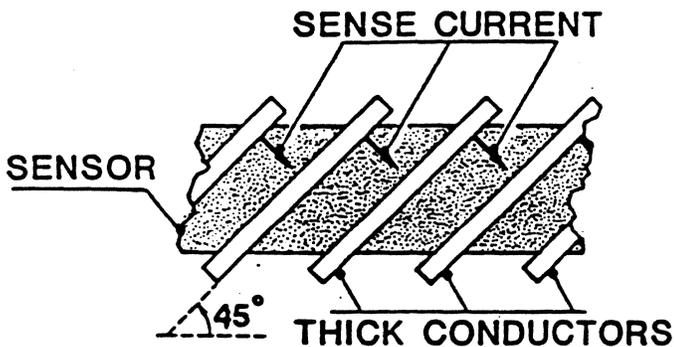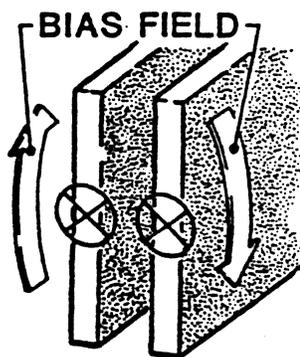# FIG. 30   MR HEAD BIAS TECHNIQUES

Courtesy of F. Jeffers

N

S

BIAS FIELD

SENSOR

① EXTERNAL MAGNET

BIAS FIELD

N

HARD LAYER

S

SENSOR

② HARD LAYER

BIAS FIELD

SOFT LAYER

N

SENSE CURRENT FIELD

S

SENSOR

③ SOFT LAYER

SHUNT

SENSE CURRENT

BIAS FIELD

SENSOR

④ SHUNT CURRENT

SHIELDS

BIAS FIELD

IMAGE

⑤ PLACEMENT IN GAP
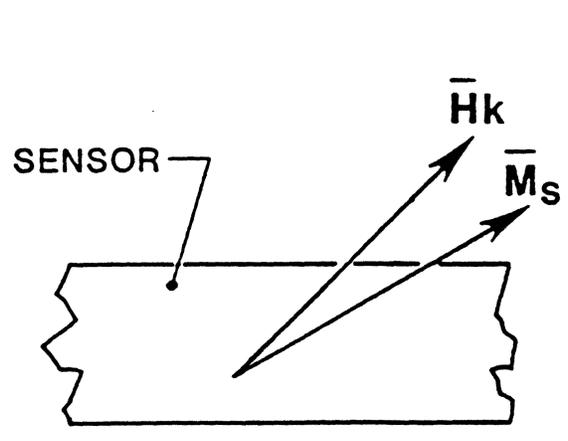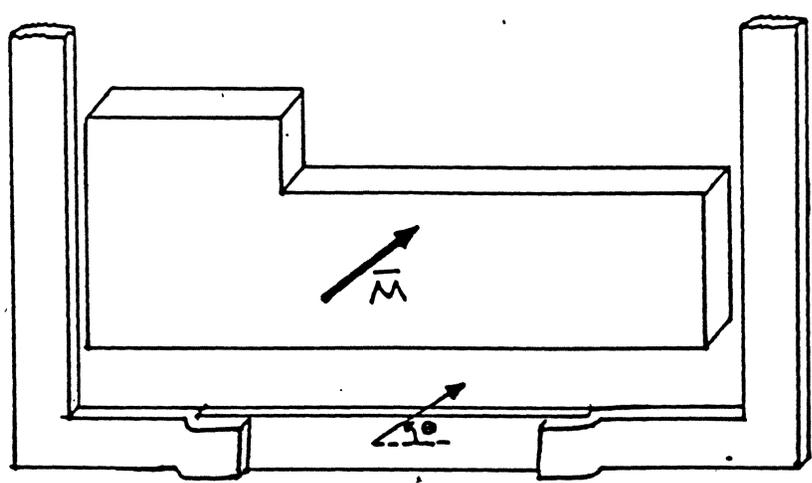
SENSE CURRENT

SENSOR

45°

THICK CONDUCTORS

⑥ BARBER POLE

BIAS FIELD

⑦ PAIRED SENSORS
(2nd harmonic and thermal noise cancellation)

FIG. 31   (MR Heads Bias Techniques Cont.)

SENSOR

$\bar{H}k$

$\bar{M}_S$

⑧ **CANTED EASY AXIS**

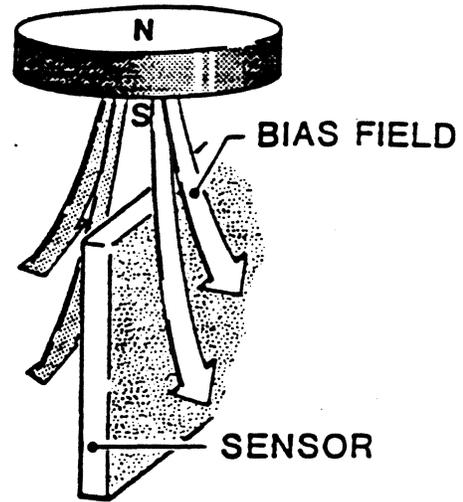MnFe ANTIFERROMAGNET

SENSOR

EXCHANGE FIELD

⑨ **EXCHANGE COUPLING**

$\bar{M}$

θ
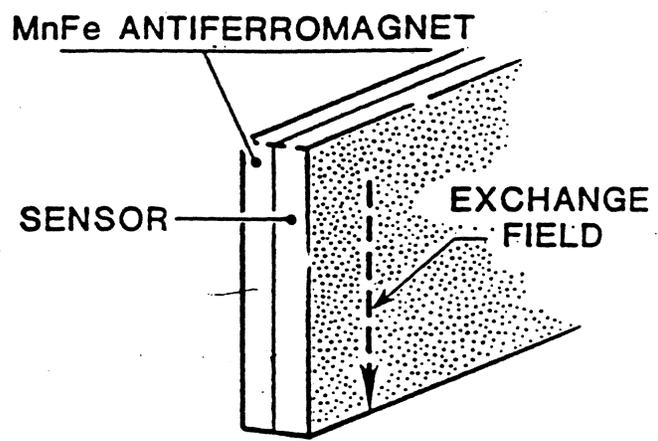
⑩ DEPOSITED HARD LAYER ABOVE MR

◆ External Magnets.

○ This was one of the first ways of biasing.

○ Problematic when shield are used.

○ External field liable to affect recorded data.

○ Complex to construct.

BIAS FIELD

SENSOR

EXTERNAL MAGNET

◆ Shunt current in adjacent nonmagnetic layers (shield needed)

○ This scheme uses the current in a conductor adjacent to the element to induce a bias field:

MR Stripe

bias conductor

H

Direction of bias current

No insulation necessary
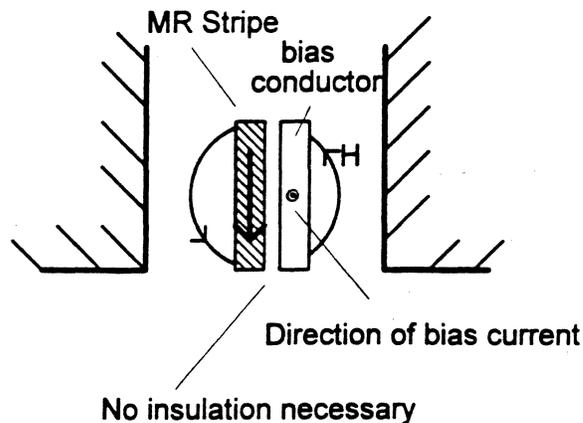
○ The two elements are in electrical contact (for ease of fabrication/configuration), therefore **common current supply**.

○ Their relative current levels is adjusted through their respective thickness and conductivities.

○ Problem with this design is **insufficient bias field** and *"Joule heating"* near the sensor.

Shunt Bias and ferrite Shields
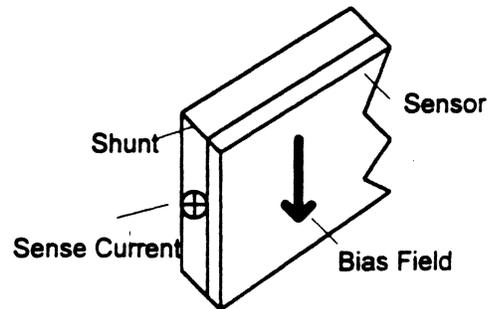
F. Jeffers

PRO

❏ Works for wide tracks and low to moderate densities (<40 KFCI).

CON

❏ Shunt lowers $\Delta R \, / \, R$ and lowers maximum signal (~7dB)

❏ Low thermal conductivity of shunt material can affect thermal noise due to sensor heating.

❏ Low I_s and poor "*bias efficiency*" result in an underbiased sensor which further lowers signal.

❏ Underbias generates second harmonic distortion which requires _center tap_ and _bridge detection_. This **results in a center dead zone** and limits maximum track width.

❏ In case NiZn ferrite shield are employed, its low $(125° C)$ T_c may cause effective gap to increase at high sensor power.

❏ NiZn develops a dead layer of 50-100 nm when run in contact with smooth tape. This can affect signal and resolution.

❏ NiZn wear rate is high, reducing head life.

51·2

◆ 'Soft' and 'hard' adjacent layers (SAL), (HAL)

○ SAL biasing calls for the placement of a thin, electrically insulated soft magnetic film adjacent to the MR element:

Electrical Insulation

Soft Bias Film   MR Sensor
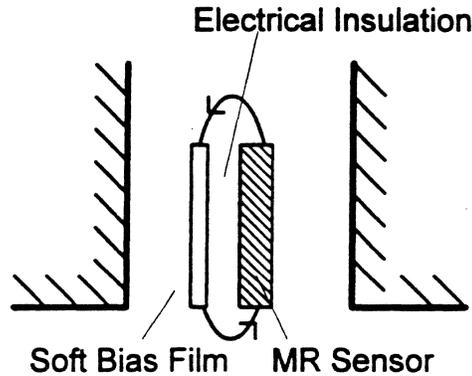
○ The current in the MR element induces a field in the **magnetically soft** layer. **This field is magnetostatically coupled back into MR element**.

○ If this current is chosen right, the SAL will saturate, **making the bias field independent of the sense current** and **amplitude of** fields from the medium.

○ The bias field must be large enough to rotate average magnetization of the sensor **by 45°**.

○ The soft layer can help to **offset the effects of demag fields**.

○ SAL can be made of *amorphus* and, therefore, **high resistivity** alloys such as **CoZrNb** and **CoZrRe**. Therefore, shorts are not as much a problem, but difficult to anneal to get stable Hk.

○**In case no insulation is used**, higher *resistivity* and *lower magneto-resistivity* than the MR element is essential.

○ Works well when the **insulator is very thin** (then risk pinholes!).

○ Shorts can also occur during operation.

○ With **HAL**, where hard magnetic material is used for biasing, *the distribution of magnetization produced is more uniform across the width of the sensor* than either **SAL** or **'shunt bias'** (this is welcome, since well-biased region near the edge of the sensor where the media signal is greatest is required).

○ Also in HAL, the spacer between the 'permanent magnet' and MR has to be at least *75 nm to avoid Barkhausen noise*.

○ Here, too, pinholes in insulator can cause local exchange coupling.

○ The **HAL** *must have high coercivity to resist signal field*.

◆ Asymmetric placement of the sensor element in a magnetic gap.

○ The resulting bias here can be considered to result from sensor current being "imaged" in the high permeability head.


Shields

MR

Image
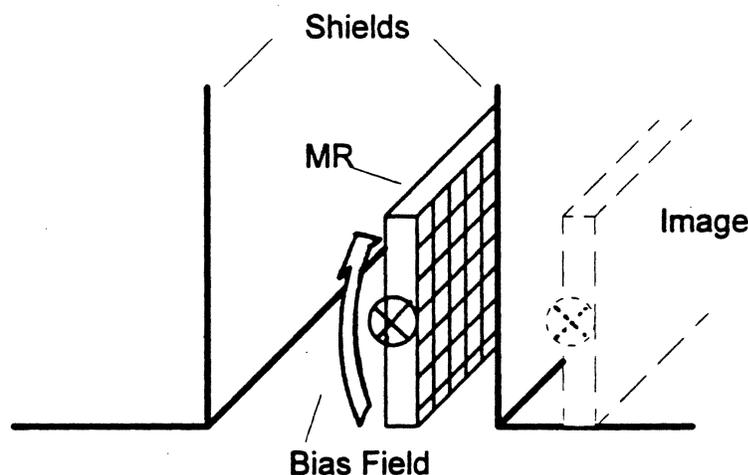
Bias Field

<u>Problems</u> : Bias provides **asymmetrical output.** Also **small bias field.** than a pure shunt bias.

<u>Good points</u>: <u>Does not suffer a loss of signal from shunting</u> effect of bias conductor, <u>nor is the Joule heating as great</u>.

◆ Rotation of current by "barber pole" conductor layer placed on the sensor layer (Canted Current).

In this mode to obtain linearization, the direction of magnetization is not altered. *Instead the current direction is effected* through adding **highly conductive bars** *at an angle to stripe*, forcing the current to pass segment of MR element in a direction normal to bars.
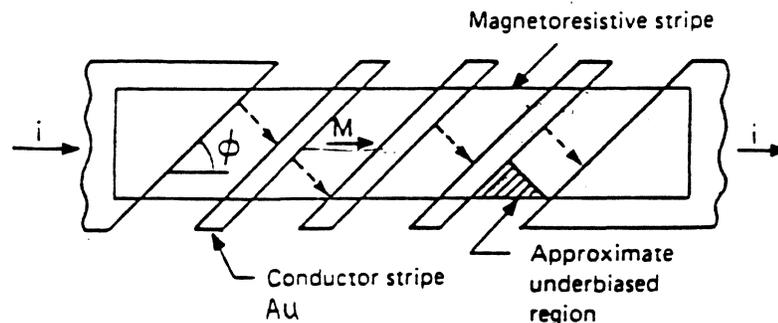
❏ Barber pole **conductors reduce effective track width** <u>by a factor of two</u>. *Intrinsic sensitivity is also twice as small.*

Only in a small area near the top and the bottom of the stripe (see above fig.) will the current direction remain close to the magnetization direction. This gives rise to **"quadratic response"** (this is somehow reduced by increasing the angle).

<u>No thickness-matching</u> problems as encountered by SAL and dual stripe heads, better linearity than shunt bias. Also, the conductor stripes themselves <u>give rise to additional fields</u>, further improving linearization.
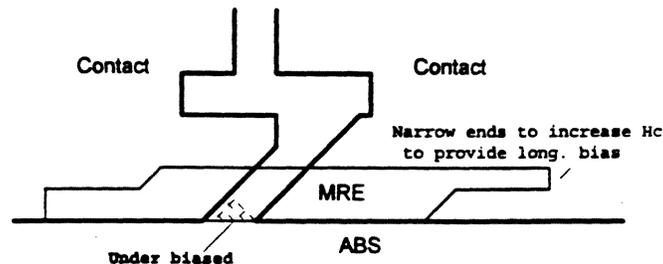Furthermore, the structure is <u>simple to construct</u> since no additional composite material is required.
The **conductor stripes should be narrow** to maximize signal amplitude associated with given track width, and the **uncovered area of the sensor should be narrow** to limit under biased sensor area (photo-lithography problem).

❏ Bias angle is **zero at sensor edge,** which reduces high density signal.

Bias is OK at low I_s . **But high I_s pushes bias angle off 45 degrees, which increases distortion.**

<u>54</u>

Slanted Contact (SC) Biasing

O This is a variation on the 'Barberpole' theme

O It is very simple to construct

O This design caters for very narrow tracks

O Narrowing the ends gradually increases the Hc so high that the structure is stabilized in a single domain state, hence, <u>no need for longitudinal bias</u>.

O It has a large *'dynamic range'* - i.e. resistance change is a linear function of field.

Disadvantages:

▼ The low current angle tends to produce underbiased regions. ∴ the read gap has to be chosen to provide additional biasing trough shield image fields.

● The long tail to the left is caused by the underbiased region. It is a disadvantage at high track densities, since it **increases cross-talk** and, the main drawback, **complicates servoing**.

Reader scan of a written track. Microtrack profile that reveals the read sensitivity function (RSF).

Juan J. Fernandez-de-Castro, Peter K. George
Seagate Technology, 7801 Computer Ave. So.,
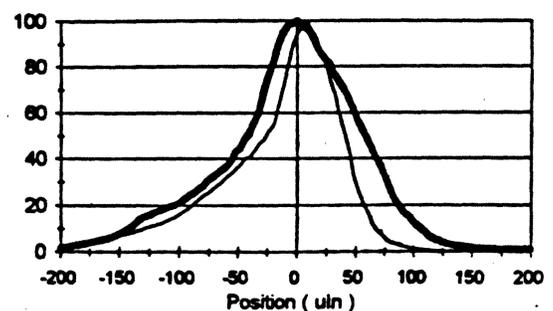
◆ Canted easy Axis
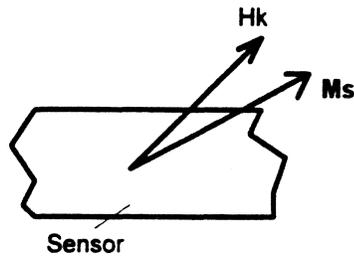
Sensor

○ Here the easy axis of Ni-Fe is made to lie at an angle to the stripe.

○ Not practical, since it requires an MR stripe with very high H_k to counter demagnetization.

◆Exchange-coupling (EC) bias (TbCo, FeMn).

○ Here, the Ni-Fe sensor is exchange-coupled at **the atomic level** to an Fe-Mn or similar **antiferromagnetic film**. Mr layer then experiences a uniform field of ~50 Oe.

Exchange Material

Sensor

Exchange field
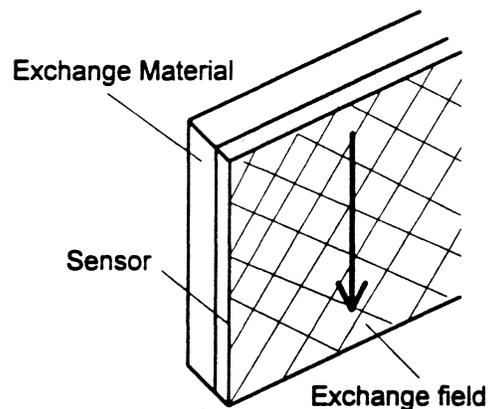
○ Just like *HAL*, this technique poses material science problems such as magnetic properties of EC media must be *stable, reproducible and free of local inhomogeneities*, which can cause *Barkhausen noise*.

○ It is often used for longitudinal biasing, to reduce Barkhausen noise.

❏ H_{ex} can serve to bias sensor, but hard to control **because effective bias filed varies with MR thickness**.
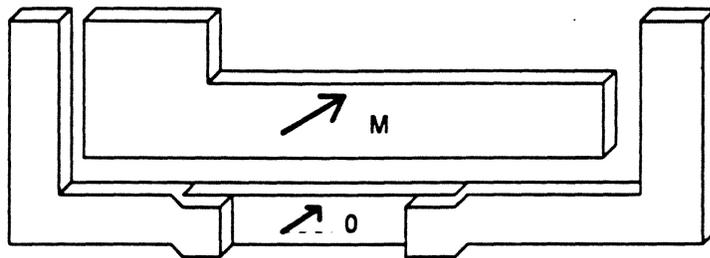
❏ H_{ex} **can have easy axis component** to eliminate *Barkhausen* noise.

❏ H_{ex} varies with temperature.

❏ Exchange material are prone to corrosion.

❏ Exchange layer somewhat <u>lowers</u> $\Delta R / R$.
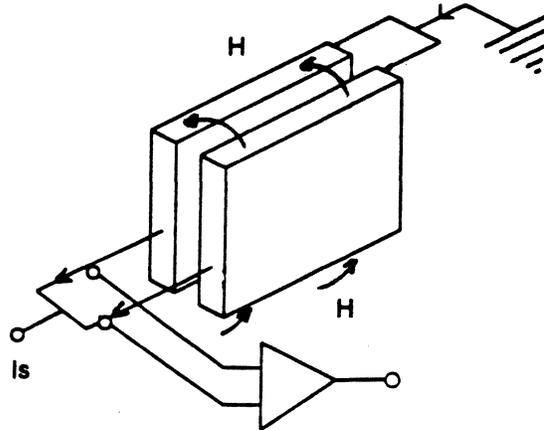
◆Deposited Hard Layer Above MR

❏ This is a variation on the *'external magnet'* biasing scheme.

❏ Permanent magnet must have **high coercivity** to resist signal field from media.

◆ Paired Sensors - *'Dual Stripe'* (DSMR), *'Dual MR'* (DMR) And *'Gradiometer'*

○ This has the features of *SAL* combined with **shunt current**.

○ Two identical MR sensors are separated by a few hundred Å, with currents flowing in either the same or opposite direction, depending on the type of head.

○ Thus, *both current and magnetization of each sensor contributes to the biasing field magnetizing its neighbor*.

○ The differential amplifier provides the output as well as a **common mode rejection of noise**.

○ It is fairly difficult to fabricate (the sensors have to be *identical*; in case of insulated sensors **pinholes** are a problem).

Dual MR Head Configurations

two most common configurations are _**dual head**_ and _**gradiometer**_:

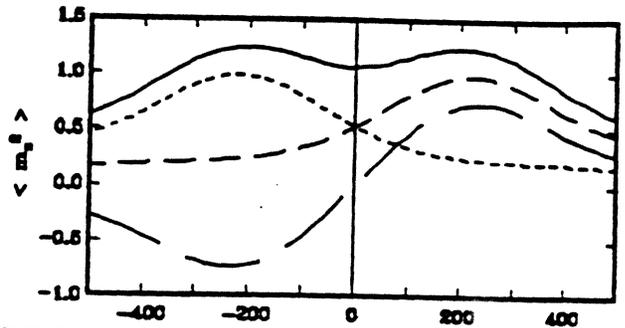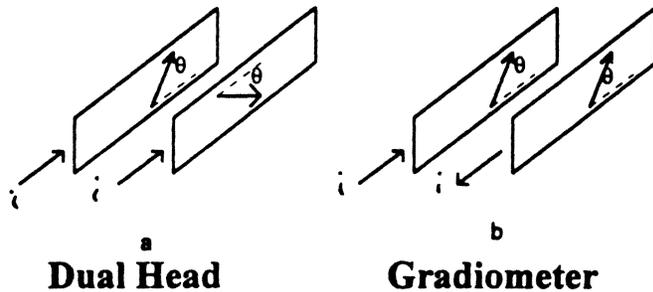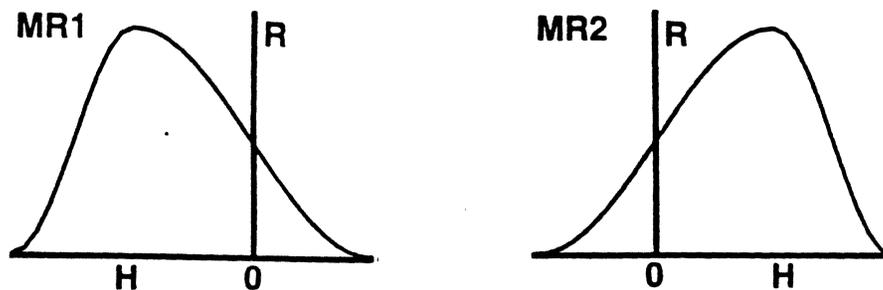**Dual Head**   **Gradiometer**

FIG. 7. Transfer curves for DMR (solid), DS (long dashed curve), and each individual MR film (intermediate dashed curves).

❑ In 'dual head' the current is applied in the same direction. The elements are ∴ _magnetized asymmetrically._

❑ Playback flux increases the resistance in one element and decreases it in the other:

❑ A voltage ∴ results only from field produced by the media that are spatially _asymmetrical_ **w.r.t. the structure** (e.g. a longitudinal magnetization transition whose center is positioned exactly between the elements produces no replay voltage- N. Bertram).

❑ The 'dual head is spatially sensitive in an **unshielded configuration**.

❑ _Dual MR_ is useful for high density applications (because of **absence of gap null**, also **shield-to-shield shorting not a problem**).

◯ In the **gradiometer** head the resulting current fields bias the element magnetization in the same direction. A replay flux ∴ yields a **common change in the resistance**. However, because the current is in opposite directions, the **net voltage** across the two elements cancels for symmetric replay fields (such as **thermal asperity** noise).

Advantages of Dual-Stripe MR

- Reduced Asymmetry

- Reduced base-line shift
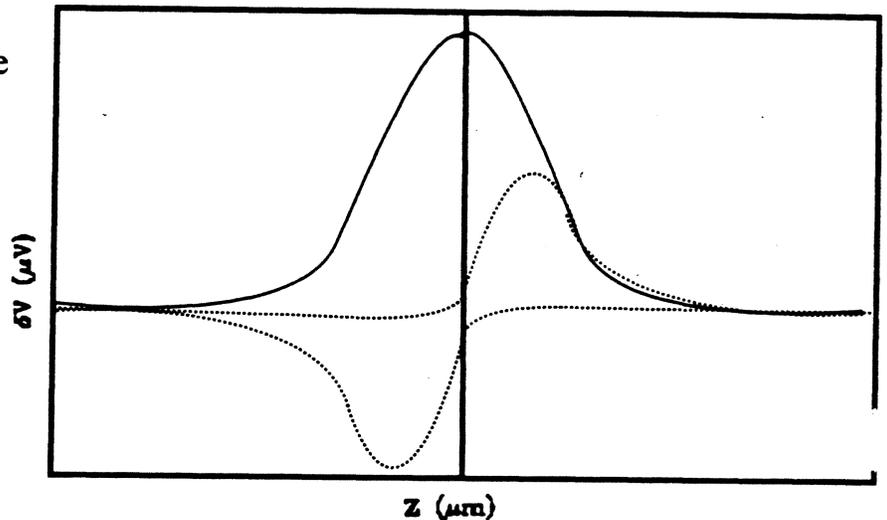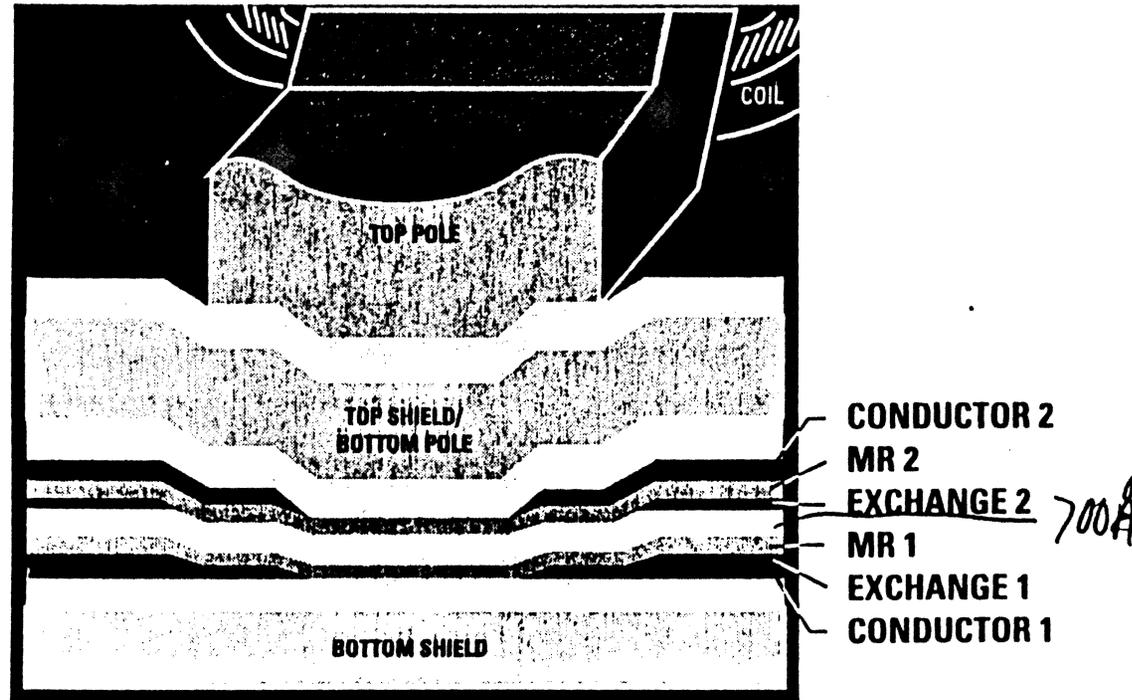
- Better off-track performance

FIG. 10. Off-track profiles for DS (solid) and each individual MR film (dashed curves).

- High, linear output.

- Pre-amp can be designed with one side of each MR element held at ground potential. This means that the disc and the drive case also can be held at ground. Thus special electrical isolation mountings are notrequired.

- Immunity to thermal aspirities

Problems Concerning Dual-Stripe MR

- For high frequency applications, the stripe separation needs to be small, difficult to keep the stripes insulated.

- The stripes need to be absolutely identical.

- Manufacturing difficulties

Dual Stripe Read/Inductive Write Head Design

Labels on figure: COIL, TOP POLE, TOP SHIELD/BOTTOM POLE, CONDUCTOR 2, MR 2, EXCHANGE 2 (700 Å), MR 1, EXCHANGE 1, CONDUCTOR 1, BOTTOM SHIELD

Write

- Shared bottom pole
- 0.5 μm write gap
- 8 turn coil
- TW = 4.5, 6.0, 8.0 μm

Read

- $g_1 = g_3 = 150$ nm, $g_2 = 70$ nm
- MR1 = MR2 = 25 nm
- TW = 4.0 μm
- Exchange recessed 2 μm

Dastek

Dual MR Heads (DMR)

This is two identical adjacent MR stripes separated by a **conductive** spacer.

- Although DSMR have signal advantages, for very hi-densities (>10GB/sq. in) the stripe separation between elements becomes <500A! rendering electrical insulation impractical. ∴ DMR are usefull since the current in the two stripes are in the same sense and *shorting not a problem*.
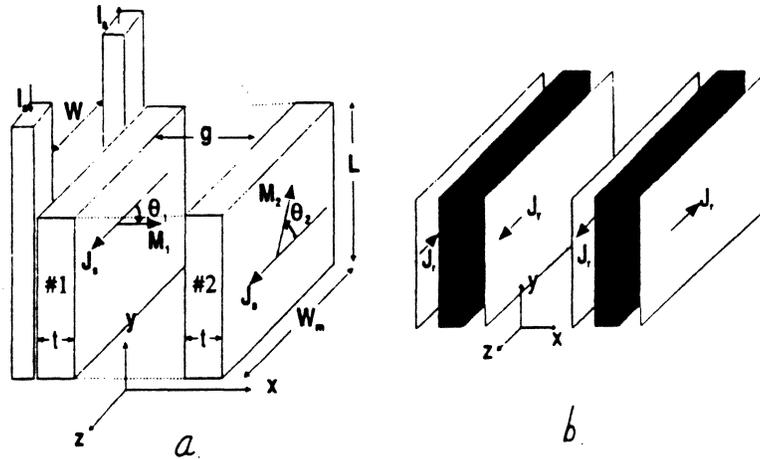
- It is self-biased.

- It is immune to electrical shorting between elements, and insusceptable to differential wear and accompanying spacing loss.

- It is simple to fabricate and very robust.

- Two MR elements are connected electrically in parallel, separated by a conductive spacer.

- The DMR sense current, I_s, flowing along Z generates biasing fields along Y of opposite polarity at either MR sensor.

- To avoid shunt losses of ~ 40%, one can use alternative higher resistivity gap such as NiCr or Cr-Si-O

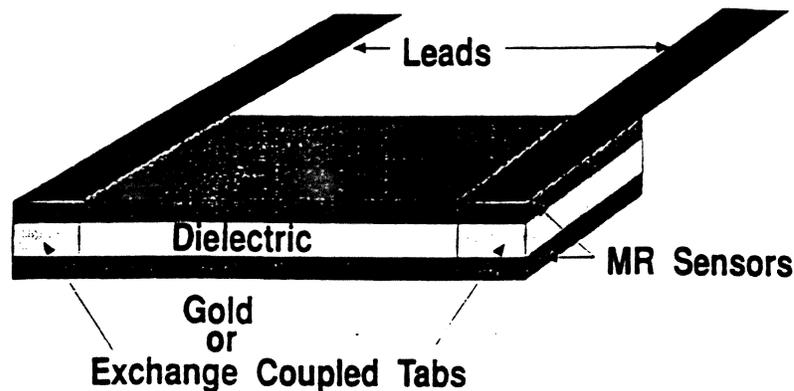FIG. 4 Illustration of two shunt-loss-free, "optimum" embodiments of a DMR reproduce head (described further in the text).
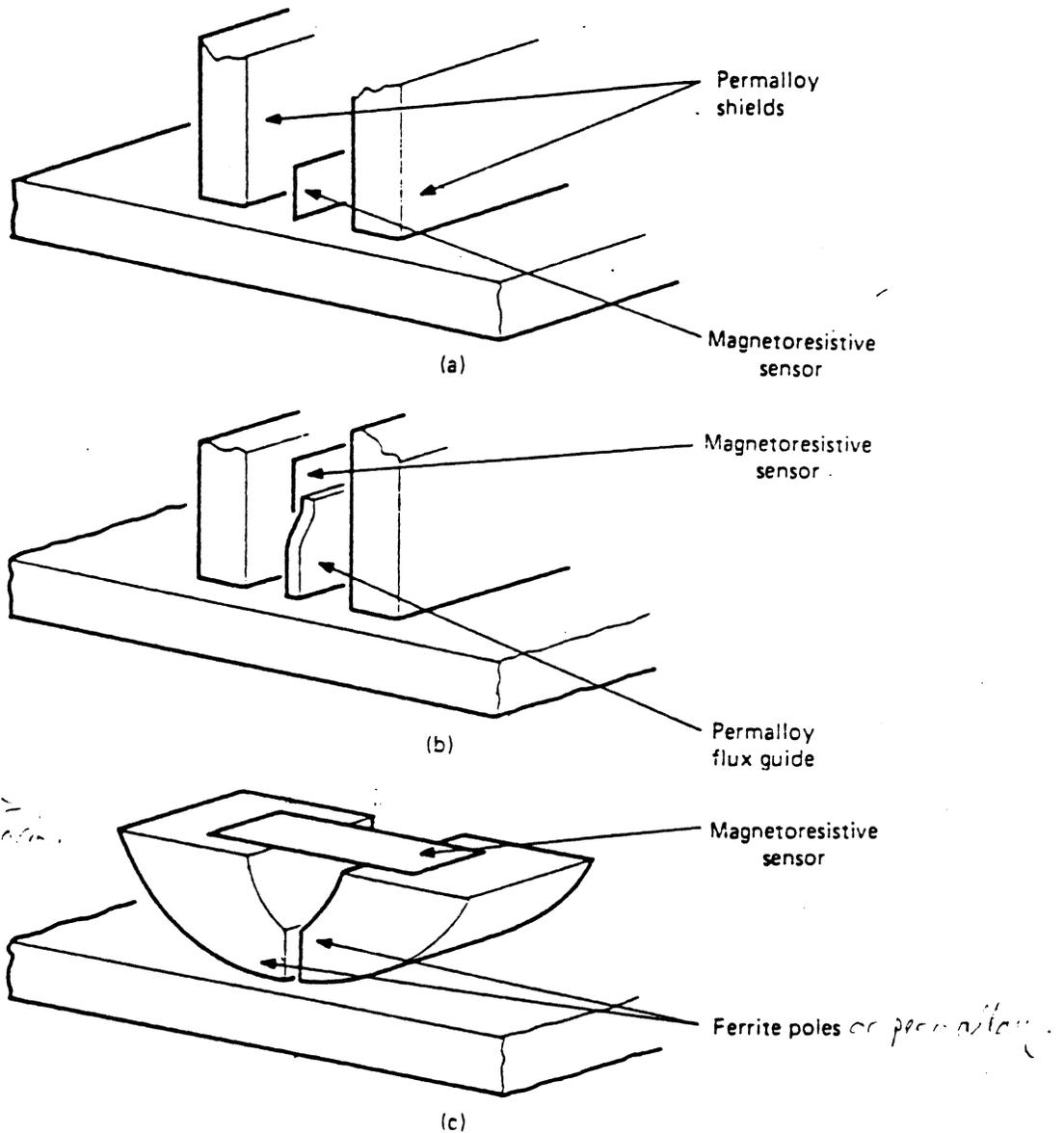
60

(a)

Permalloy shields

Magnetoresistive sensor

(b)

Magnetoresistive sensor

Permalloy flux guide

a conductor — is placed for feedback.

(c)

Magnetoresistive sensor

Ferrite poles or permalloy.

Figure shows various magnetoresistive head designs.
Magnetic feedback can be applied to (c) . See below

•*Permalloy shields* are placed on either side (a), or in series with the element
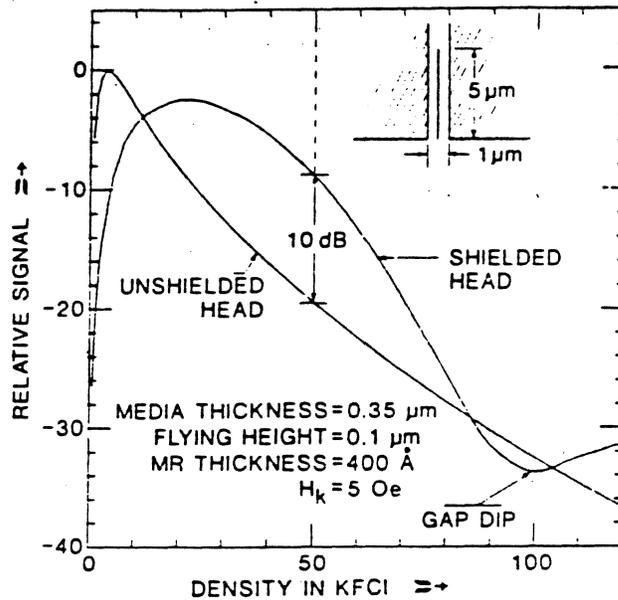(b & c) to improve resolution. (It responds to vertical fields, $\therefore$ can sense a
signal from adjacent bit).

Continued

Fig. Shielded and unshielded MR head response curve (F. Jeffers)

- The use of *flux guide* permits the positioning of MR element away from wear region.

- Using feedback *from* MR to reading field, it can be kept ~zero→reduce Barkhausen noise.

  This is done by placing a conductor near the element, carrying the read current...

- In *dual -element* read-write head designs, separate read and write are deposited on top of each other (*piggy-back* heads).

One particular design ... which is ... is amenable :
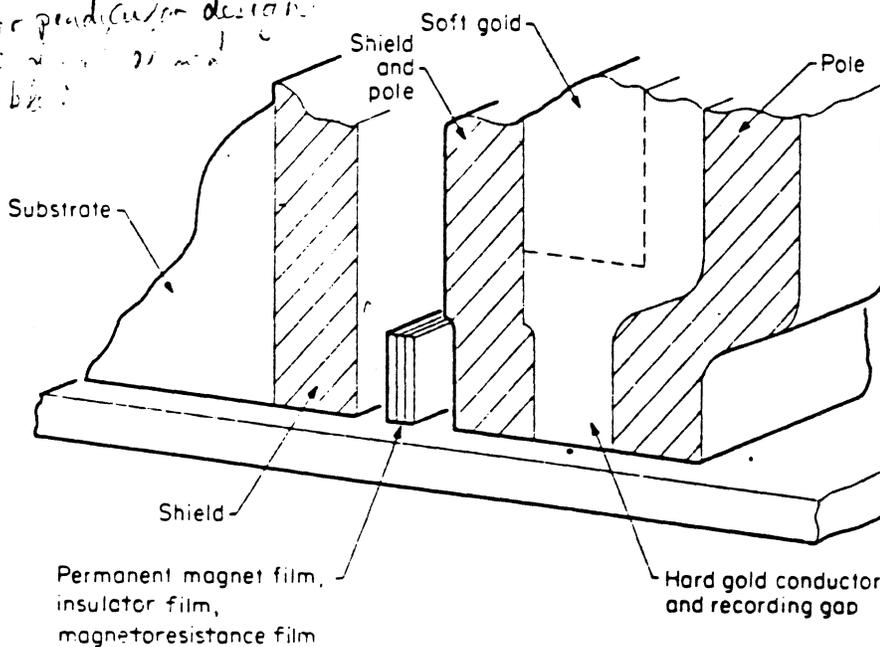
Fig. A *dual-element film head*: inductive write and magnetoresistive read (R. E. Jones).
Note that the center pole also acts as a shield. Difficult to construct (too many layers)

Some of the major advantages are:

♣ **The two elements can be optimized separately**.

♣ **Ability to read immediately after write**.

♣ Allows for tracking misregistration through wider write than read track.

Another design is the **_Yoke MR head_**: *uses No shields !*

GAP ── ┐
PERMALLOY
TOP POLE ─
TRACK WIDTH
FERRITE SUBSTRATE ─

ELEMENT LENGTH

HEAVY GOLD LEADS

PERMEABILITY

SENSOR

BIAS LINE
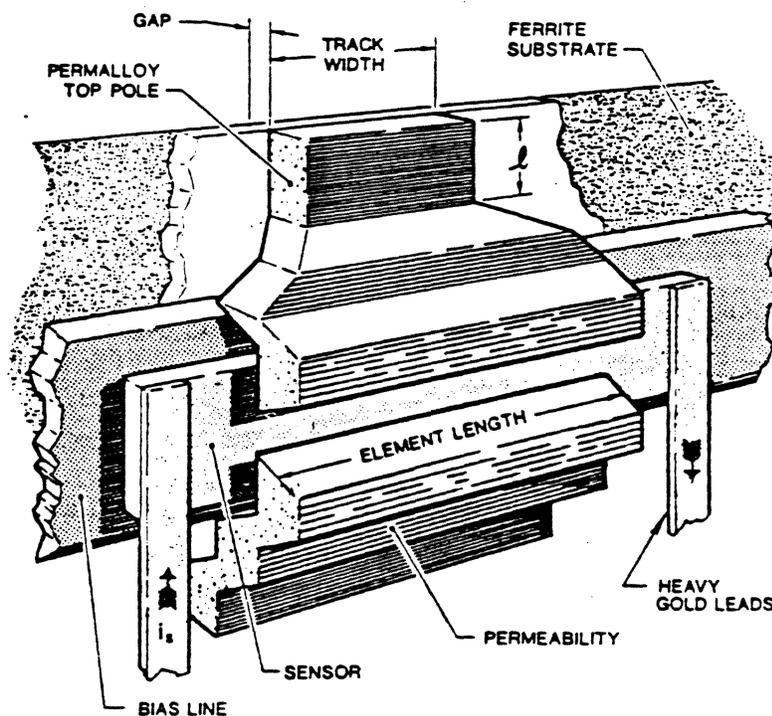
Yoke MR head. (Drawing not to scale.)

Figure shows one of the designs where MR element is remote from the gap (Jeffers).
Note that the *ferrite substrate is used as a pole* (to reduce the number of layers)

• **MR element away from ABS**, therefore less wear.

• **Capable of reading long wavelengths too**, since no shields are used.

• They have **more signal than inductive heads** at low media speed, *But less signal Than inductive heads"*
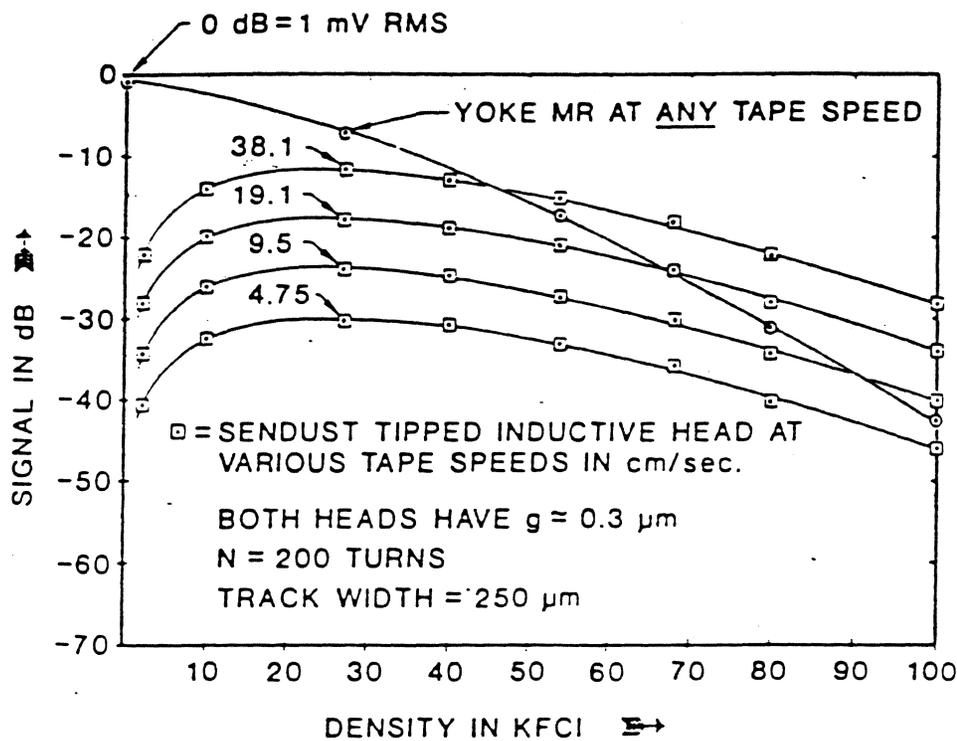
Yoke MR and inductive heads compared (F. Jeffers)

- Note that as the tape speed increases, <u>the signal advantage decreases</u>.
- Also <u>difficult to construct.</u>

The first MR head was IBM 3480. Feature:

> * Ferrite shields to solve resolution problems.
> * Transverse biasing was solved using *shunt bias*.
> * Still, thermal noise and Barkhausen noise was present (not detrimental).
> * A **thirty six track** head (3490) has recently been developed.

For disk drives:

> * Thin film heads are doing OK. (MR advantageous at >300Mb/sq.in).
> * Shunt biasing inadequate. Other schemes have to be employed.
> * Barkhausen noise much more severe.
> * Actuator mechanism used → misalignment of write and read element.
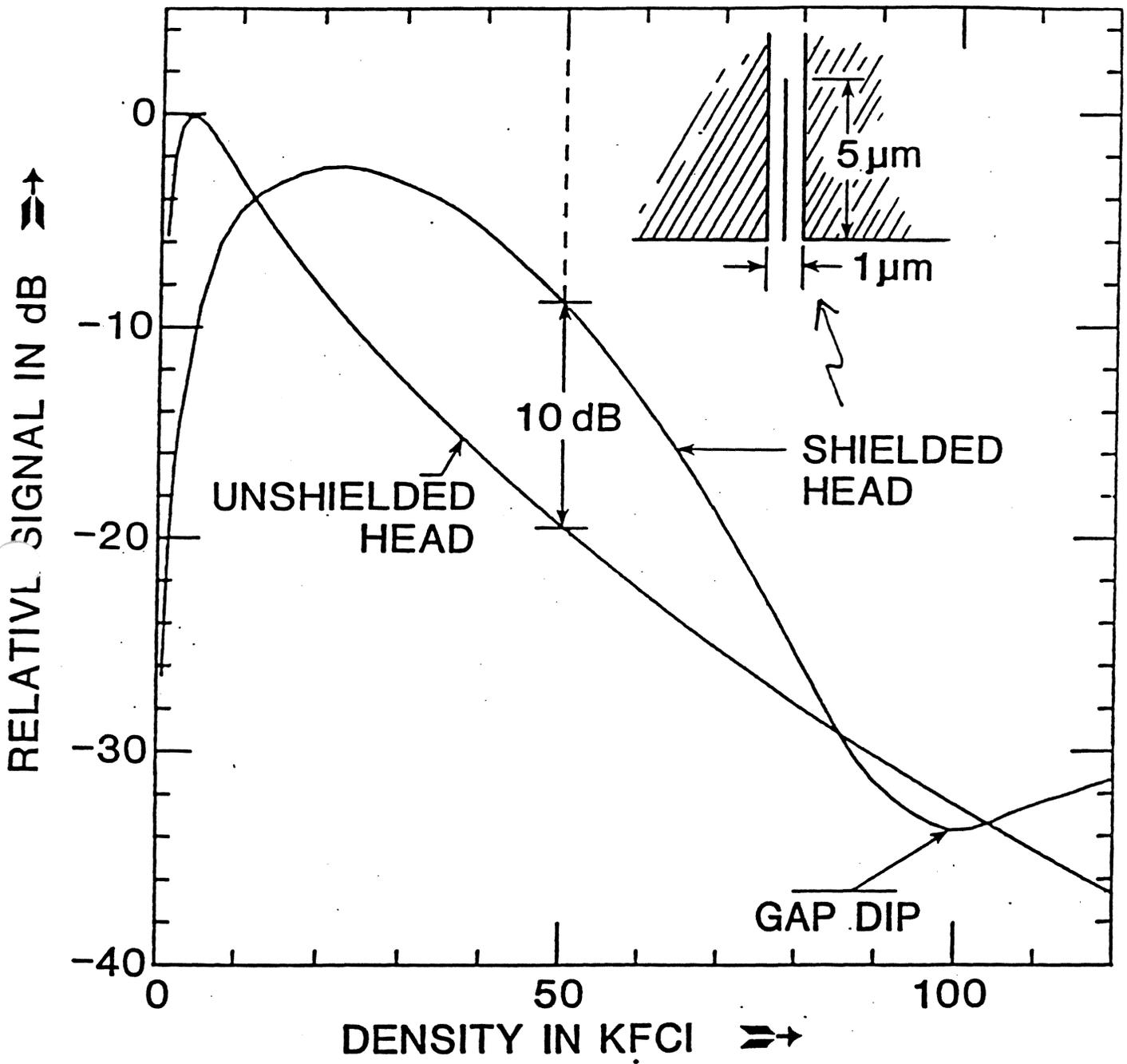
Comparison of shielded and unshielded
MR head response curves.(assumes both
heads have the same bias contour.)

SHIELDED MR HEADS

(F. Jeffers)

PRO

- <u>Resolution</u> is considerably improved

- When correctly biased, <u>midband</u> $(\lambda \sim G)$ <u>signal is ~ 10dB higher</u>.

- When there are shields, <u>the relative density response becomes less dependent on element height</u>. However, signal level still depends on element height.

CON

- <u>All inside -the-shields bias schemes are hard to control</u> and increase the risk of shorting to the shields.

- the small shield-to-shield spacing required for high density <u>puts a constraint on the biasing scheme</u>, and *'Exchange Coupling'* with its myriad problems, becomes the only viable option for longitudinal biasing.

- _Barkhausen_ noise from the shields may be a problem.

- As linear density increases (and the gap length decreases) shorting the shields becomes more likely, especially in contact applications where smearing occurs.

- For $V_s \sim 1V$, E between sensor and shield can be as high as 50KV/cm. Moisture on the head can cause burnout.

- Gap fields of several hundred Oe can be generated by the sense current and shields. This field can partially erase the signal or, at least, generate second-harmonic distortion during read.

- High density requires small gap spacing and lots of equalization which increases out-of-band noise.

- Deposited shields erode during contact use, causing separation loss.

Electrostatic Discharge Damage (ESD)

i) Electrothermal failure
Localized Joule heating within MR element
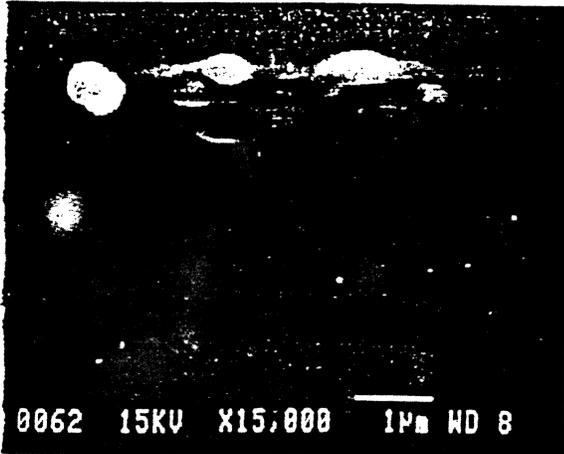
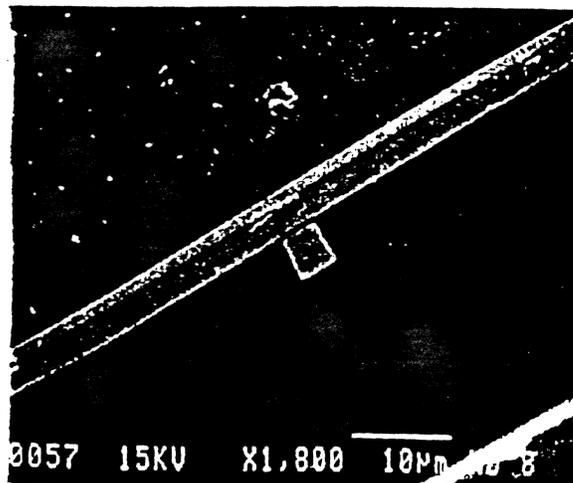ESD Electothermal damaged MR head .
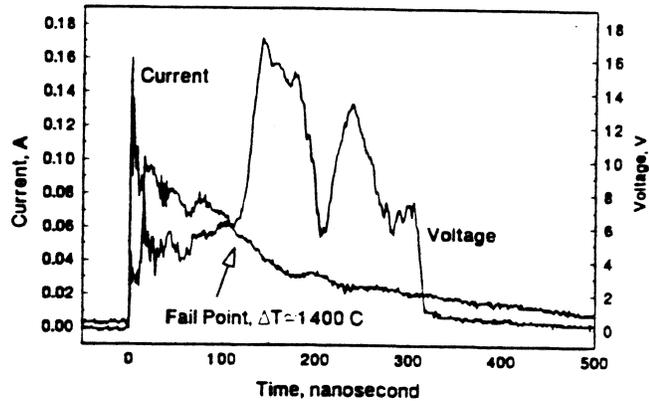
Current and voltage profiles during ESD.

After H. Tian

ii) Dielectric breakdown
Here, the shields are broken down and the MR element can be melted

ESD dielectric breakdown damaged head.

iii) 'Fatigue' mode
MR element or shield changes as a result of multiple discharge at lower level.

MR HEAD NOISE

I) THERMAL NOISE

a) The *'Temperature Coefficient of Resistance"* for NiFe is ~0.28%/ºC. The element can rise upto 20º in temperature during operation. Where the media serves as a *heat sink*, <u>intermittent contact between the head and the media</u> -due to particles etc.- can lead to spikes.

$$\frac{d\rho}{dT} \cong 0.28\% \, / \, ^{\circ}C, \quad \Delta T = 4^{\circ}C \rightarrow 1.2\% \quad \Delta\rho = \text{Max Signal}$$

b) Another source of thermal noise is **'frictional heating'** caused by hard dust particles dragging.

For these reasons **hard** substrates with **high thermal conductivity**, such as **sapphire**, are used.

II) RUBBING NOISE

Generated in materials with non-zero magnetostriction

$\Delta H_K \propto \lambda \Delta S$, where ΔS = magnetostriction const.

$\therefore \Delta S \rightarrow \Delta H_K \rightarrow \Delta Q \rightarrow \text{NOISE}$

• <u>Differential thermal expansion</u> can also lead to RN. This is reduced when **polycrystalline** materials are used - <u>random orientation leads to cancellation of magnetostrictive effect</u>.

Thermal Asperity Solutions

- Dual MR (VMR, Yoke MR, Flux guide)

- Recessed Pole Tip

- Use Smooth Media

- Increase Flying Height

- Use Signal Processing, Error Correction

- Use material with small TCR & large magnetoresistance

- Thermal characteristics of the element is important.

- Large element height is desirable (also good for efficiency).

III) *BARKHAUSEN* NOISE

Narrow T.W. => Large H_d => Domain Wall
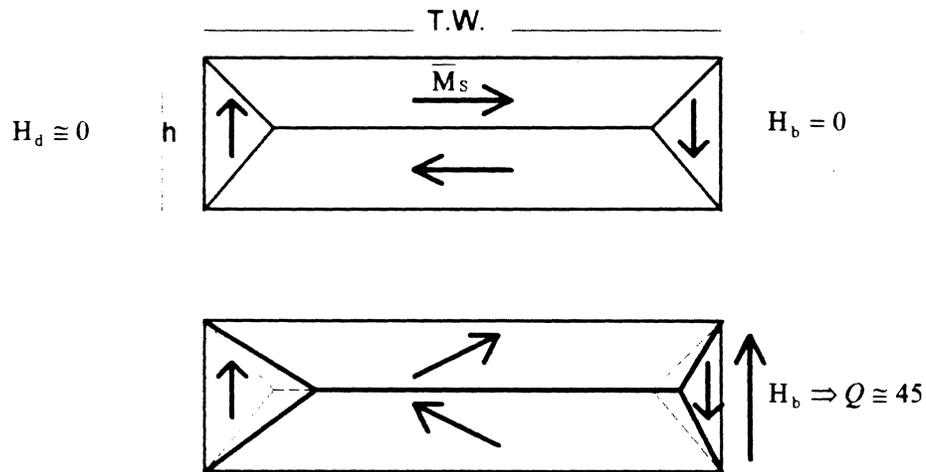
Large signal fields move domain walls at end
which **"snap"** over pinholes etc.
                    => Barkhausen Noise
Generally not a problem for T.W.>50μ, h~5μ, T~700μ.

Barkhausen noise is reduced through:

    I) Careful micromagnetic design.

    II) Use of multilayers.

    III) Longitudinal bias.

Longitudinal Biasing

- Application of longitudinal bias to reduce **Barkhausen** noise :-

  Barkhausen noise is caused by domains originating from either,

  I) *shape demagnetization* due to finite planar geometry of the sensor,
or
  II) from *material effects* such as dispersion of anisotropy easy-axis direction.

- There are **two** principle ways of suppressing this noise;-

  a) Reduce the longitudinal demagnetization field in MR element.

  I) Increase element length, or, magnetically through constructing various flux closure schemes to increase the effective **"magnetic length" of the element.**

  II) **Apply a longitudinal bias to create a single-domain state.**

- One way of generating this bias is to use *exchange biasing*.

  Here, a layer of antiferromagnetic material, i.e. FeMn, is deposited on top of NiFe sensor. As a result, a large *'exchange-bias field'* is created.

❏ b) Origin Of Barkhausen Noise In Magnetoresistive Heads

Opposite is the hard axis response of a 20x60 μm rectangular **unbiased** MR stripe as the field decreases from saturation (Decker & Tsang):

- D(H) => a relatively smooth curve is traced as **H**=> 0, with only a few Barkhausen Jumps.

- T(H) => this region is characterized by a a large No. of abrupt decreases in MR.

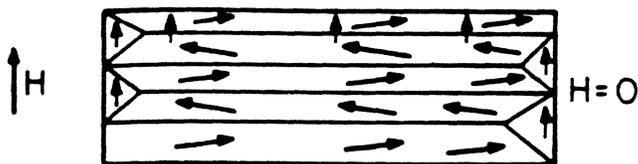- S(H) => as **H** increases towards saturation, the response again follows a smooth curve.
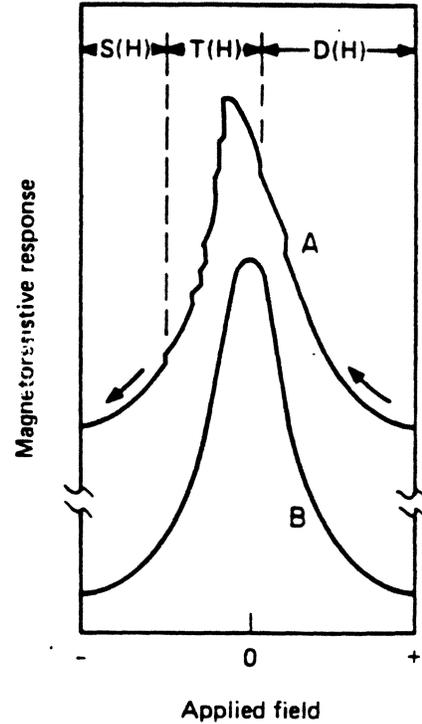
Domain patterns in a hard-axis cycle:
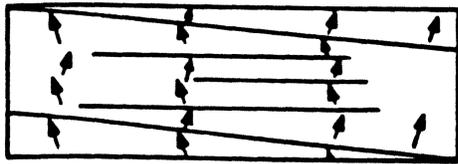
a) A positive field of ~15 Oe *'ripples'* **start to appear.**

• Small θ_D ,∴ large No of domains

(Ripples are the result of demag. fields near the edges)

b) Field is reduced zero.

• Here, ripples turns into **_Buckling_** domain structure with closure domains at the end.

θ_D becomes larger (i.e. wall energy increases). **Walls merge and disappear.**
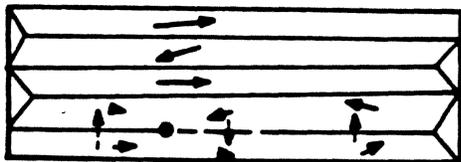
c) Singularity develops
• **Abrupt change in resistance**

d) Reverse saturation
• Through **rotation and smooth** expansion of favored **closure domains.**

SOLUTIONS?

○ **Fields in the easy direction** induce a quiet MR response. These *longitudinal* fields **would inhibit the formation of buckling domains**.

○ **Electrically shorting the ends** so that sensor becomes insensitive to the motion of closure domains.

○ **Bias the MR properly** so that excursions to near zero field do not induce noisy neel wall-state transition (R. Jones et al).

○ Use caution when designing the micromagnetics (aspect ratio, etc)

○ Use *multilayer structure* when possible.
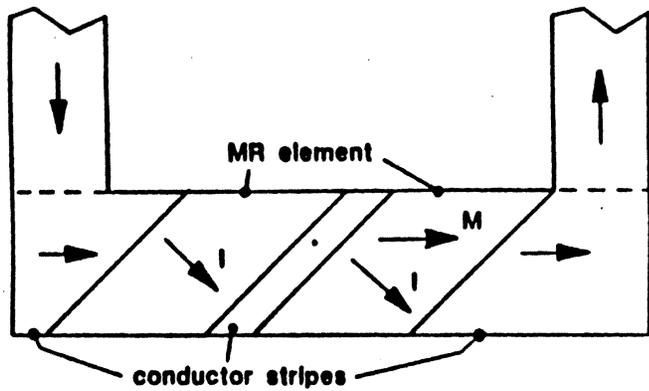
- rotate **current** vector with respect to magnetization

Figure 13. The "Barber Pole" linearization scheme.

(a) **MR element in multi-domain state**

(b) **MR element in single-domain state**
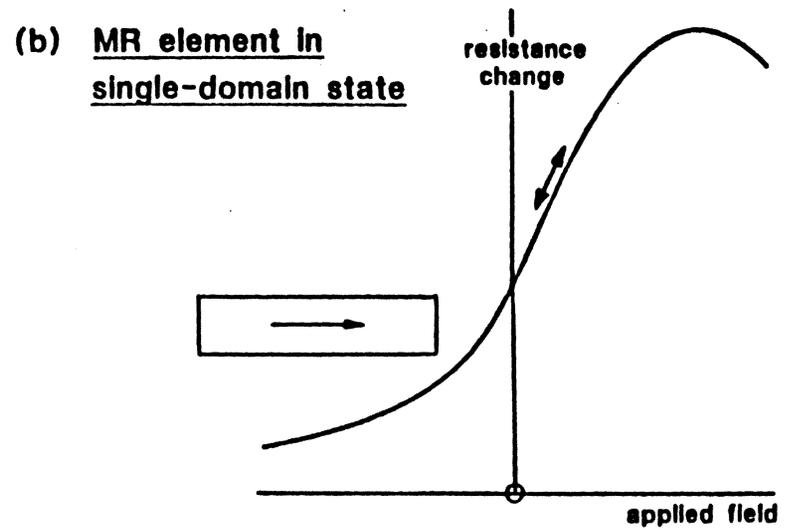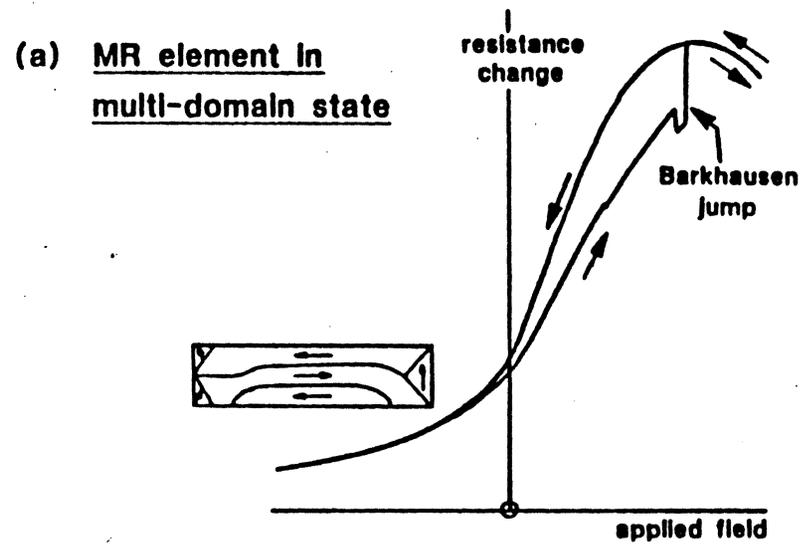
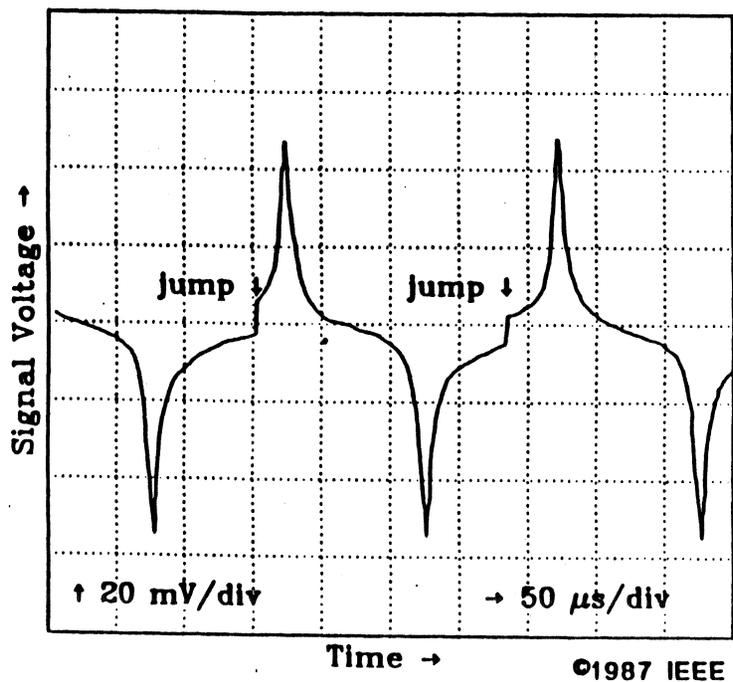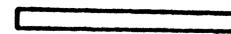Figure 14. The origin of Barkhausen noise.

Figure 15. Recorded transitions reproduced with Barkhausen noise.

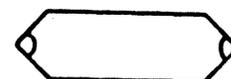- **Application of field along MR easy axis**
  - external field source
  - field derived from canted "barberpole" conductors
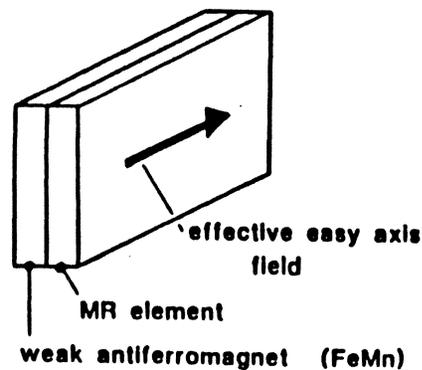 - effective field from canted exchange layer magnetization

- **Geometry**
  - large length/height ratio
  - control of domains at ends
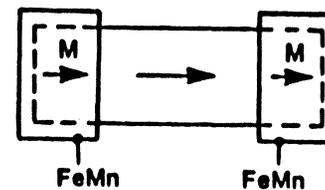
- **Exchange bias**

Figure 16. Barkhausen noise elimination techniques.

Patterned Exchange Biasing

Despite all its benefits, longitudinal bias may significantly degrade the performance of the sensor by ***stiffening the magnetization* *against rotation*** into transverse direction (C. Tsang 89).
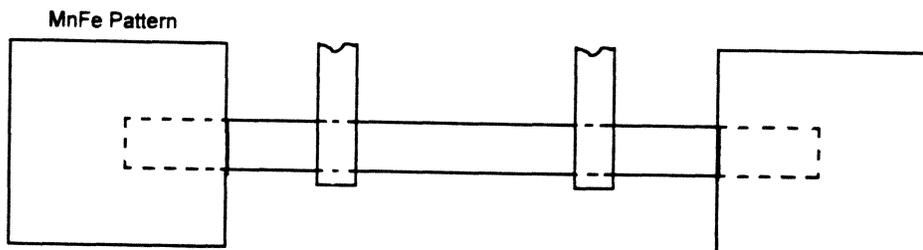
This can make **transverse biasing difficult** and **reduces signal field**.

Solution?

- Adjust the long. bias so that it is not too large to cause transverse permeability loss- this is hard in case of exchange biasing.
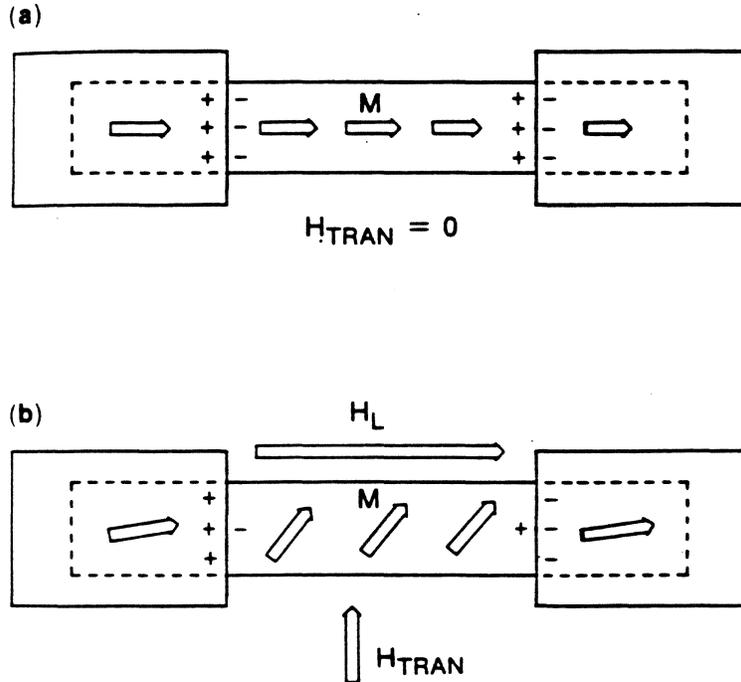
- Use **Patterned Exchange Bias.**
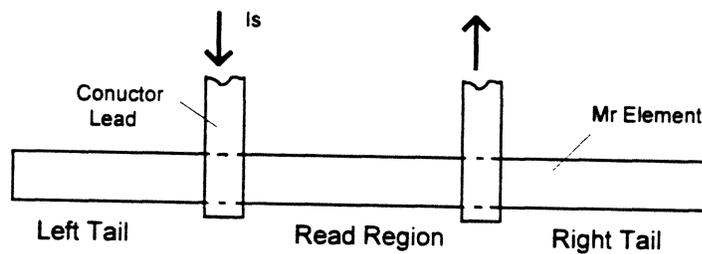
(a)

(b)

Schematic of MR sensor elements (a) Conventional design: (b) Patterned Exchange-Bias design (C. Tsang)

Provided the read portion is not too long, biasing the tail regions into a single domain state tends to force the center read region through **magnetostatic** and **exchange** interactions.

(a)

$$H_{TRAN} = 0$$

(b)

$$H_{TRAN}$$

Magnetics of the Pattern Exchange-Biased MR (a) Without signal field; (b) With transverse signal field

On application of a transverse signal field, magnetization of the middle region is appreciably more rotated than the tail regions

=>   a) *net charges* at the tails => *net longitudinal field*. (Note that its magnitude is geometry determined).

b) At the boundary of the exchange pattern with NiFe, **exchange field is excited**.

The total longitudinal bias is the sum of these two fields.

Permanent Magnet For Longitudinal Biasing

O This is done by exchange coupling a P.M. with the soft NiFe.

O The **SAL** layer is **NiFe+Cr** since it has little magnetoresistance.

O CoNiCr or CoNiPt is deposited on a Cr underlayer to produce Hc of upto 1000 Oe.
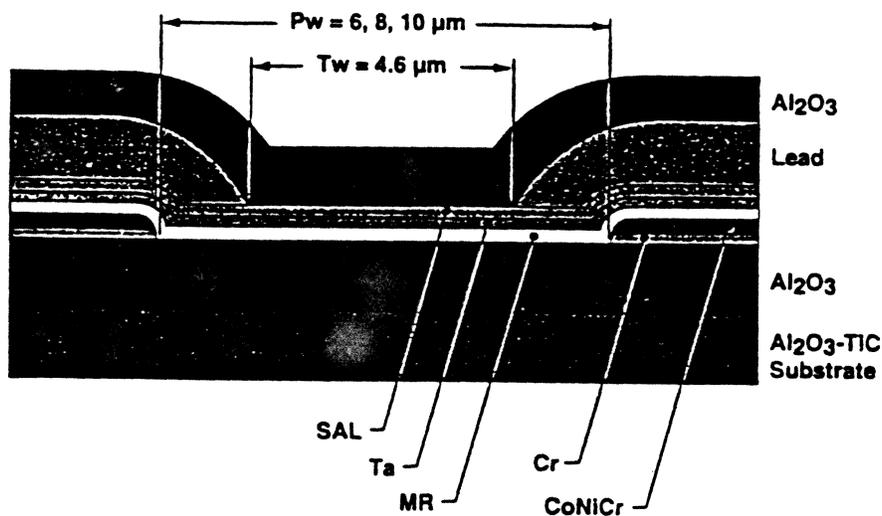
O Gradually beveled edge of P.M. assures magnetic continuity.

O Ta is used because of its **high resistivity** *in order* to adjust current to **SAL**.

O P.M. materials are less prone to corrosion more compatible with wafer fabrication process (The exchange coupling actually improves at high temperatures).
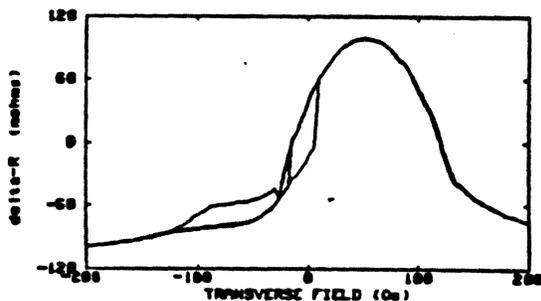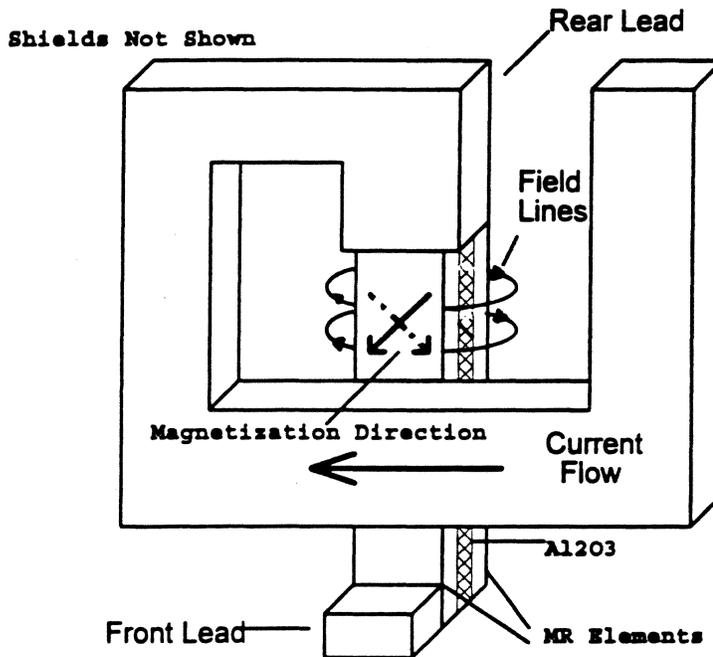

(a)
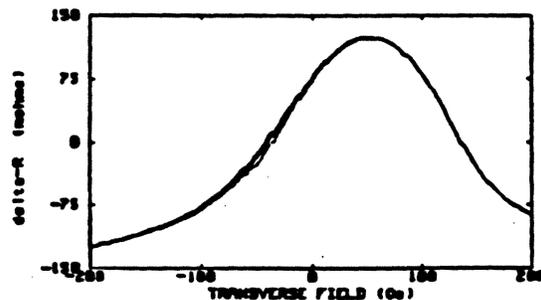
(b)

Measured transverse transfer curves of a
(a) PM/MR/Ta/SAL device before annealing
(b) PM/MR/Ta/SAL device after annealing.

Simon H. Liao, Terry Torng, Toshio Kobayashi

Vertical Magnetoresistive Heads
(VMR)

Features:
- Two terminal design, *sense current is also used as bias current*.
- *Low crosstalk* (since the sensor is narrow).
- For the same reason, *low sensitivity to thermally induced noise* The magnetic circuit is designed so that the *circular* magnetic field in the MR element caused by the sense current and longitudinal field give the required *45 degrees* operation point.
- Front lead exposed to the ABS and the upper shield are grounded. The upper shield acts as a lightning rod for MR.
- MR element is recessed by ~ 1 μ m, therefore, it is insensitive to shorting by smearing. (Note, because of recess, output level may require compensation by ,e.g., increasing permeability).
- Signal output does not depend on the trackwidth, hence, it has good potential for high density recording.
- Symmetrical offtrack performance, since the element is narrow.

Giant Magnetoresistance (GMR)

- In general, presence of magnetic field alters trajectory of an electron moving through that field.
  This effect is more pronounced in magnetic metals.

- For GMR to appear:

  a) must be able to change the relative orientations of magnetization in adjacent magnetic metal layer.
 In Fe/Cr, antiferromagnetic coupling between adjacent Fe layers is the case.
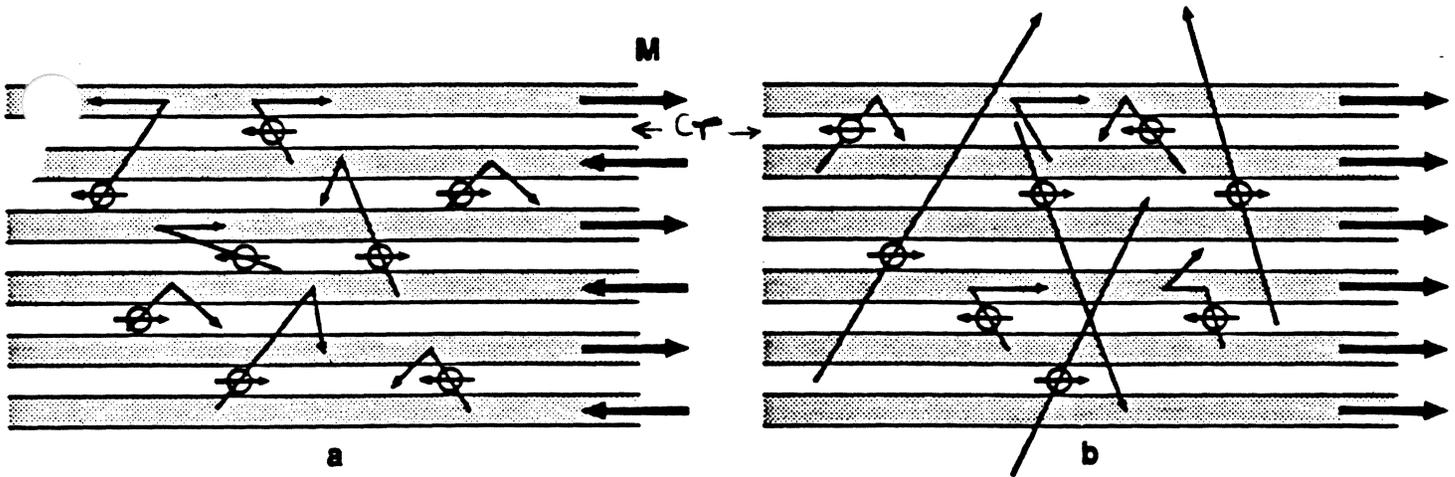
  b) film thickness involved must be less than the mean free path of an electron in multilayer array.

- Cr is not the only spacer material where this effect is present.

- The sign of magnetization changes from anti- to ferro-magnetic with spacer thickness.

GMR Heads

▶ This is a phenomenon of scattering of electrons at interfaces

low resistance   **high resistance**

magnetic field ➡   **magnetic field ⬅**
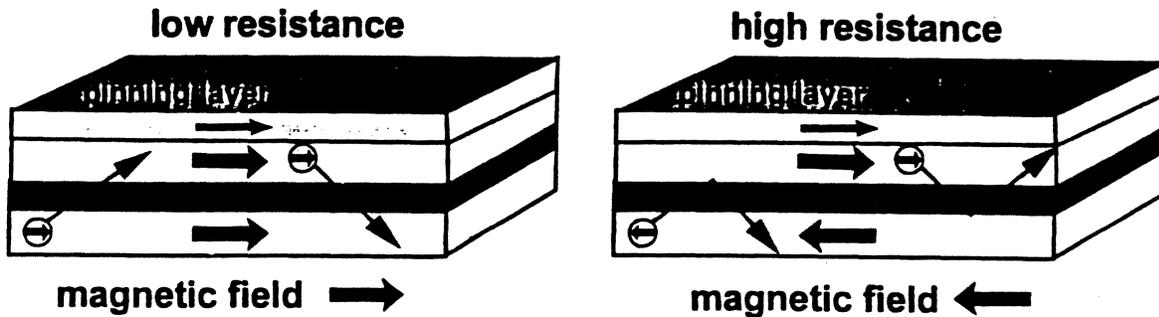
▶ All thin film systems, such as Fe/Cr, for which successive layers, in zero applied field, are held anti-parallel by an exchange interaction through spacer require fields in excess of 20KG to switch the array from parallel to an anti-parallel configuration.

When in a three layer system two *inequivalent* thin magnetic films are separated by a thin non-magnetic spacer, the fields required are considerably less than 20KG. These system is termed **'spin-valve'.**

Because of the number of layers involved the field from various layers is more difficult to balance.

Pinned Film

Sense Film

After Jim Brug, H.P.

79
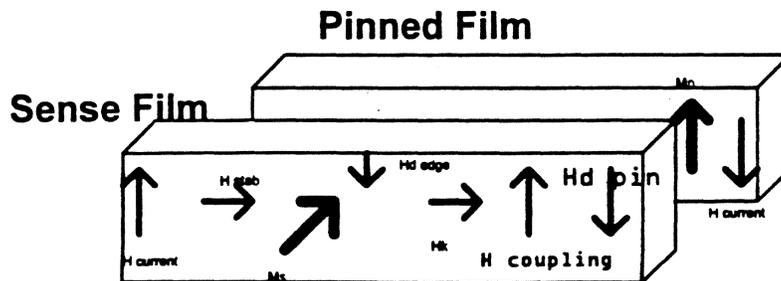
If the upper layer can be pinned in orientation, for instance by antisymmetric exchange coupling to an antiferromagnet, the lower layer can be switched back and forth with respect to the upper, the resulting hysteresis loop and magnetoresistive behavior is shown below:
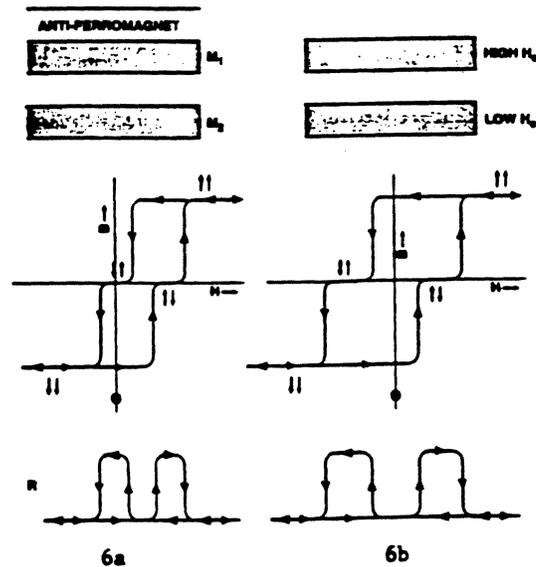

Fig. 6. Diagram of spin valve configurations showing hysteresis loops and resistance changes for antiferromagnetic pinning (6a) and different coercive forces (6b).
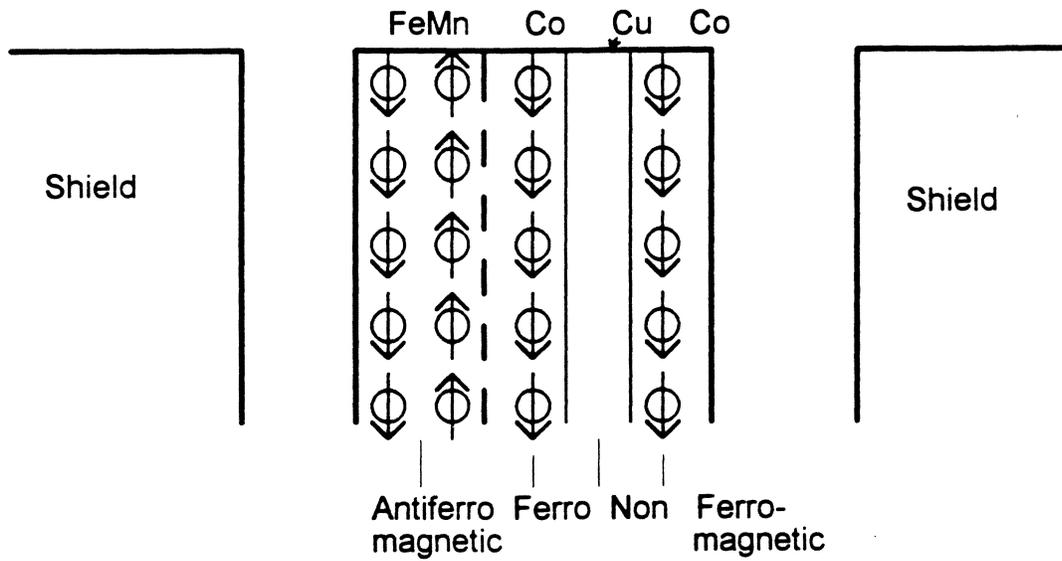
Advantages of GMR:

▲ Larger signal

▲ Symmetric crosstrack response

▲ Very thin films possible - smaller shield-to-shield spacing

▲ Similar to present MR technology

Disadvantages:

▼ Complex material systems

▼ Present deposition systems probably not suitable

▼ Lifetime issues more important

Spin-Valve Structure For
GMR

GMR Parameters

❏ **Normalized change in resistance** $\Delta R / R$

❏ **The field needed to saturate the response**

❏ **Permeability**

- May be limited by intrinsic anisotropy and the exchange coupling. Also its frequency response matters for hi-frequency.

❏ **Size effects due to demagnetizing fields & discrete switching events**

- Generally, as the device becomes smaller, the response broadens and individual switching events are observed as jumps in the response - *Barkhausen noise.*

❏ **The effect of large applied currents**

- **Large currents,** $(2 \times 10^7 \, A / cm^2 \text{ in GMR})$, **can generate** *'self fields'* **and** *heating.* **These fields can reduce the response by as much as 30%** (R. William et al & M. R. Parker et al)
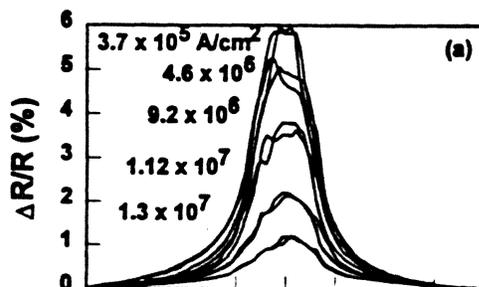
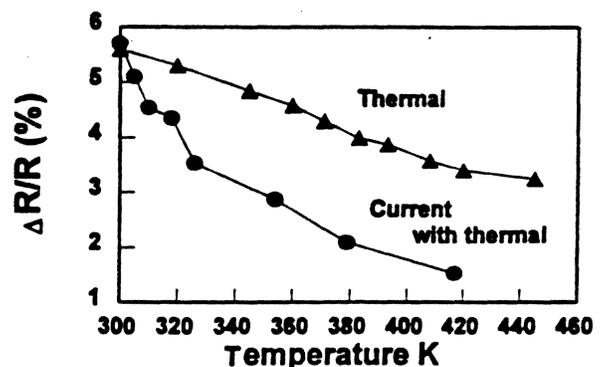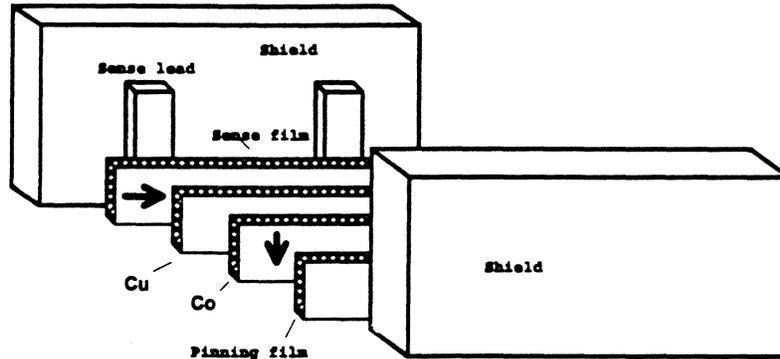Fig. 3. Plots of GMR response as a function of (a) applied current density

Fig. 4. Plots $\Delta R/R$ as a function of temperature for a NiCoFe/Cu device with

Spin Valve Read Head

○ In the above there is <u>ferromagnetic</u> coupling between the *Co* and the *sense film*.

○ The direction of magnetization in the sense film is then rotate through 90 degrees through a combination of ***depositing the sense film in a magnetic*** field, and ***adjusting the sense current*** (note that the majority of the sense current actually flows through the Cu layer since it is a good conductor. The field generated by this layer <u>can rotate the direction of magnetization of the sense layer</u>)

○ Various demagnetizing fields related to the thickness vs stripe height try to rotate the magnetization away from being parallel to the track. They <u>even try to rotate the direction of the pinned</u> layer, i.e. the Co layer, away from perpendicular!

○ Resistance vs magnetic field transfer curve for the above structure has hysteresis due to switching of magnetization in the sense film.

In spin valve in addition to the shape anisotropy, there is an induced anisotropy in the same direction by an external magnetic field.

The biased NiFe can acquire its magnetization direction either as above and/or by annealing after wards above FeMn *'blocking temperature'* in a magnetic field.
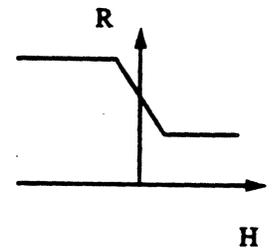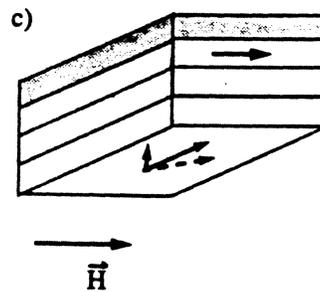
There are at least two choices of anisotropy direction:

Aligned anisotropies　　　　**Crossed anisotropies**
H along easy axis
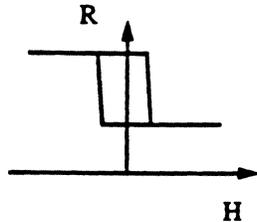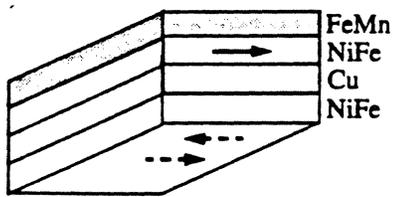
With hysteresis　　　　No hysteresis
Involves noisy　　　　Less noisy
domain wall motion

- In comparison to anisotropic magnetoresistive sensors AMR, the giant magnetoresistive sensors deliver much larger sensitivities and amplitudes.

After R. Scranton
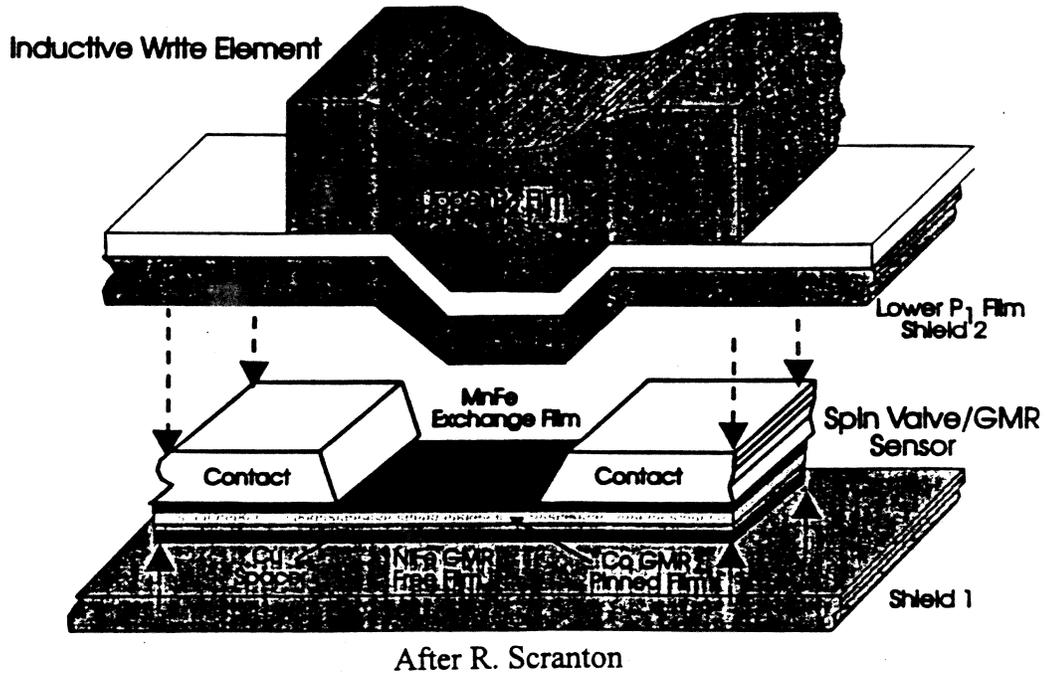
- The structure below is a GMR head with a read trackwidth of 2μm, read gap of 0.25 μm, and an MR sensor height of 1μm. The structure is a 100Å NiFe/25Å Cu/22Å Co/110Å FeMn yielding a spin-valve coefficient ~3.5%.

Fig. 1. Schematic of a spin-valve sensor (M: magnetic moment, θ: angle from the longitudinal direction).

After C. Tsang

82

- The magnetic moment of the pinned layer is fixed in the transverse direction, while that of the free layer is allowed to rotate.
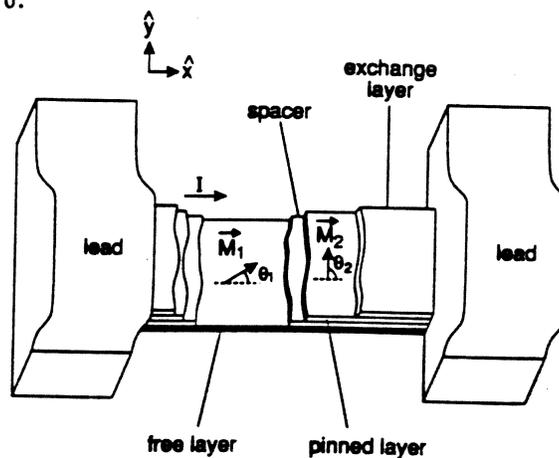
- The resultant spinvalve response is:

$$\Delta R \propto \cos(\theta_1 - \theta_2)$$

$$\propto \sin\theta_1$$

i.e, the response is linear

- By sandwiching the $(Ni_{1.58nm} / Fe_{0.42nm} / Cu_{2.1nm})_8$ layers between two **5** and **7nm** thick magnetically soft $NiFe$ layers the MR ratio a remarkable increase, and considerable reduction in FWHM
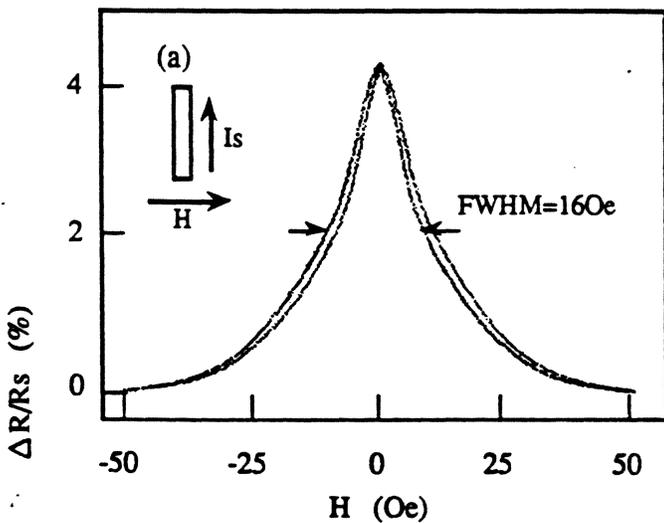
Fig. 1 MR curves for a (Ni/Fe/Cu)$_8$ multilayer.   MR curves for a NiFe(Ni/Fe/Cu)$_8$/NiFe multilayer.
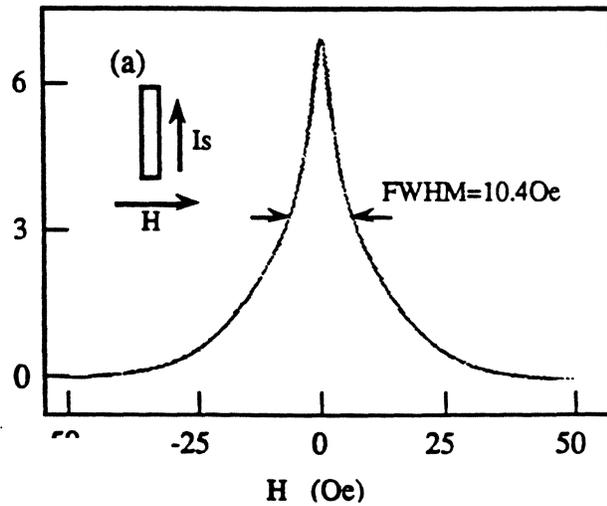
This is due to the antiferromagnetic coupling of the two NiFe layers with their adjacent Ni/Fe layers.

- The respective layer thicknesses are optimized for maximum signal and minimum FWHM:
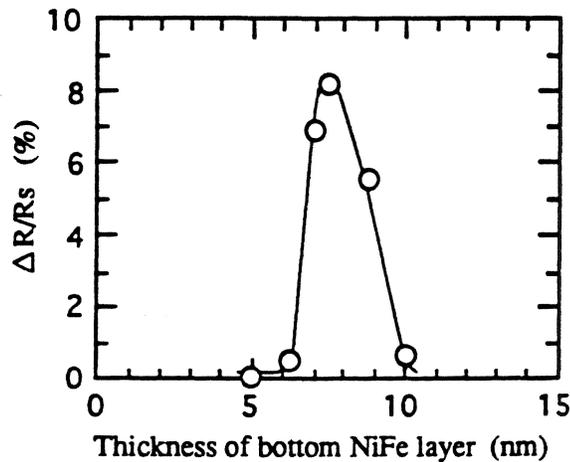
Fig. 4 Dependence of GMR ratio on bottom NiFe layer thickness in a NiFe(Ni/Fe/Cu)n/NiFe multilayer.
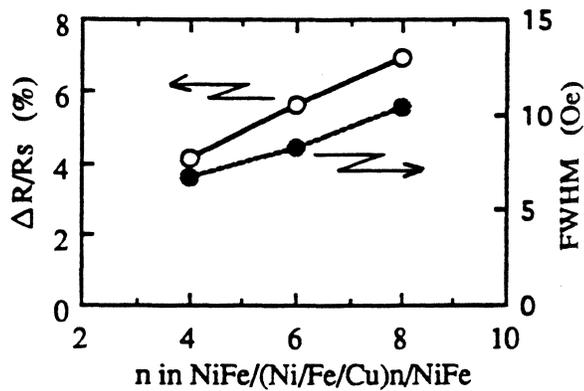
Fig. 5 Dependence of GMR ratio and FWHM on n, number of multilayer periods, in a NiFe(Ni/Fe/Cu)n/NiFe multilayer.
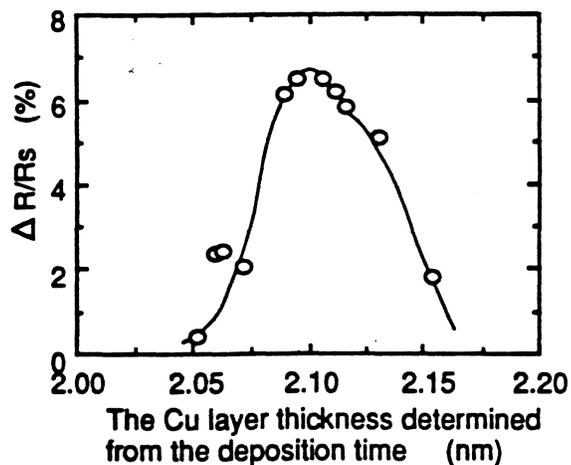
Fig. 6 Dependence of GMR ratio on Cu layer thickness in a NiFe(Ni/Fe/Cu)n/NiFe multilayer.

84

NiFe thickness dependence of H_U

Anisotropy field resulting from exchange coupling is NiFe film thickness dependent, <u>indicating interface nature of exchange coupling</u>:
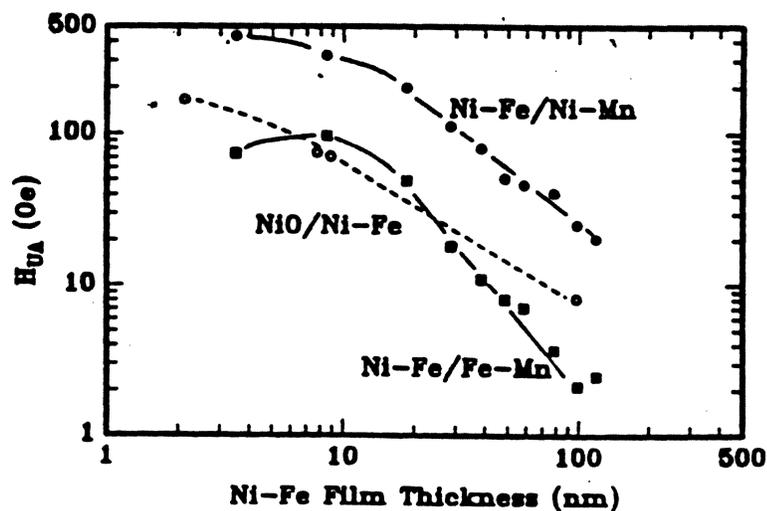
H_{UA} vs Ni-Fe film thickness for annealed Ni-Fe/Ni-Mn(50.4 nm), Ni-Fe/Fe-Mn(50.4 nm) and NiO(40 nm)/Ni-Fe films.

After T. Lin et al

It is also antiferromagnetic film thickness dependent:
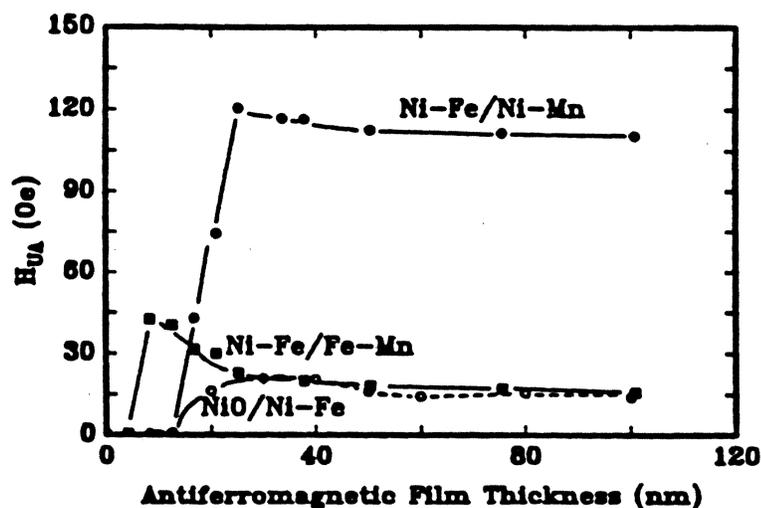
H_{UA} vs antiferromagnetic film thickness for annealed Ni-Fe(28.5 nm)/Ni-Mn, Ni-Fe(28.5 nm)/Fe-Mn and NiO(40 nm)/Ni-Fe(28.5 nm) films.

84.1

NiO As Antiferromagnetic Layer

i) Corrosion Resistant

ii) High Neel temperature

iii) Electrically insulating (can reduce sense current flow outside of a flux sensing free layer as well as heat generation at the sensor region)

iv) High thermal Stability (when thin Co layers are inserted between NiFe and Cu)

v) Longitudinal bias may be necessary to suppress Barkhausen jumps.
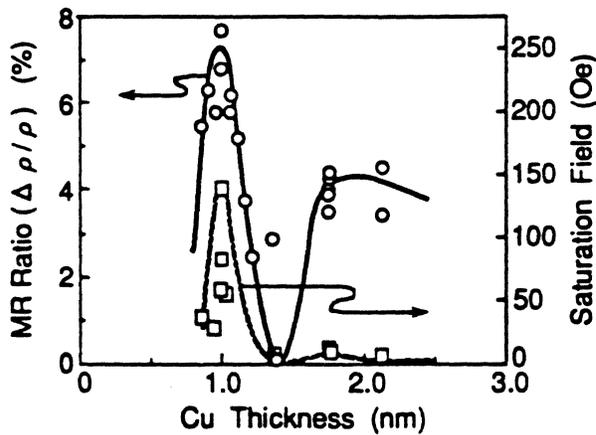
Figure 1. MR Ratio and Saturation Field as a function of Cu Thickness
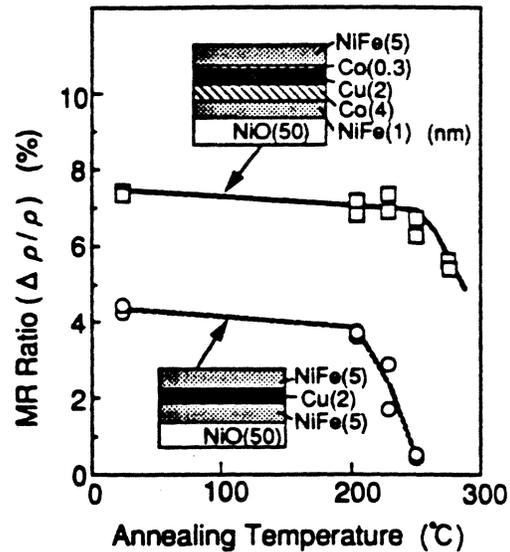
Figure 2. Thermal Stability of Spin-Valve Structures
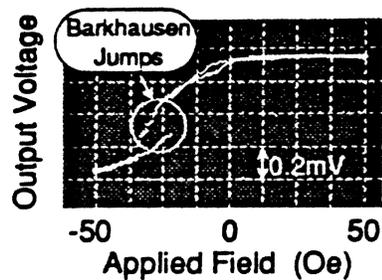
(a) without Longitudinal Bias
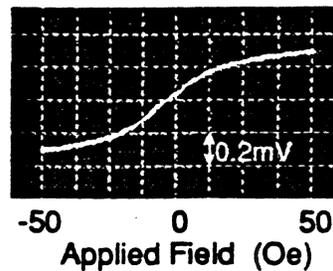
(b) with Longitudinal Bias

Figure 3. Transfer Curves of the Fabricated Sensors

84·2

1. Takashi Kawabe   Central Laboratory Office, Hitachi Research Laboratory

Permanent magnet, both **abutted** juntion form or **overlaid** structure, can be used for domain stabilization:
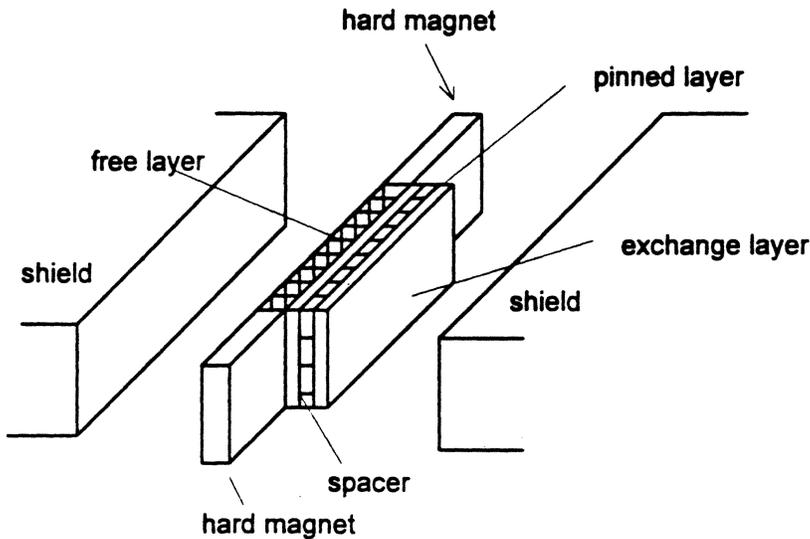
GMR Spin Valve Head With Abutting Permanent Magnet
Longitudinal Bias

The linear dynamic range is a much higher for short sensor height. Also, for insufficient field strength the transfer curve can exhibit irregular response (D. Lu, et al, 95) :
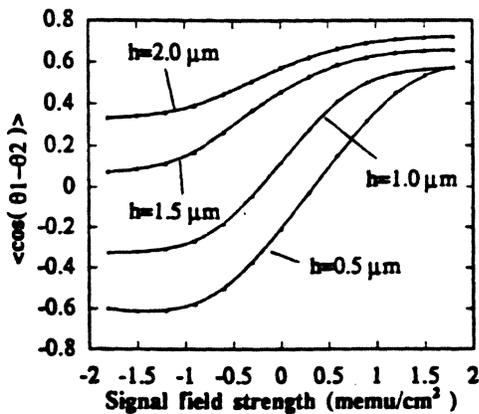
Calculated transfer curves for various sensor heights (h). The width of the sensor is W=1 μm.
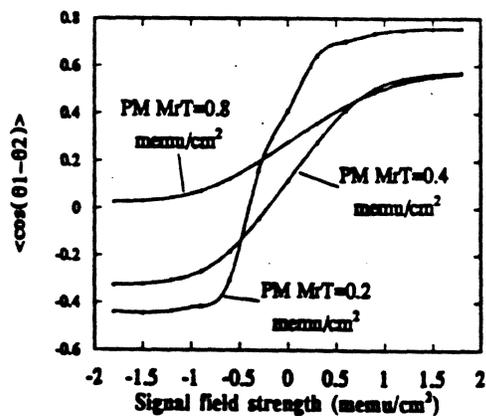
The transfer curves for various values of permanent magnet (PM) strength. The sensor is 1 μm wide and 1 μm high

84·3

Write Coil

Shields

Conductors

I

I

Biasing Magnet
GMR Multilayer
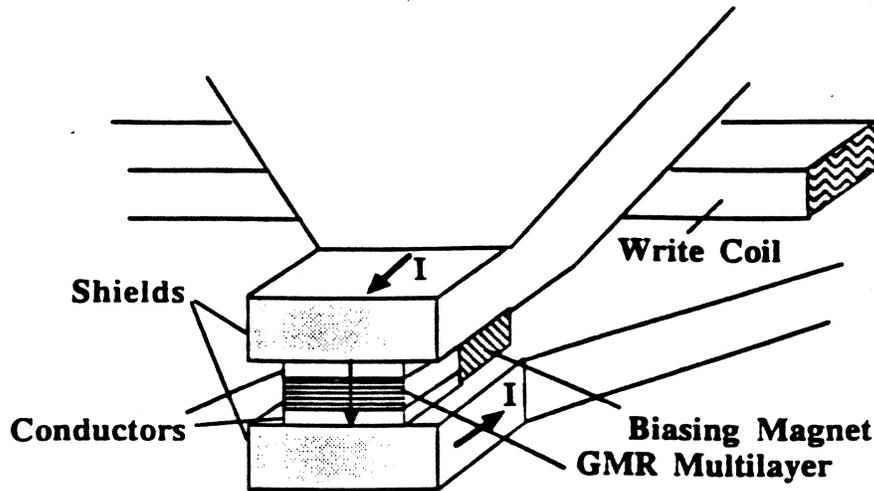
Figure 1. Schematic drawing of the new head design. The GMR sensor is in-between the two shields which also function as writing poles. The arrows indicate the direction of sense current in the read mode. The biasing magnet is a soft magnetic film exchange coupled with an antiferromangetic film.

Biasing Magnet

GMR Sensor

ABS
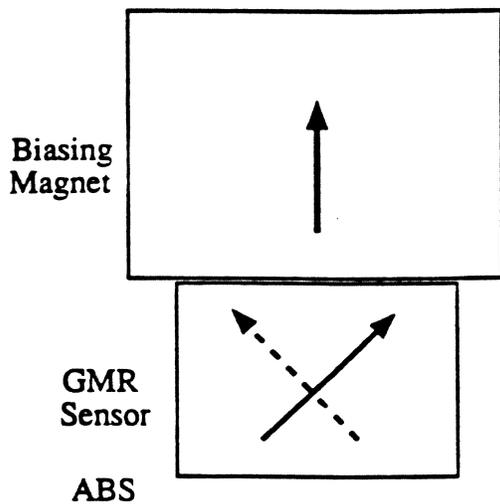
Figure 2. Schematic drawing of the magnetization orientation in the adjacent magnetic layers of the multilayer GMR film under the transverse biasing at quiescent state.

2nm/2nm/2nm
$M_{pm}=225$ emu/cm^3
$\delta_{pm}=20$ nm

fly-height=30 nm
$W=0.5\mu m$
$h=0.25\mu m$

Output $<\cos(\Delta\Theta)>$

Transition Excitation (memu/cm^2)

$W=0.5\mu m$
$h=0.25\mu m$
$g_{s-s}=0.2\mu m$

Output $<\cos(\Delta\Theta)>$

Along track position (μm)
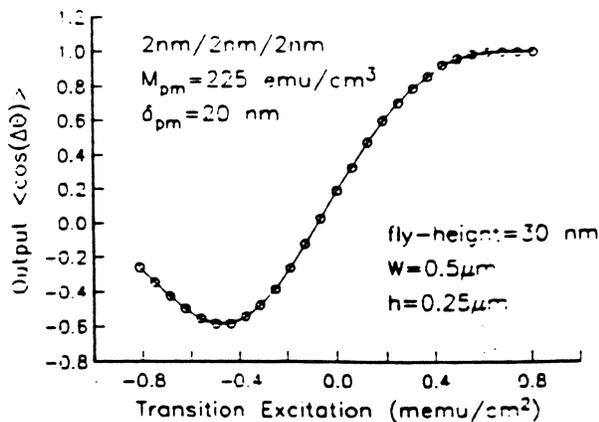
Figure 3. Calculated transfer curve with a transition excitation. The linear dynamic range covers more than 70% of the full-possible change.
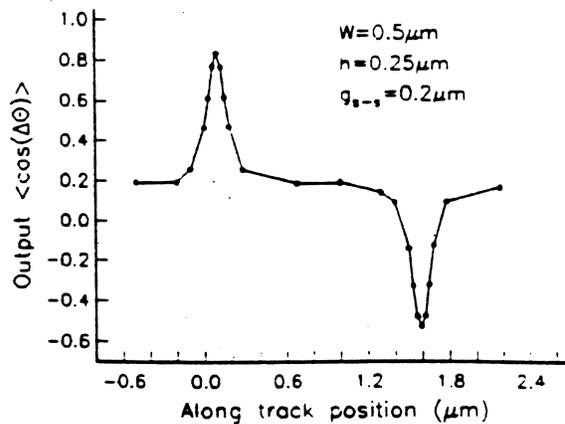
Figure 4. Calculated voltage pulses for positive and negative transitions.

Robert Rottmayer[1] and Jian-Gang Zhu[2]

85

Giant Magneto-resistancs (GMR)

- Was first observed in transition metal multilayers - Co/Ag, Fe/Cr, Co/Cu (antiferromagnetically coupled ferromagnetic layers are separated by non-magnetic interlayers).

    This exploits "spin-valve physics", and is limited to multilayers.

    High Electrical Resistivity

    Low Electrical Resistivity
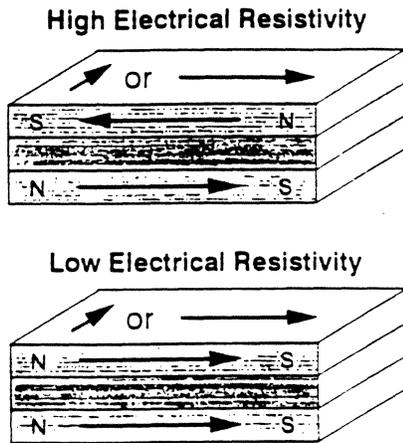
    - Magnetic layers separated by ≈ 10 Å spacers
    - Antiparallel magnetic state due to exchange coupling across spacer layer

    (K. Howard)

- In case of Co/Cu, an Fe "buffer" increases GMR effect as observed in CoFe/Cu.

    EXPERIMENTAL DATA FOR SANDWICHES WITH 80 Å MAGNETIC LAYERS AND 25 Å OR 30 Å NON-MAGNETIC LAYERS.

materials	GMR (%)	AMR (%)	M_s (rel.)	R_0' (Ω)
NiFe, CuNi A	0.68	1.14	.051	175.7
NiFe, CuNi B	1.47	1.19	.051	78.4
NiFe, CuNi C	1.72	1.21	.053	88.2
NiFe, Cu	1.99	1.16	.055	98.3
NiFeCo,Cu	1.71	1.01	.052	103.6
NiFeCo,CuZn	1.22	0.95	.056	614.2
CoFe,Cu pre-anneal	3.21	0.81	.084	88.58
CoFe,Cu post anneal	6.01	.995	.084	78.14

- Also, it is strongly a function of 'sense current':
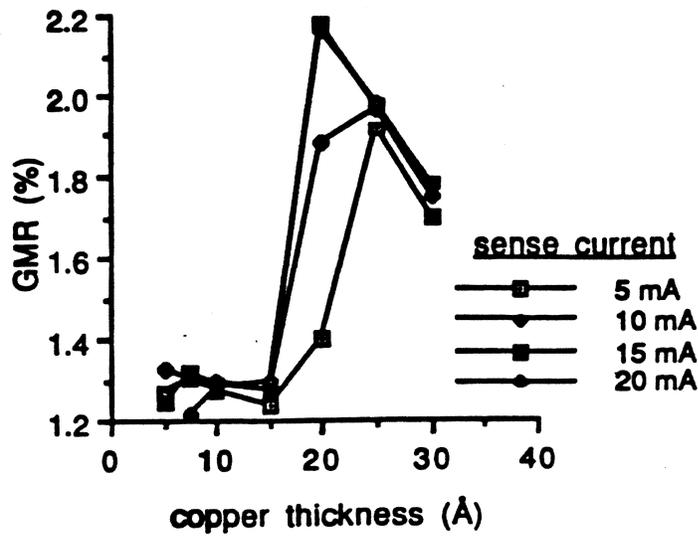
Fig. 3 The GMR measurements for a series with 80 Å NiFe magnetic layers show the effects of pinholes in the Cu layers. The linewidth of these samples was 6 μm.

◆ Magnetoresistance, $\Delta R / R$, is defined in terms of the FWHM of the field :-

Discontinuous Multilayer
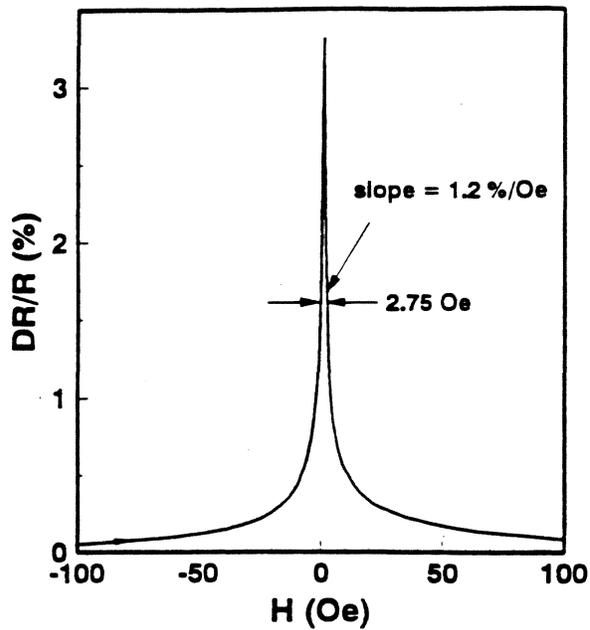
◆ Problem with multilayer is that it requires finite film thickness:-

Number of Atomic Layers

Signal (DR/R %) vs **Layer Thickness (Å)**
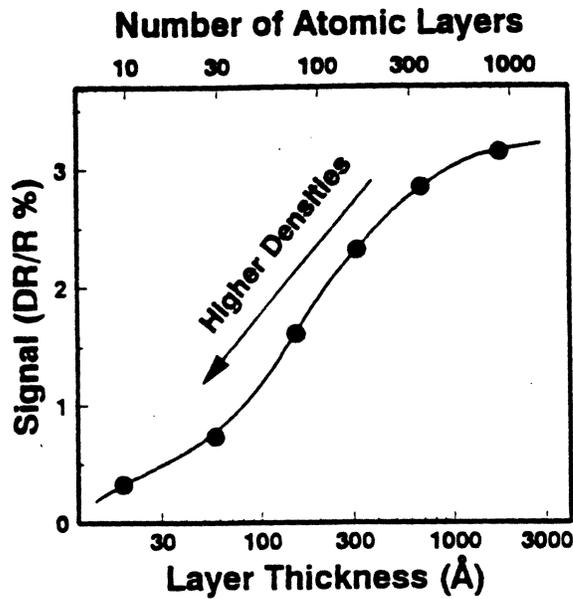
Higher Densities

- Ability to scale AMR head to higher densities is limited by loss of signal

(K. Howard)

◆ MR can also be observed in **<u>discontinuous magnetic layers</u>'** (DML)

Discontinuous Multilayers

High Electrical Resistivity

↗ or ⟶

Low Electrical Resistivity

↗ or ⟶
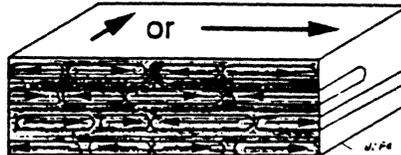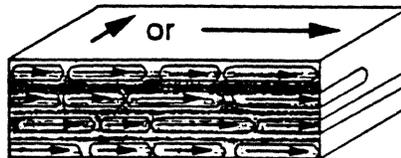
- "Pancake" shaped magnetic regions
- Magnetic state determined by magnetostatic interactions (exchange coupling weak)

(K. Howard)

This technique is an extension of *'granular thin films'*:

88

Granular Thin Films

High Electrical Resistivity
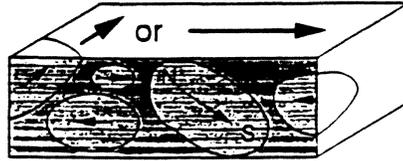
Low Electrical Resistivity
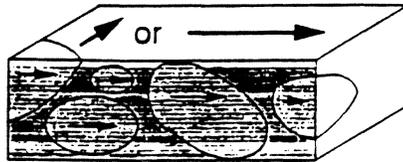
● Magnetic regions and spacer regions

● Magnetic state determined by thermal
fluctuations and magnetostatic interactions

which suffer from:-

    a) Disorienting effect of thermal agitation (due to particle size~30Å).

    b) Shape-anisotropy, due to departure from perfect sphere can **>10 Oe**.

    c) Crystalline anisotropy can be > 10Oe.

DML *takes advantage of shape anisotropy* to reduce required field.

    DMLs are made of **annealed multilayers of NiFe and Ag**:

       ◆ Annealing process results in magneto-resistance, and

       ◆ After annealing the NiFe acquires **flat** platelets configuration
(reduced in-plane demag.).

◆ The magnetoresistance in such structures is strongly a function of annealing:-

Annealed Films
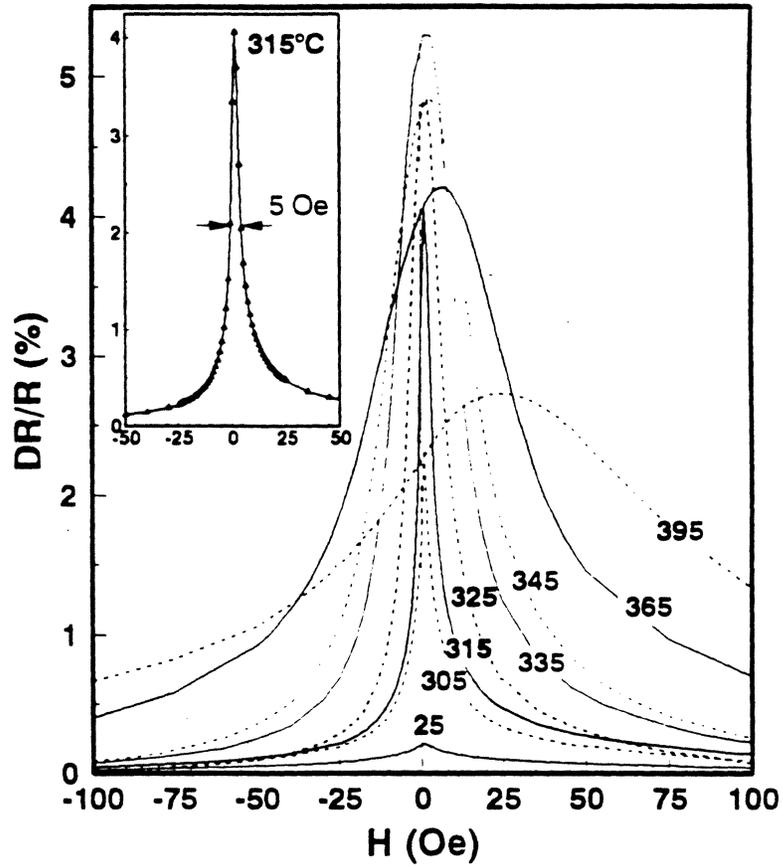
● Discontinuous multilayers **suffer from domain noise related issues**.

Colossal MR Material

- The MR effect here is due to <u>atomic level conduction</u>

high resistance   **low resistance**

magnetic field ⟵   **magnetic field ⟶**

⬤▶ Manganese
◯ Praseodymium/Ca
⬤ Oxygen
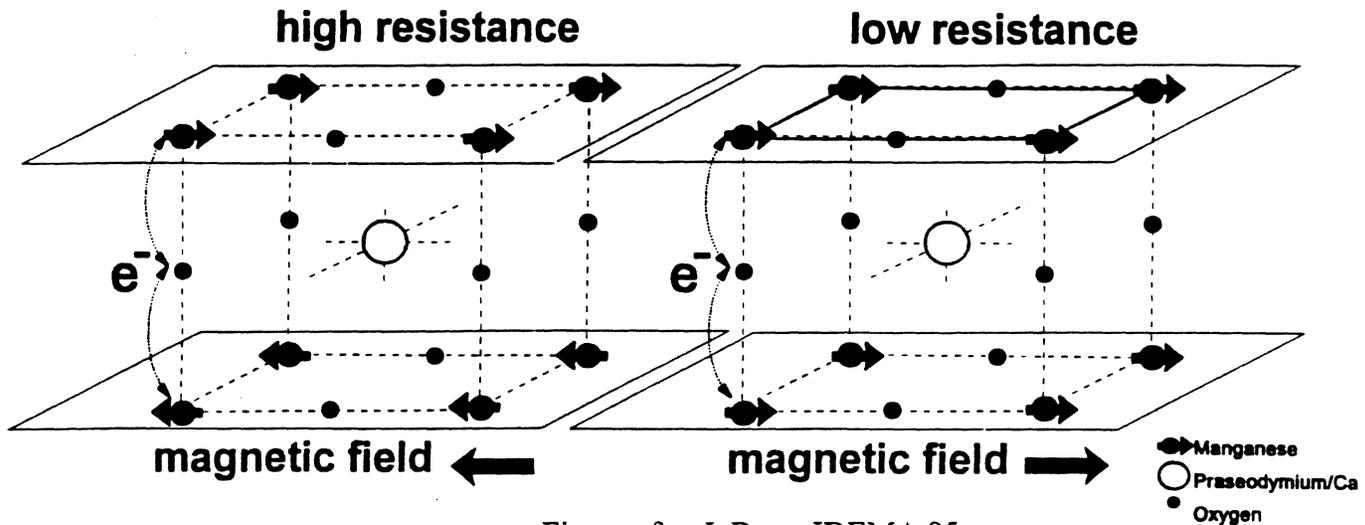
Figure after J. Brug, IDEMA 95

- there can be as much as 127000% change in resistance!
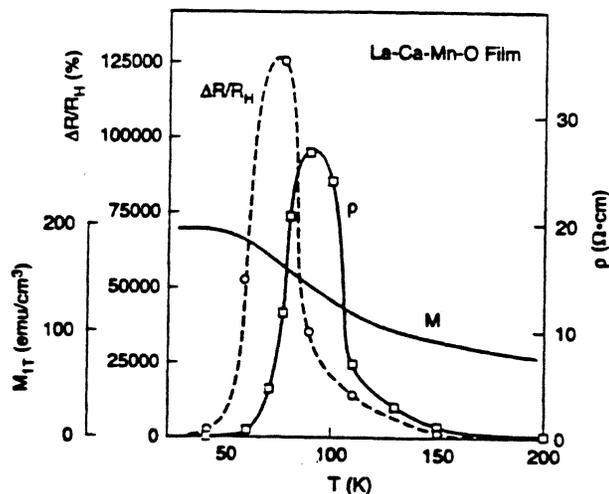
- The signal would be high enough for 100 Gbits/in² recording.
- Problem is the change occurs at <u>high fields</u> and <u>low temperatures</u>.

MR/Inductive Head Parametric Differences

❑ **Similarities:**

- TAA (track average amplitude), PW_{50}, Overwrite, Resolution and Bitshift

❑ **Peculiar to MR head:**

✦ TAA Asymmetry, PW Asymmetry - leads to signal nonlinearity

• For low currents, when the SAL is not yet saturated, large Asy.

• There is asymmetry with regard to read current polarity

(x100 micro inches)
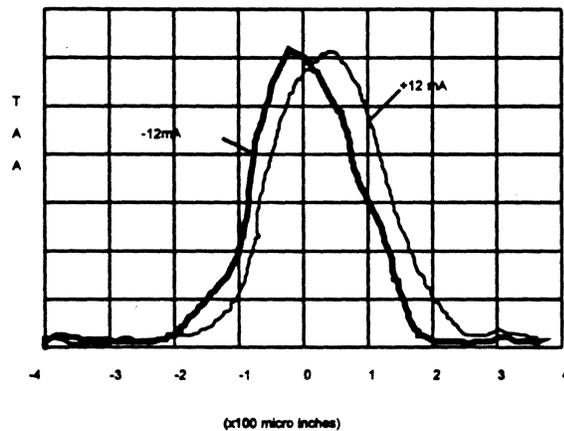
<u>Note the shift from +ve to -ve polarity</u>

✦ Magnetic read center

✦ Magnetic read width

✦MR resistance

✦ Thermal asperity sensitivity

MR Design Issues

On-Track

- Signal Amplitude

- Pulse Width

- Amplitude Asymmetry

- Pulse Width Asymmetry

- Head Stability

Off-track

- Asymmetric Profile Shape

- Side Lobes (Base Line Popping)

- Stability

Parametric testing priorities

Inductive :   Overwrite => Bitshift/Margin => Amp/Res
=> Modulation => Defects => Media noise

MR: Defects => Bitshift/Margin => Media noise
=> Modulation => Amp /Res => Overwrite

93

Track Profile vs Micro-track Profile

■ Micro-track prfile is **1/2** μ against **5** μ of **full track** profile.

• One can either use a special head with a very narrow width or a regular head (and use only a portion of it) for this purpose.

• It is used to give the details of full track profile.

• It can also provide effective track width.

• It can provide detail of head asymmetry.

• Element noise and Barkhausen jumps can be traced.
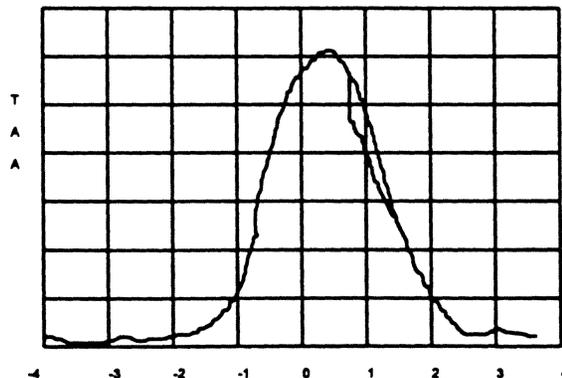
MR Head Design Factors

- **Inductive-write** and **magnetoresistive-read** element.

- Write element has eight turns, **0.4** μ gap, **4**μ **m** thick permolloy pole tips

- Read head is shielded MR head right below the write head with 0.25μm read gap and track width of 0.5μm narrower than write head.

Merged Magnetoresistive Head

Inductive Write Head P2 Layer

Copper Write Coils

Inductive Head P1 +MR Shield2

MR Contact

MR Shield1

MR Read Element

R. A. Scranton
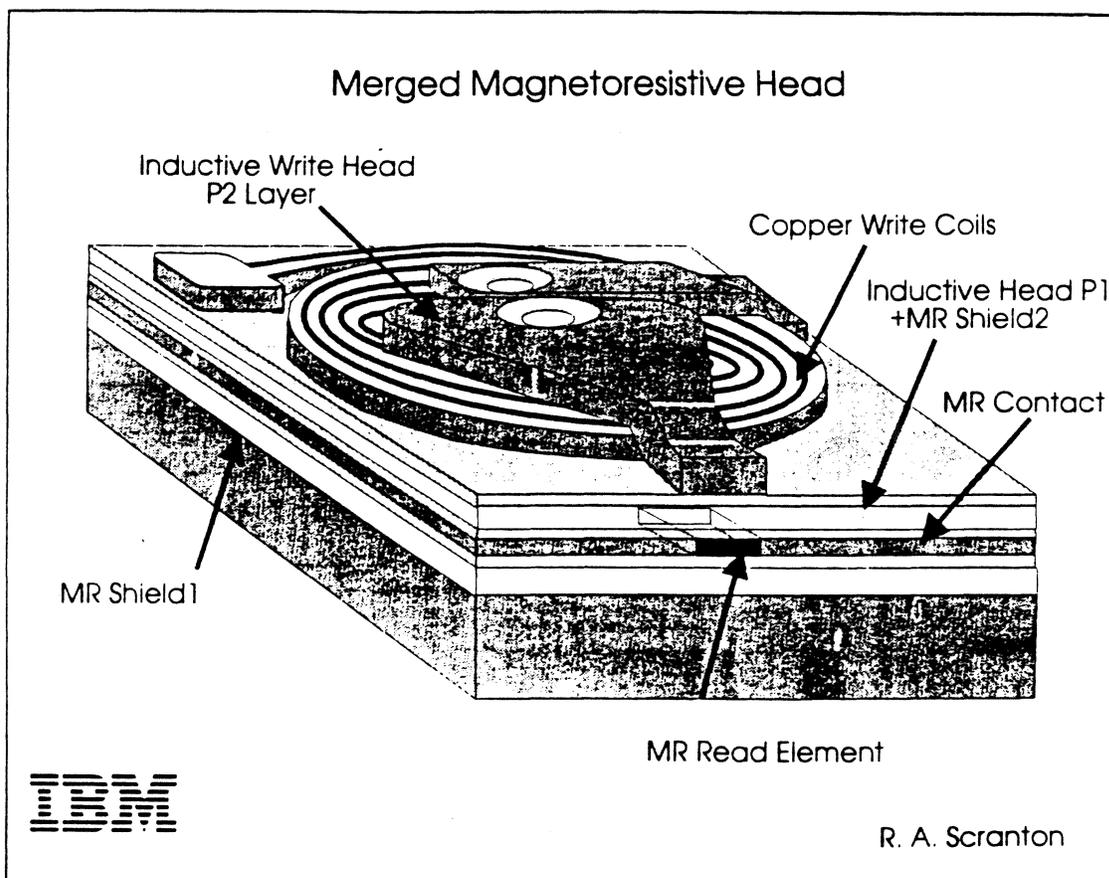
- Shields are electroplated, ~ 3μm thick.

Design and Performance Considerations

I) Linear Resolution

- Thin-film heads suffer from **"undershoots"** in the isolated output pulse, in the positions corresponding to outer pole tip edges. These can make equalization difficult.
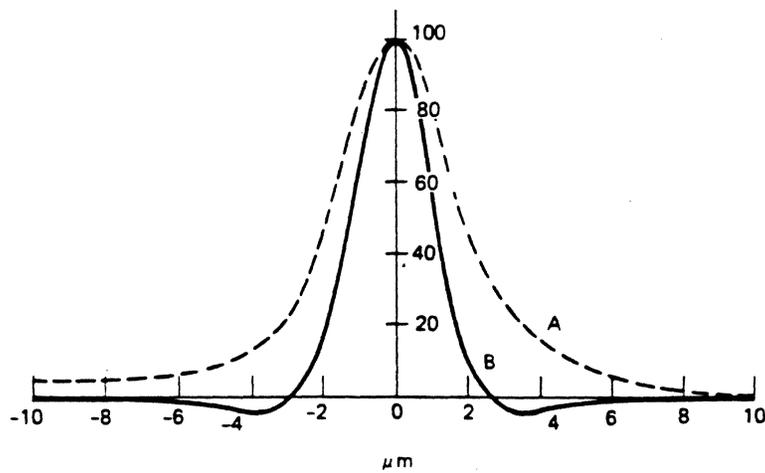
short-pole heads normalized for equal amplitude *(Valstyn and Shew, 1973)*.

In MR heads, <u>because of nearly 'ideal' waveform</u>, a <u>lower unequalized resolution is acceptable</u> than TF heads.

However, **'base-line popping'** can generate overshoots, affecting resolution.

- **"Write resolution"** is determined by the write head and the media to support sharp transitions. **"Read resolution"** is the ability of the read head to resolve closely spaced transitions.

A small change of magnetic spacing can drastically affect D_{50}.
(the <u>density</u> at which the amplitude is half its peak amplitude)
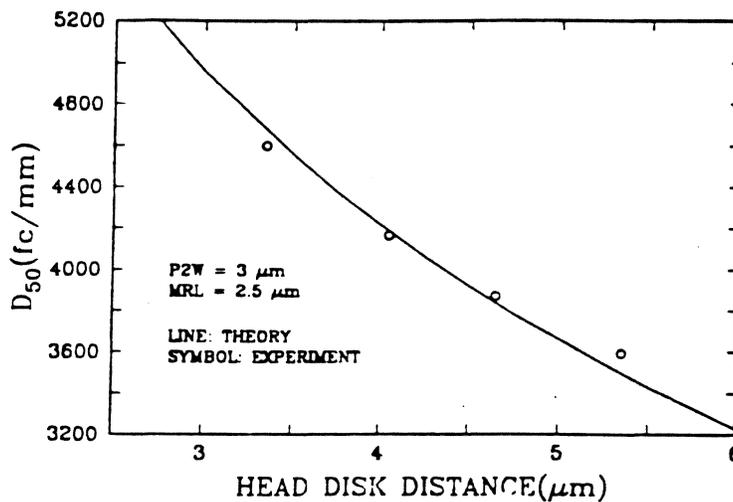
Experimental and theoretical D_{50}
vs head-disk spacing(C. Tsang)

Therefore:
a) Reduce **head-disc spacing**.
b) Reduce **overcoat** thickness.
c) Reduce **'head recession'** from the slider air-baring surface.

- **Read gap** is, also, an important parameter for linear resolution.

The problem in reducing it is that in the limit the material deposited in the gap may not provide enough coverage, **<u>resulting in shorting</u>**.

97

- Reduction of **disk moment** will improve linear resolution, but will lead to SNR degradation.

- **High coercivity => high resolution**, since sharper transitions can be written. But write head has to be also improved:

  - ◆ Use **thick write pole tips**.

  - ◆ Reduce further **head-disc spacing**.

- Increase **coercivity squareness**, S* => increase resolution as well as writability.

  Down side is it leads to intergranular coupling increase => noisy media.

II) Track Density Resolution:

This is a **write-head** as well as a **read-head** design problem.

a) Write-head resolution:

- Improve write track resolution, write well defined, narrow tracks using **narrow 'trailing pole tips'**.

  a) Risk side-track erasure problem. (apart from the data track. side tracks are generated where the data is not well written due to insufficient field gradient. They are, nevertheless capable of erasing previously (adjacent) written data. thus limiting track proximity).

  I) Reduce write gap

II) Reduce head pole asymmetry.
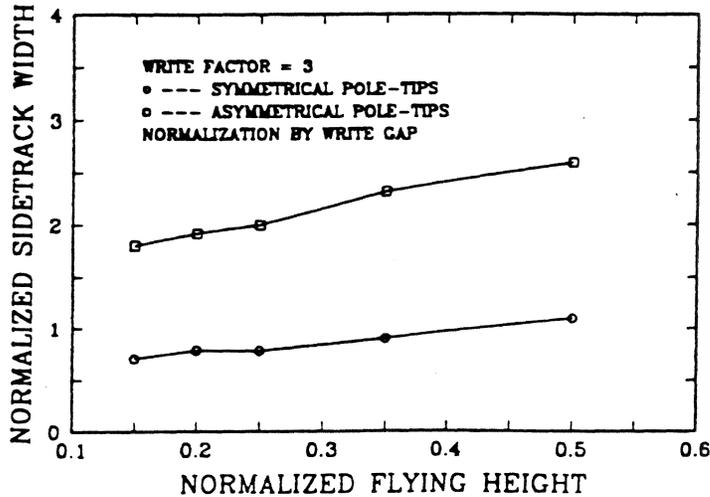
Sidetrack width vs flying height for symmetrical and asymmetrical heads.
(Ching Tsang)

Note that reducing head-disk spacing does not have much effect.
However, **reducing pole-tip asymmetry** reduces side-track width
considerably.
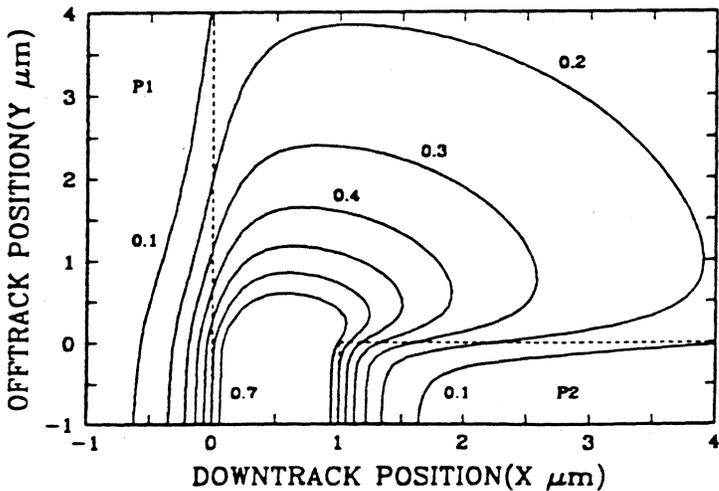
a) **Non-Ideal case** (unequal P1 and P2)
The contours are highly <u>asymmetrical</u> about
the gap center <u>& extend further into side track</u>
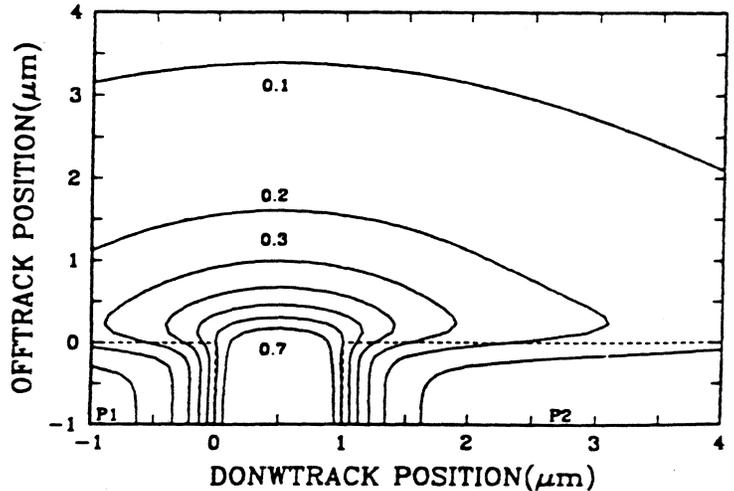
b) **Ideal case** (equal P1 and P2)
Here 0.3 contour, e.g , extends only
0.1 μm, vs 2.4 μm of non-ideal case.

99
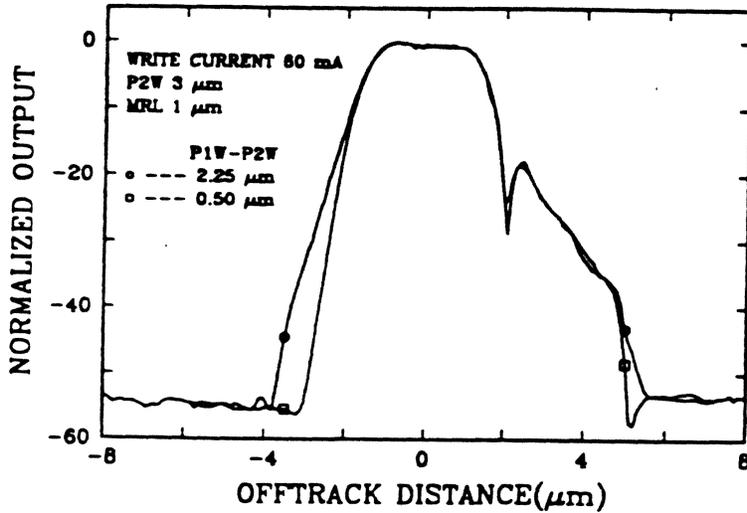
Track profiles of normal vs ion-milled gigabit write heads.

Reducing the upper pole tip to lower pole tip difference to 0.5μm significantly affects the signal profile (broadening)below -20dB.(C. Tsang)

b) Read-head resolution:

- For a shielded MR head the track resolution (ability to resolve closely packed tracks) is limited by the **side reading behavior** of the sensor.(flux from the neighboring tracks is guided from the tail of the sensor to the center).
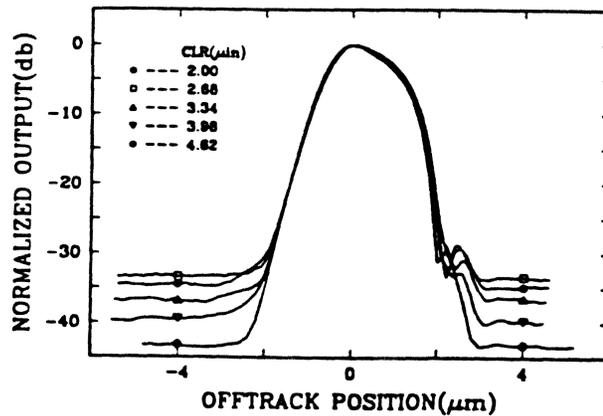
MR head microtrack profiles for different head-disk clearances.

Evidently, the width of track profile is not much affected by flying height. It is better to use *short MR sensors* => may run into domain noise problems. Alternatively **reduce permeability of the tail regions(P.E.B).**

II) Signal Asymmetry

This can be **either amplitude** and/or **pulse-width related**. It is mainly due to improper transverse biasing (leading to *second harmonic distortion*) and MR sensor saturation.

- Apply the right transverse bias:
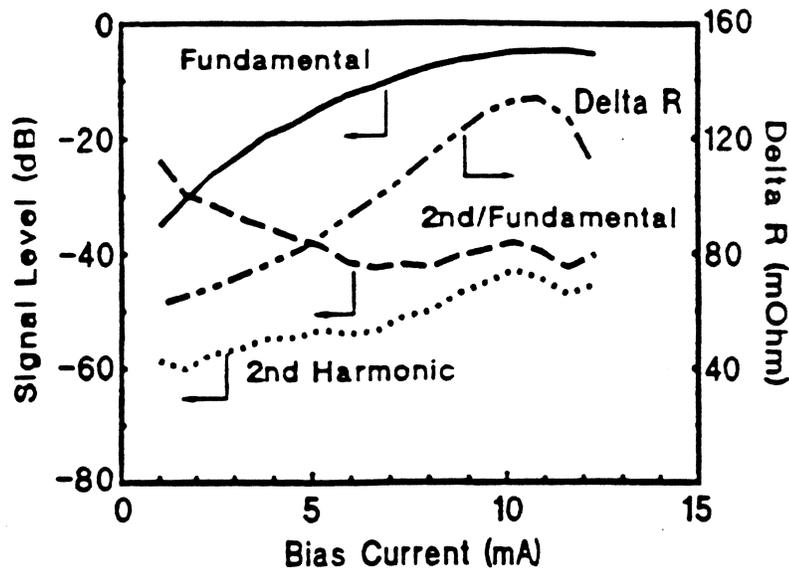
Bias current dependencies of the fundamental, second harmonic, second harmonic suppression, and ΔR for a DSMR head at 10 kfci.

(T. C. Anthony)

As is evident from above, maximum signal follows maximum ΔR, and second **harmonic suppression > 35 dB** (as indicated by the ratio curve) over a broad range of current about the bias point for DSMR.

♦ Second harmonic suppression is also strongly a <u>function of head position</u>:
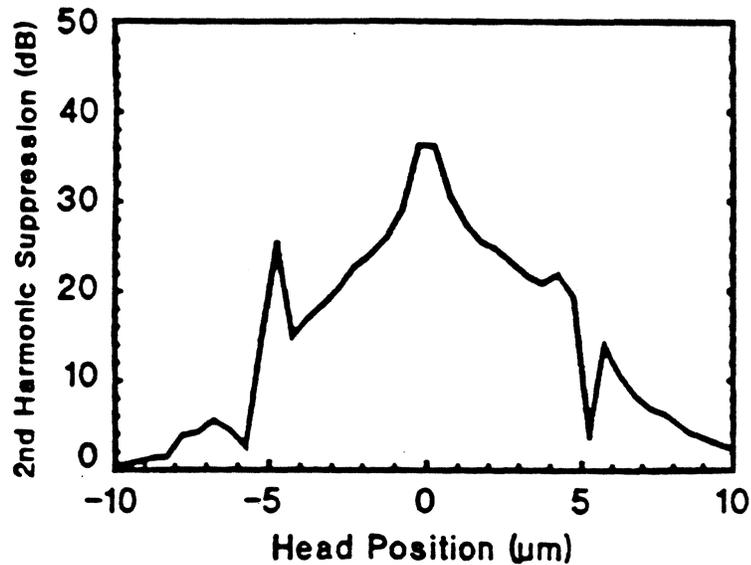
Second harmonic suppression of a 4 μm DSMR read/4.5 μm write head with respect to cross-track position. Linear density=10 kfci.

- Keep the <u>flux into the stripe low</u> to avoid saturation.

    a) Keep **Mrt low**, and

    b) keep **gap thickness low**. This is limited by sensor-to-shield shorts.

    These <u>also improve resolution</u>.

- Keep sensor <u>stripe thickness high</u>, therefore, need more flux to saturate the stripe (this may reduce amplitude and resolution).

AND

- Choose the right *'sense current'*:
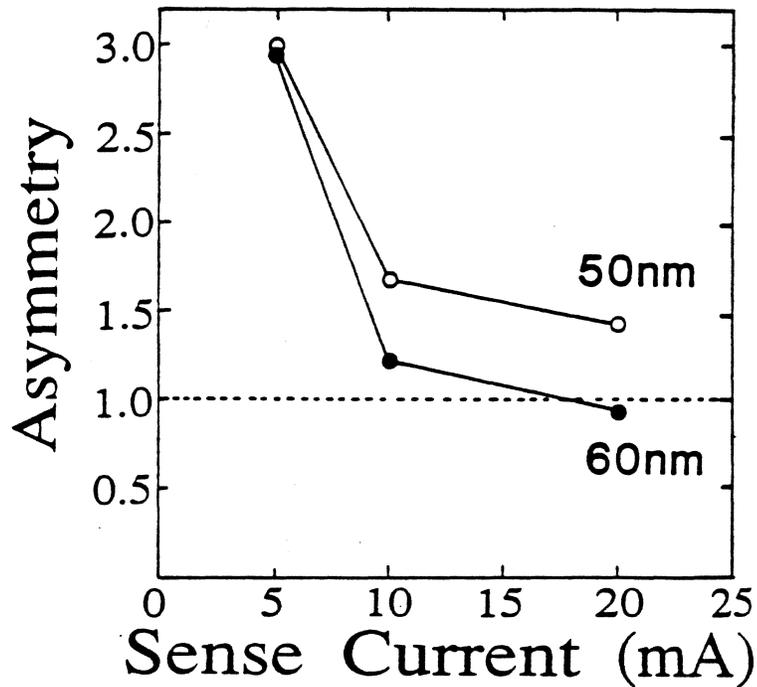
Simulation result, indicating sense current dependence of reproduced waveform asymmetry for two different SAL thicknesses.

(K. Yamada)

Note that in the above asymmetry is defined as the plus to minus pulse height ratio: <u>Symmetrical waveforms are, therefore, obtained when its value is equal to 1</u>.

III) Base-Line Shift

Base-line shift (BLS) can occur due to <u>track edge domains in the media</u>:
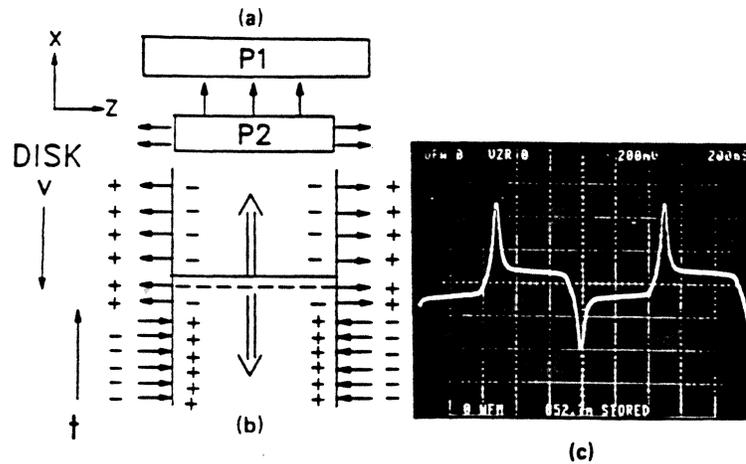
Write field, magnetic dipoles and base-line shift, (a) Z-directed (transverse) write field near lateral edges of P2, (b) Magnetic dipoles along each edge of a data track, (c) The observed BLS of MR readback signal resulted from reading part of the edge dipole charges. (J. L. SU)

BLS can be effectively **removed by side erasure**:
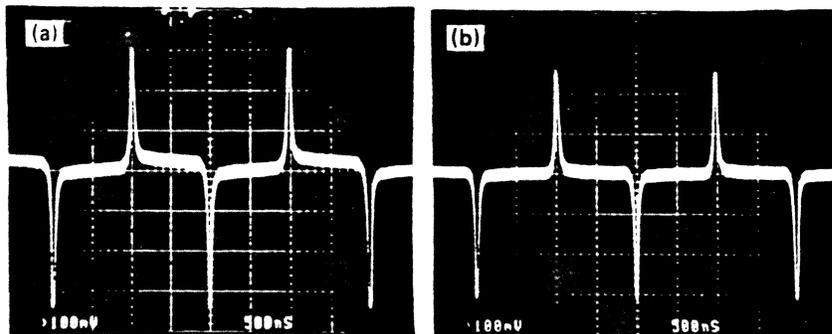
Erasure of track edges to eliminate the base-line shift, (a) On-track MR readback signal on an isotropic film disk, (b) Signal after dc erasure of both edges of the same track.

(J. L. Su)
Note: This phenomenon is less noticeable in dual stripe head.

IV) Off-track Performance

This is characterized by the *distance the head can move off track before some specified unacceptable error rate is reached.*

- It is affected by **read-to-write head alignment**.
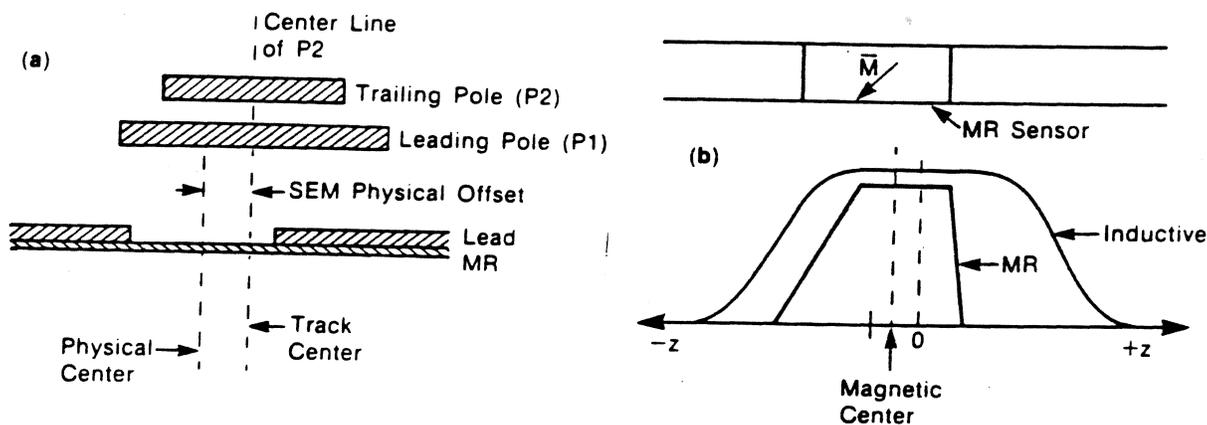
- Note that some well-controlled, **intentional** read/write *offset* which compensates for *'magnetic center'* shift *may be necessary*, as is indicated above. However, too much misalignment can be detrimental.

- Excessive *misalignment* can lead to:

  a) additional **mechanism for track misregistration** *(TMR)*.

  b) **reduced signal amplitude** (due to anisotropic flux propagation along the directions perpendicular to bias magnetization in MR stripe).

(a)

(b)
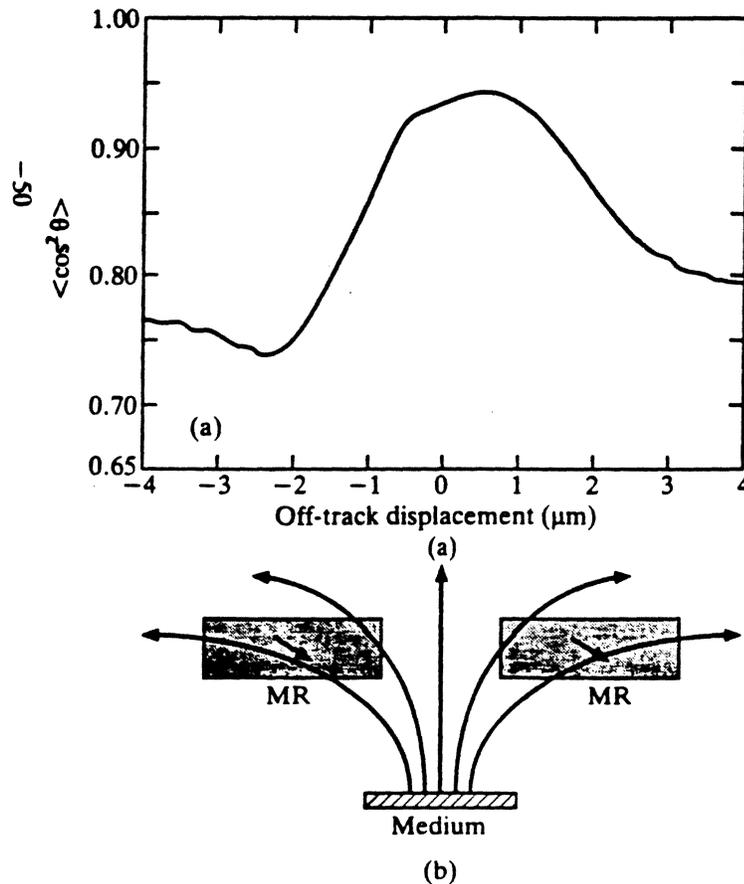
- For the element on the right $(\Delta z > 0)$ the signal field is generally orthogonal to the MR bias magnetization. *∴ torque on the magnetization is large*.

- As the element is moved off-track towards $\Delta z < 0$, at a specific location the field is approximately parallel to MR magnetization *minimizing the response*.

- On track $(\Delta z = 0)$ the response is not the largest due to *non-uniform bias magnetization*.

(a)

signal flux propagation

(active region)

test track positions
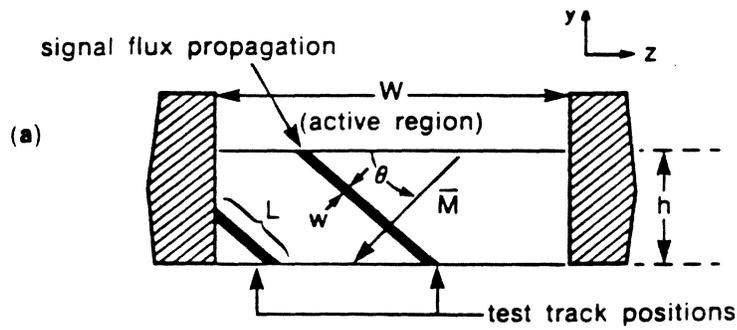
$$\Delta R \simeq \frac{\Delta\theta^* w \Delta\rho \sin 2\theta_b}{2th^2} L(z_t).$$

$\Delta\theta^*$ is the value of $\Delta\theta$ at the edge of the MR film. The flux path length $L(z_t)$ depends on the position z_t of the test track, as can be seen in Fig. 3(a).

(b)

ΔR (normalized)

$\frac{h}{2} \tan\theta_b$

physical center

magnetic center

$\frac{h}{4} \tan\theta_b$
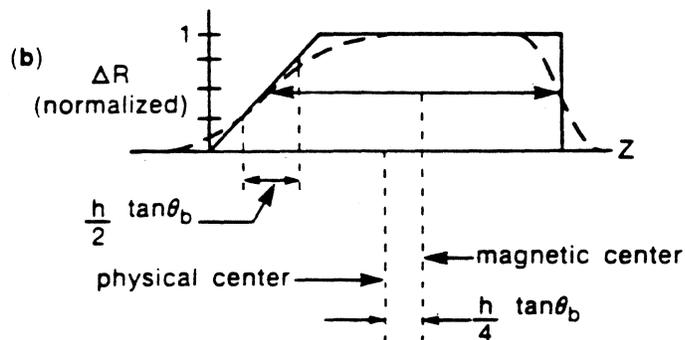
MR stripe shown with relevant parameters used in the model.
(A. Wallash, et. al., 1991)

To alleviate this:

I) reduce the stripe height:
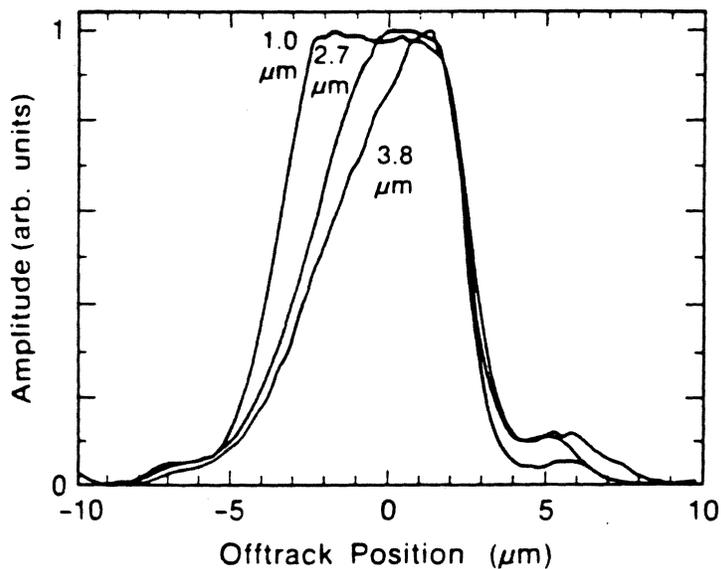
II) Use dual stripe sensors:
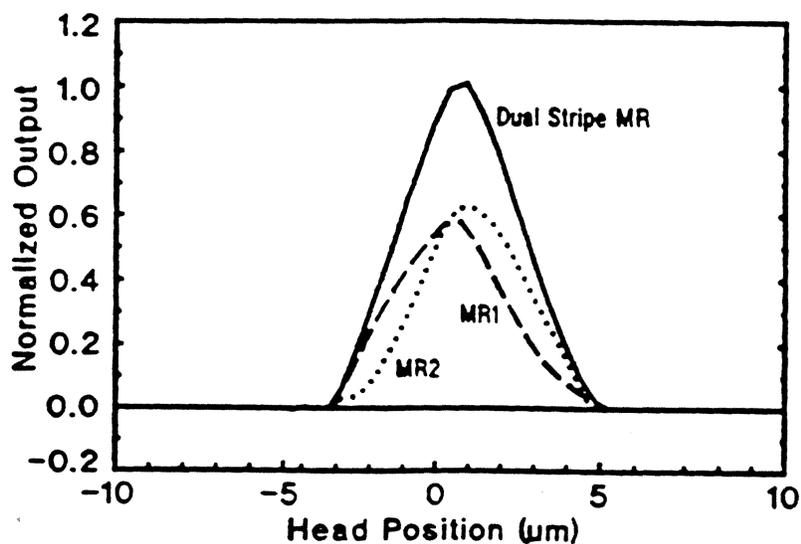
Cross-track profiles from exchange-stabilized 4μm DSMR read/
4.5 μm write head.

Skew And Crosstrack Asymmetry
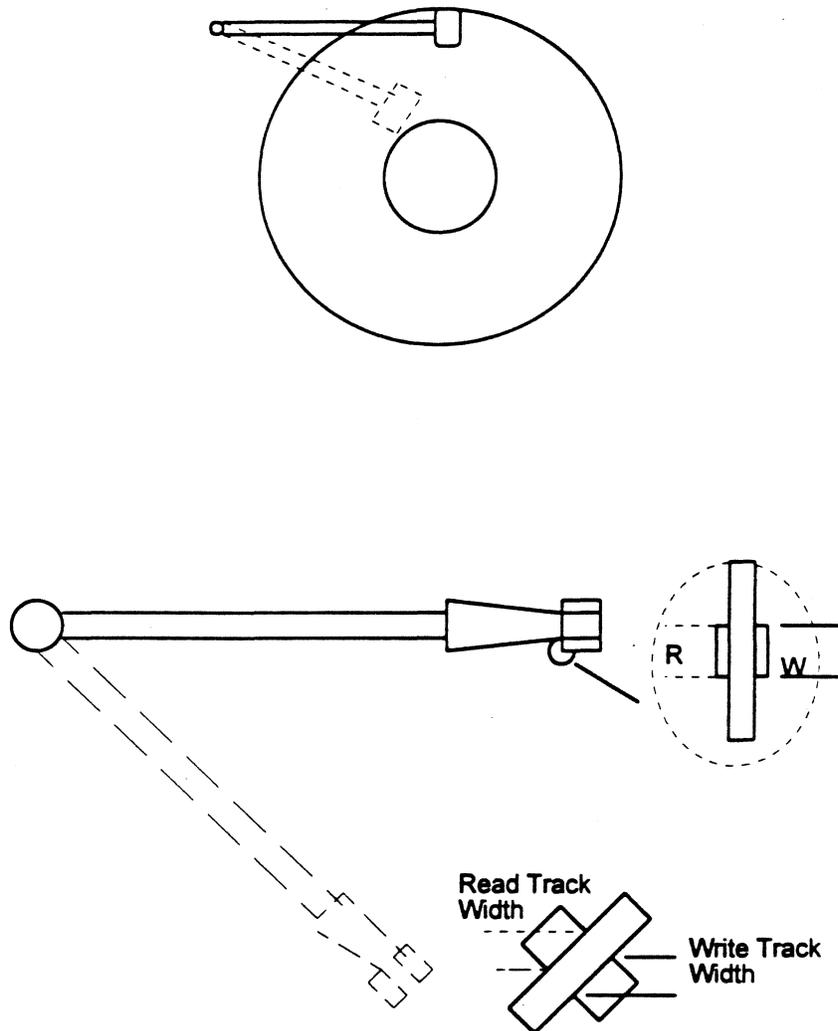
Solution?

- **'Micro-jogging'** can help reduce <u>asymmetry resulting from skew</u>.

V) Mechanical Factors

- **Shorting of the sensor:** This is caused by smearing of the (conductive) shields during polishing.

  This can be alleviated by <u>using a ferrite slider</u> as the first shield, and <u>using less ductile materials</u>.

- Thermally induced noise: These spurious, particle-impact generated, noises can best be contained through use of <u>differential designs</u>. Also, optimize stripe height and thickness to reduce electromigration. This may result in amplitude reduction.

Constant Current
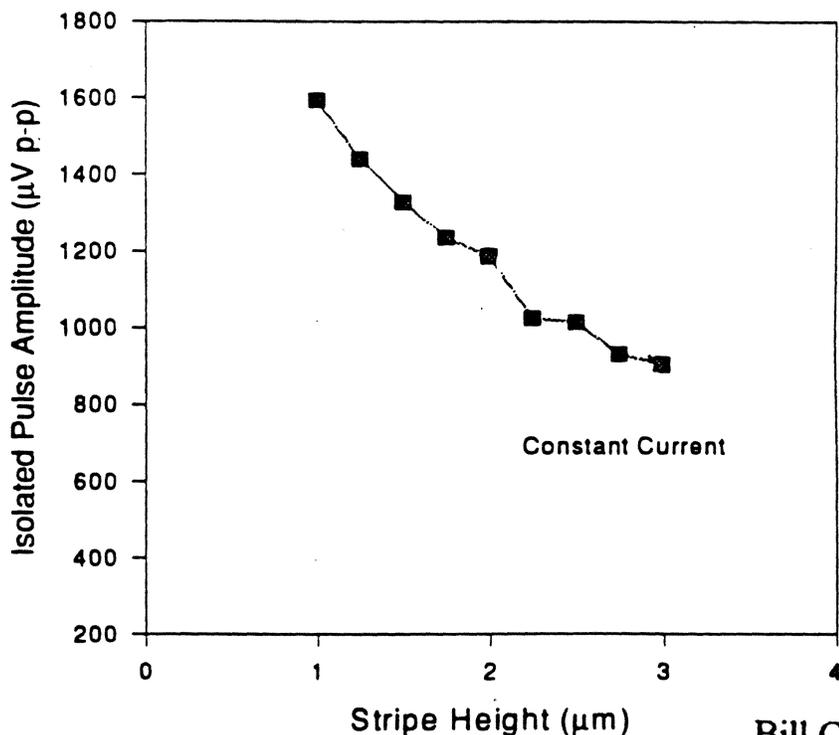
Bill Cain

Mr Heads and High Track Densities

This requires tight control of the following parameters:

❑ **Separate read and write widths.**

The read width depends on critical wafer-level dimensions and on stripe height. Therefore, **precise lapping becomes especially critical**. This is because a wide reader, although shows good on-track properties, will be too sensitive to off-track interference in the presence of track misregistration (K. Weisen). A too narrow a reader, on the other hand, will suffer from a low SNR and inadequate servo performance.

❑ **the across-track offset of read and write centers.**
(This can have three causes. Firstly, the location of the top pole of the inductive writer cannot be positioned perfectly on the wafer. Secondly asymmetric side reading causes the magnetic center of the MR stripe to be offset from the physical center by about half micron. Thirdly, the skew angle will displace the read and write elements in the down track direction)

❑ **Non linear track profile shape.**

This can affect the ability to servo accurately. Minimizing this requires good stripe height control and small variations in the MR stripe magnetic properties.

MR head Signal Sensing Schemes

1) Constant current Biasing, voltage sensing $\Delta V_s = \Delta R_h \bullet I_b$

2) Constant voltage biasing, voltage sensing

$$\Delta V = (\Delta R_h / R_h) \bullet V_b$$

- This has an *advantage* with respect to the life time of sensor.
  ## Mean Time To Failure
  $$\text{MTTF} = A \cdot J^{-n} e^{E/kT}$$

  where E is the activation energy of the ions diffusing in MR.

  Therefore, **life-time~1/current**

- The *disadvantage* is that for a short sensor the current is too low to maintain adequate biasing.

3) Constant current biasing, current sensing

$$\Delta I_s = -(\Delta R_h / R_h) \bullet I_b$$

- this method of biasing involves large currents, especially for short stripe heights, therefore it is bad for life-time.

4) Constant voltage biasing, current sensing

$$\Delta I_s = -(\Delta R_h \: / \: R_h^2) \bullet V_b$$

- This too has the same lifetime problem.

- **Voltage sense preamps is used today**

  Amplitude is proportional to the absolute change in resistance:

  Higher resistance leads to higher amplitude

  => Vendor-to-vendor differences
  => Stripe lapped to shorter hieghts 'appears' to be better

- **Current sense preamps are being phased in**

  Amplitude is proportional to the relative change in resistance.
  => current head/media tests data base will not be valid

*Manufacturing concerns:

●MR heads <u>have to be robust</u> enough to withstand alterations in the read and write throat height dimensions during final lapping.

●Risk of inter-diffusion between layers resulting from repeated temp. cycling. This is yet to be investigated.

●Both thickness and magnetic properties require strict monitoring.

●Alignment of write and MR element very critical.

TABLE I. MR SENSOR PROCESS COMPLEXITY

| DEVICE STRUCTURE	PHOTO STEPS	LAYERS ALL (MAG)	SUBTRACTIVE PATTERNING	ADDITIVE PATTERNING	TOTAL STEPS
Barberpole	2	2 (1)	2 (1)	0 (1)	6
Current Shunt	2	3 (1)	1	1	7
Soft Adjacent Layer (no exchange)	2	4 (2)	1	1	8
Soft Adjacent Layer (full exchange)	2	5 (3)	1	1	9
Soft Adjacent Layer (pattern exchange) (leads/exchange aligned)	2	5 (3)	1	1	9
Soft Adjacent Layer (pattern exchange) (leads/exchange overlap)	3	5 (3)	1	2	11
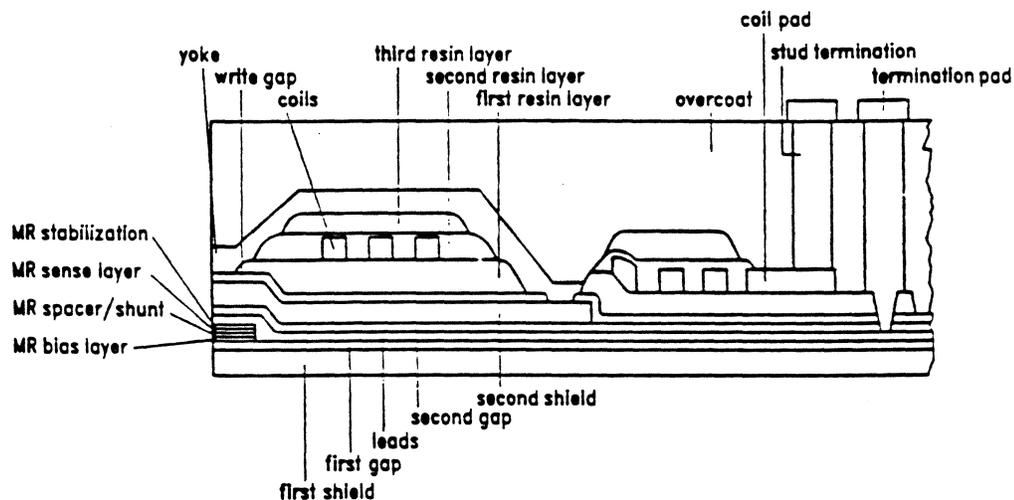
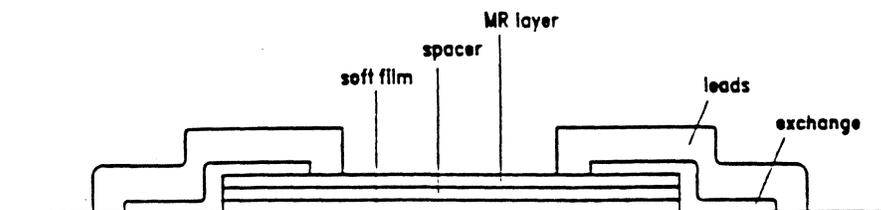Figure 1. Cross section view of MR thin film head

Figure 2. Cross section view of soft adjacent layer MR sensor

V. HEAD CONSTRUCTION

Many substrates have been tested such as oxidized silicon, aluminium coated with alumina, glass, etc. The glass substrate offers large mechanical hardness. Many heads are aligned on the same substrate using only one mask. The wire connections are then soldered, and heads are covered with a protective coating. Separated heads or whole head group are cut, and the plane facing the recording medium is obtained by grinding with a diamond wheel. Fig. 8 shows a gap and the pole faces of multilayer legs.

VI. CONCLUSIONS

We have seen that the present integrated magnetic head offers many advantages over classical heads: mass production, miniaturization, efficiency, and very large frequency bandwidth. Fig. 9 shows an integrated magnetic head. In spite of the fact that the write current is still too high ($I_w < 500$ mA), the results are very encouraging. New possibilities are opened by this head model; with an appropriate thickness distribution of the magnetic films which form the multilayer leg, it may be possible to determine a potential function at the pole faces of the magnetic legs. (In a classical head, this potential function is fixed and assumed to be an equipotential.)

REFERENCES

[1] E. P. Valstyn and D. W. Kosy, "The write field of a magnetic-film recording head," IEEE Trans. Magn., vol. MAG-5, Sept. 1969, pp. 442–445.
[2] M. S. Cohen, "Magnetic properties of Ni–Fe–Cr films," J. Appl. Phys., vol. 35, Mar. 1964, pp. S34–S35.
[3] J. P. Lazzari et al., French Patent EN 69 36 S64.
[4] J. P. Lazzari et al., "Experimental studies using in-contact recording on chromium-cobalt films," IEEE Trans. Magn., vol. MAG-5, Dec. 1969, pp. 955–959.

A Magnetoresistive Readout Transducer

ROBERT P. HUNT, MEMBER, IEEE

Abstract—A new type of reproduce transducer for reading magnetically recorded tapes is described. The device structure, which utilizes the magnetoresistive effect in a thin magnetic film deposited onto a nonmagnetic substrate, provides wavelength response characteristics comparable to existing technology. Indigenous noise effects are subordinate to tape noise. No intrinsic frequency limitations are experienced for recording bandwidths in existence today. Since the device detects the tape's fringing fields directly, the output is not a function of tape velocity. The device construction lends itself nicely to multichannel head assemblies. The transducer may also be used to detect digitally recorded information.

INTRODUCTION

A NEW type of transducer which reads stored magnetic information and performs comparably to ring type heads conventional to magnetic recording is described. The device makes use of the magnetoresistive effect in thin magnetic film strips which are deposited onto a nonconductive substrate. Two possible geometries are indicated in Fig. 1. The plane of the film strip may lie either parallel to the plane of the storage medium (horizontal configuration) or perpendicular to the plane of the storage medium (vertical configuration). From the point of view of wear resistance, the vertical structure is preferred since the substrate then takes the brunt of the
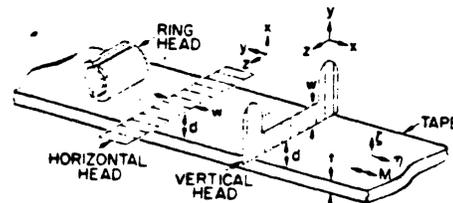
Fig. 1.   Horizontal and vertical head configurations.

abrasive action caused by the relative motion between transducer and storage structure.

In magnetoresistive materials, such as unoriented polycrystals with isotropic resistance, the resistivity ρ has a uniaxial anisotropy with a symmetry axis parallel to the direction of magnetization [1]. Thus

$$\rho = \rho_0 + \Delta\rho \cos^2 \theta \qquad (1)$$

where ρ_0 is the isotropic portion of the resistivity, $\Delta\rho$ is the magnetoresistivity, and θ is the angle between the magnetization M and the current density vector. For materials such as Permalloy and cobalt–iron alloys, $\Delta\rho$ amounts to about 2–6 percent of ρ_0 at room temperature [2]. In the geometry of Fig. 1, the fringing fields of the stored information operate on the magnetization of the film strip to cause a variation in the angle θ. By supplying the device with a constant current, a terminal voltage proportional to $\cos^2 \theta$ arises.

To describe the device's operation analytically, a functional relationship between the applied field H and the

Giant Magnetoresistance: A Primer

Robert L. White
Department of Materials Science and Engineering
Stanford University, Stanford, CA 94305

Abstract - - **The giant magnetoresistive effect appears in a number of ultra-thin multilayer systems in which thin magnetic films, a few tens of Å thick, are separated by non-magnetic metal films, also on the order of tens of Å thick. For the effect to appear, the primary requirement is that the relative orientation of successive magnetic layers must be susceptible to change by the application of a magnetic field. The basic physical origin of the effect is the differential scattering of electrons parallel to and antiparallel to the local magnetization. This differential scattering arises either from the character of the scattering centers or in the different density of states functions for the two spin species. The giant magnetoresistive effect is of great interest because of its potential utility in magnetoresistive "read" heads in the information storage industry.**

I. INTRODUCTION

The purpose of this article is to give an introduction to the phenomenon of giant magnetoresistance. My intent is to convey an understanding of what giant magnetoresistance is, under what circumstances it appears, to present a simplistic heuristic explanation of its occurrence, and to indicate some of the application areas driving much of the interest in giant magnetoresistance. For more penetrating treatment of the physics underlying this effect, for more extensive treatment of the thin film systems in which it occurs, and for more thorough treatment of the applications, the reader is directed to the references cited, including those corresponding to the papers by Fert [1], Speriosu [2], Parkin [3] and Daughton [4], following immediately in the Intermag conference session to which this is the introduction.

II. THE DISCOVERY

Because the presence of a magnetic field alters the trajectory of an electron moving through that field, the resistance of a metal is different in the presence of a magnetic field than in the absence of such a field, an effect which is especially pronounced in magnetic metals. The change in resistance for a current parallel to the applied field (or magnetization) and the change in resistance for a current perpendicular to the

applied field are different, and this difference is the classical magnetoresistive effect. For many metals this effect is vanishingly small; in the most extreme case the angular variation is on the order of 5%. It was therefore a most striking event when, in 1988, Baibich et al. [5] reported changes in resistance of as much as 50% at low temperatures with applied magnetic field in $(Fe/Cr)_n$ multilayer ultrathin films (Fig. 1). This enormous magnetoresistive effect, subsequently found to occur in a number of multilayer ultrathin magnetic film systems, was immediately labelled the "giant magnetoresistance" effect, and is the subject of this paper. As we will see the physical origin of the giant magnetoresistive effect, often abbreviated to the GMR effect, are quite different from those of the classical bulk metal magnetoresistive effect.

III. CONDITIONS FOR APPEARANCE OF THE GMR EFFECT

The giant magnetoresistive effect occurs in ultrathin multilayer films, in particular in multilayer arrays consisting of alternate layers of a magnetic metal separated by layers of a non-magnetic metal. For the giant magnetoresistance effect to appear two conditions must be met:
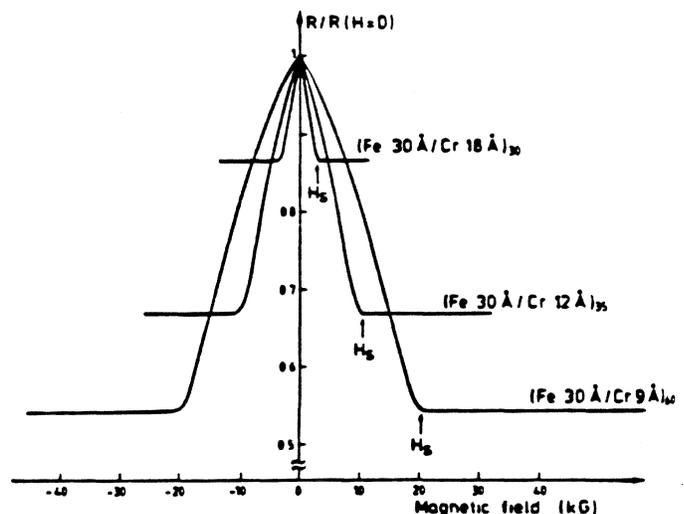

Fig. 1. Giant magnetoresistance effect as first reported by Baibich et al. [Ref. 1]

114

Very large magnetoresistance in perovskite-like La-Ca-Mn-O thin films

M. McCormack, S. Jin, T. H. Tiefel, R. M. Fleming, and Julia M. Phillips

AT&T Bell Laboratories, Murray Hill, New Jersey 07974

R. Ramesh

Bellcore, Redbank, New Jersey 07701

Colossal magnetoresistance with more than a thousandfold change in resistivity ($\Delta R/R_H = 127\,000\%$ at 77 K, $H = 6$ T) has been obtained in epitaxially grown La-Ca-Mn-O thin films. This magnetoresistance value is about three orders of magnitude higher than is typically seen in the giant-magnetoresistance-type metallic, superlattice films. The temperature of peak magnetoresistance is located in the region of metallic resistivity behavior. As the magnetoresistance peak occurs not at the temperature of magnetic transition but at a temperature where the magnetization is still substantial, the spin-disorder scattering is not likely to be the main mechanism in these highly magnetoresistive films. The peak can be shifted to near room temperature by adjusting processing parameters. Near-room-temperature $\Delta R/R_H$ values of $\sim 1300\%$ at 260 K and $\sim 400\%$ at 280 K have been observed. The presence of grain boundaries appears to be very detrimental to achieving large magnetoresistance in the lanthanum manganite compounds. The fact that the electrical resistivity of a material can be manipulated by magnetic field to change by orders of magnitude could be useful for various device applications.

Perovskite-structured lanthanum manganite ($LaMnO_3$) can be made to exhibit both strong ferromagnetism and metallic conductivity by partial substitution of La ions (3+ valence) with 2+ valence ions such as Ca, Ba, Sr, Pb, and Cd. This results in a Mn^{3+}/Mn^{4+} mixed valence state creating mobile charge carriers and canting of Mn spins.[1-10]

The magnetoresistance (MR) behavior of these La-manganite thin films has recently been reported for La-Ba-Mn-O[11] (with the MR ratio of $\sim 150\%$ at room temperature) and La-Ca-Mn-O[12] (MR ratio of $\sim 110\%$ at 220 K and near zero at room temperature). The MR ratio is defined here as $\Delta R/R_H = (R_H - R_0)/R_H$ where R_0 is the zero field resistance and R_H is the resistivity in the applied magnetic field. The data reported in this paper are mostly for $H = 6$ T. These oxide films exhibit large magnetoresistance comparable to the higher end of the values for the so-called "giant-magnetoresistance" (GMR) type materials consisting of metallic multilayer or heterogeneous films[13-16] with the MR values typically in the range of 5–150 %.

In this paper we report the electrical, magnetic, and magnetoresistance behavior in epitaxial La-Ca-Mn-O films with extraordinary MR values in excess of 100 000%, about three orders of magnitude greater than were previously reported for the GMR-type or La-manganite films.

Thin films of La-Mn-Ca-O, ~ 1000 Å thick, were deposited on (100) $LaAlO_3$ substrates by pulsed laser deposition (PLD). The substrate temperature was 650–700 °C, and the oxygen partial pressure in the chamber was maintained at 100–300 mTorr. The nominal target composition was $La_{0.67}Ca_{0.33}MnO_x$. The chemical composition of the deposited film was found to be similiar to that of the bulk target used for the deposition by scanning electron microanalysis and Rutherford backscattering analysis. X-ray diffraction and rocking angle analysis indicate that the films have the perovskite-type cubic structure with a lattice parameter of $a = 3.89$ Å (or $a = 7.78$ Å from crystallographic point of

view) and grow epitaxially on the $LaAlO_3$ substrate ($a = 3.79$ Å).

The electrical resistance and magnetoresistance of the films were measured as a function of temperature and magnetic field by four-point technique (using a constant current) in a superconducting magnet with the maximum applied field of $H = 6$ T. For most of the films, the field direction was parallel to the current direction. Some of the measurements were carried out with the field applied perpendicular to the current direction in the film (either by in-plane field or perpendicular field). The MR behavior in the La-Ca-Mn-O films is almost always negative and essentially isotropic with respect to the field direction if the demagnetizing factor is taken into consideration. The M-H loops were obtained by using a vibrating sample magnetometer.

The as-deposited La-Ca-Mn-O films yield low MR ratios of typically less than $\sim 500\%$ over a broad temperature range of 50–300 K (low MR only in a relative sense as this is still quite impressive). It has been found that a post heat treatment of the deposited films is essential in order to maximize the MR behavior.[17] The highest MR ratio so far has been obtained by heat treatment at 900 °C/30 min. in an oxygen atmosphere (3 atm. oxygen). As shown by the R vs H curves in Fig. 1, the La-Ca-Mn-O film exhibits an astoundingly large magnetoresistance value of 127 000% at 77 K (more than a thousandfold decrease in resistivity). The zero-field resistivity of the film, $\rho \sim 11.6$ Ω cm ($R = 1.35$ MΩ for the sample size of ~ 1000 Å thick$\times 2$ mm wide$\times 4$ mm long), decreased in the presence of applied field $H = 6$ T to ~ 9.1 mΩ cm ($R = 1.06$ kΩ). The 77 K data indicate that the major part of the resistivity drop occurs at $H < 2$ T. The 127 000% MR value in this film is colossal when compared to the 5–150 % magnetoresistance in the GMR multilayer films.

As this particular film has been heat treated so as to exhibit the peak MR value near the liquid nitrogen temperature (77 K), other measurement temperatures gave lower MR

115

MEDIA

Thin-Film Media

Advantages:

Higher magnetization -∴ higher signal and track density- than particulate media.

This means thinner media needed → reduced demagnetization and the fields from the entire recorded bit extend into a smaller space.

Higher S/N ratio, especially when electronic and head noise are significant compared to media noise.
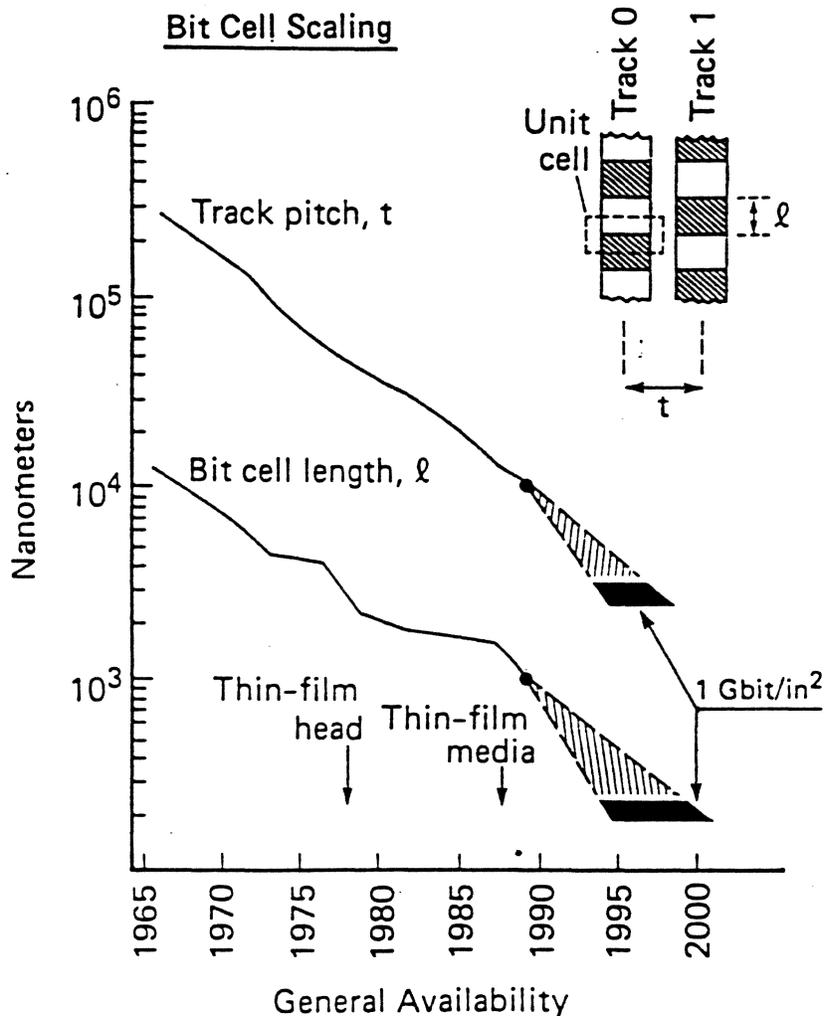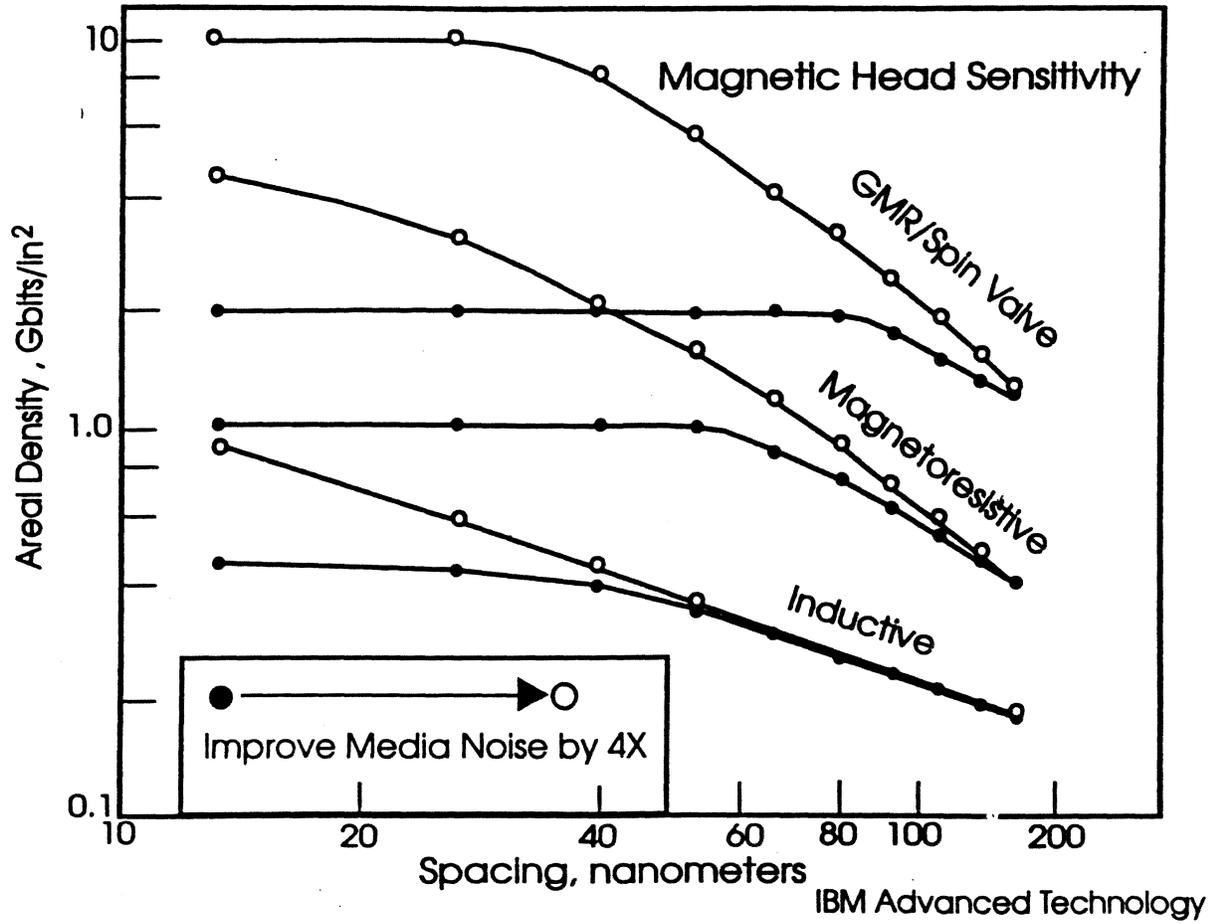

Figure shows the progress in the track pitch and bit cell length as a function of the year available (after I. L. Sanders et. al.).

Effect of Jitter on Mr Heads

After R. A. Scranton

[handwritten notes at top of page, partially legible]

Because films have M advantage ... ⟋ ... they the grains will ... expected to be higher. This is indeed the case at low t₁
2) As freq. T, the micromagnetic and inter-granular coupling be very important.

Noise in thin films and magnetization reversal

Nb → The information is recorded by forcing reversals through the head field. ∴ it is important to control these reversals.

i.e. → Although H_c gives the macroscopic (or average) behavior, microscopic crystallite configuration and behavior very important (micromagnetic problem).

Magnetization Reversal Mechanism

a) *Individual grains undergo reversal independently.*

Here, coercivity is determined by magnetocrystalline anisotropy in a grain, grain-shape and its magnetostrictive properties (stresses).

b) *Local groups of grains which are magnetically coupled undergo reversal in groups, but each group independently of others.*

In this mode, the factors in (a) apply plus the type of grain coupling within a cluster.

c) *Long range coupling of grains → domain formation and the movement of these domains constitutes reversal.*

Wall energy controls coercivity → magnetocrystalline anisotropy, magnetostatic energy at the wall, stress variations, compositional irregularities (stacking faults, e.g.), and film roughness.

This is because grains with different switching fields, when coupled together take on a common switching field. → improved write-ability since saturation is achieved at lower applied fields. However, this leads to lower coercivities.
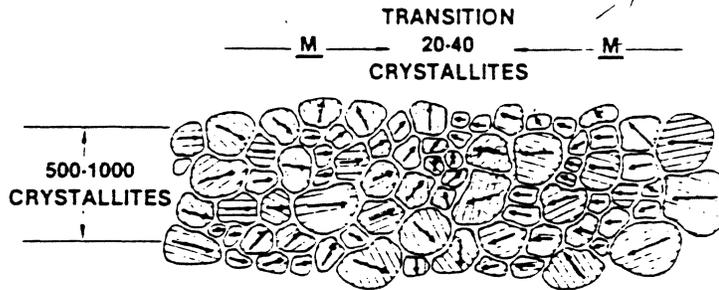
Note: boundary not as shar...

TRANSITION
————— M ————— 20-40 ————— M —————
CRYSTALLITES

500-1000
CRYSTALLITES

Fig. 5. Illustration of a written magnetization transition in a medium which undergoes reversal by grain-cluster switching. The irregular reversal boundary tends to be a delineation of grains or grain clusters, rather than a sharp zig-zag

M_r x thickness, kA/m x μm

Fe₂O₃ particulate

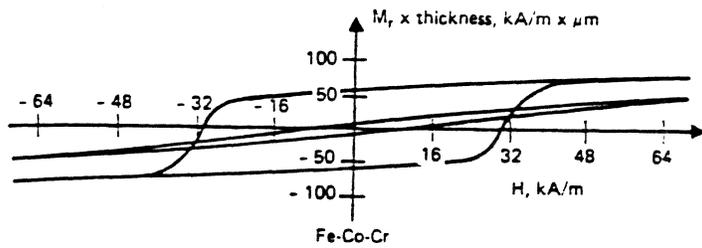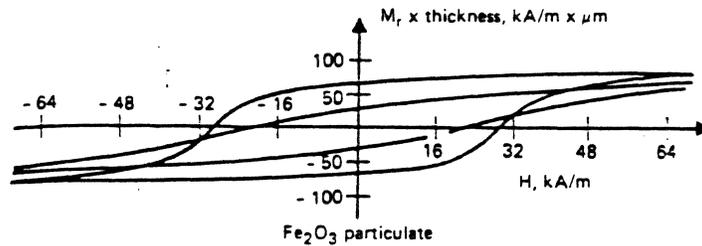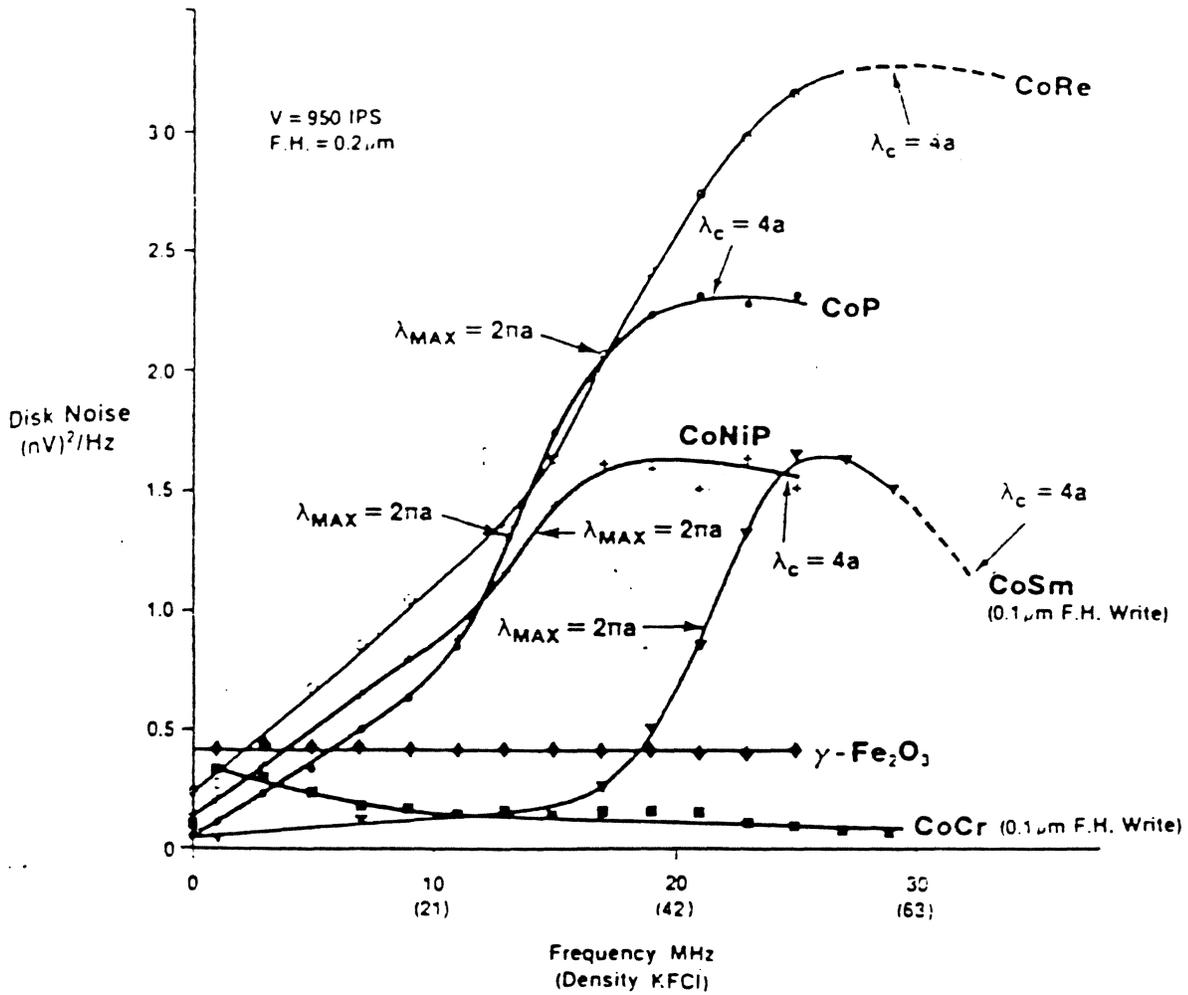M_r x thickness, kA/m x μm

Fe-Co-Cr

Figure shows comparison of hysteresis loops of typical iron oxide particle coating with that of Fe-Co-Cr thin film, where a squarer film is observed (due to stronger grain coupling). (after Rossi).

→ In both the particulate and longitudinal media *reversible rotation regions* exist:

- at the beginning of the demagnetization legs of the loop and,

- near the saturation region.

Disk Noise $(nV)^2/Hz$ vs Frequency MHz (Density KFCI)

V = 950 IPS
F.H. = 0.2 μm

CoRe, $\lambda_c = 4a$

$\lambda_c = 4a$, CoP

$\lambda_{MAX} = 2\pi a$

CoNiP

$\lambda_{MAX} = 2\pi a$

$\lambda_{MAX} = 2\pi a$

$\lambda_c = 4a$

$\lambda_c = 4a$, CoSm (0.1 μm F.H. Write)

$\lambda_{MAX} = 2\pi a$

γ-Fe_2O_3

CoCr (0.1 μm F.H. Write)

1) Co alone would be low H_c ∴ PT, Sm and Ta are

present
2) Co aids, Corrosion. Also migrates to boundaries.

121

Figure 3.41 A portion of a recorded track showing two magnetization reversals written by a film head on an obliquely evaporated Fe-Co-Cr film medium, which is highly oriented in the direction of the track. For the medium, H_c = 40 kA/m (500 Oe), M_r = 900 kA/m (emu/cm³), and film thickness is about 35 nm. The texture lines, running from top to bottom in the track direction, are from the substrate. *(Photo courtesy of H. C. Tong.)*

The above figure shows the real situation encountered.

These zig-zag domains would not really be of concern had it not been for their irregular appearance.

Lets see what happens in case of polycrystalline films

Cluster Formation:

When magnetization reversal proceeds by irreversible rotation it <u>probably does so in a cooperative manner</u>.

This is due to **magnetic coupling** which is <u>related to grain boundaries</u>.

The greater coupling produces higher remanent and coercive squareness:

With such *'cooperative'* phenomenon one observes *square hysteresis loops*. ⇒ lower Hc
and higher M
But this is a two edged sward:

a) <u>Leads to a noisy media</u>   Because 1) Cluster size becomes smaller unit
2) Magnetization cannot vary smoothly in the transition region, but in discrete

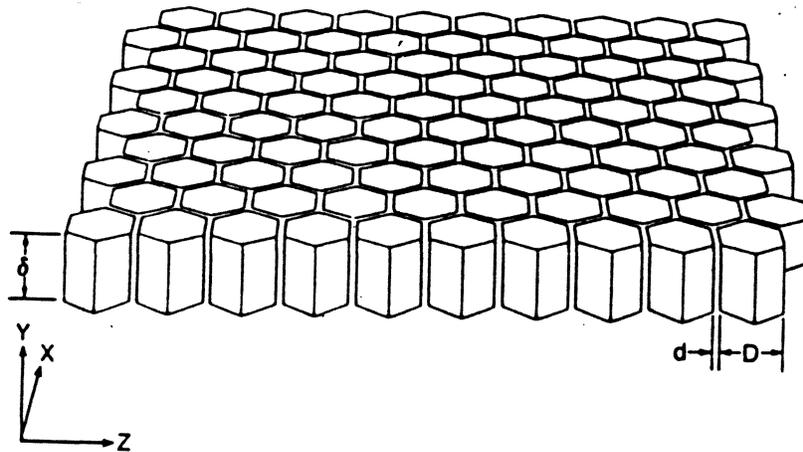b) <u>makes the transition width narrower</u> (sharper transition); & the width.
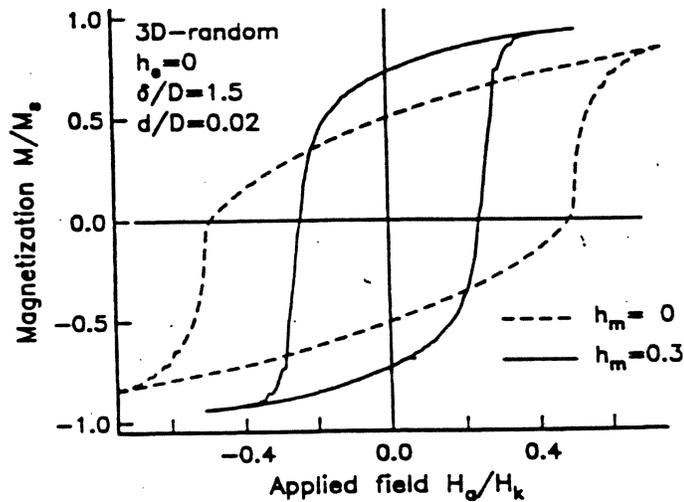
Reversal Process & Domain Structure
(J. Zhu et al)

Through mathematical modeling using two-dimentional array of **64 x 64** hexagonally shaped grains similar to:

for two different values of magnetostatic interaction, $h_m = 0$ and $h_m = 0.3$, and **zero exchange coupling,** the following is calculated:

3D—random
$h_e = 0$
$\delta/D = 1.5$
$d/D = 0.02$

- - - - $h_m = 0$
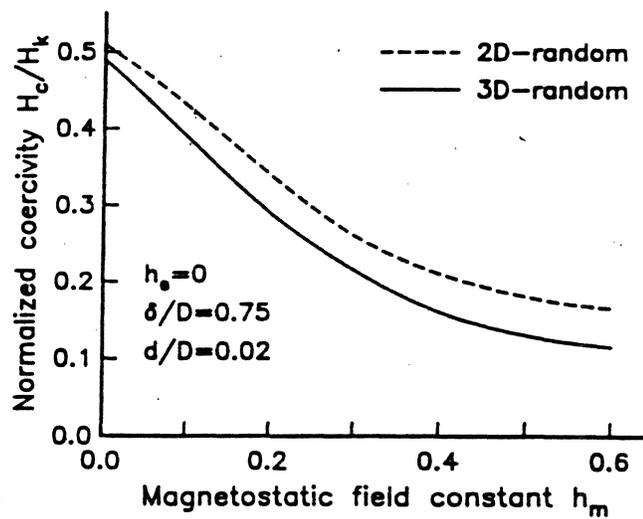———— $h_m = 0.3$

Magnetization M/M_s

Applied field H_a/H_k

G. T.

123

Note that:

- In the noninteracting case, reversal is governed by external applied field relative to local crystalline anisotropies. ∴ high **Hc**, low **S** and **S***.

- With magnetostatic interaction, $h_m = 0.3$, **Hc** is low, **S** and **S*** are high.

They represent general properties:

"Coercivity always decreases with interactions".

The **width of nonmagnetic grain boundary also affects the coercivity**. Increasing grain separation, while keeping the film thickness constant results in coercivity incraese (since the magnetostatic interaction is reduced).

The effect of *intergranular exchange coupling* is shown below:

124
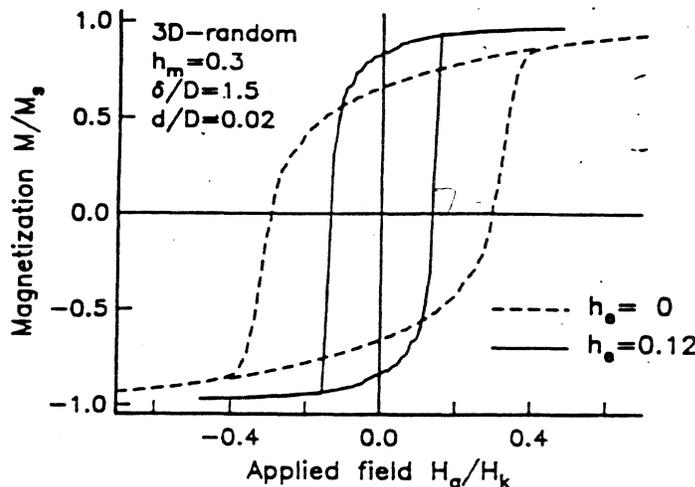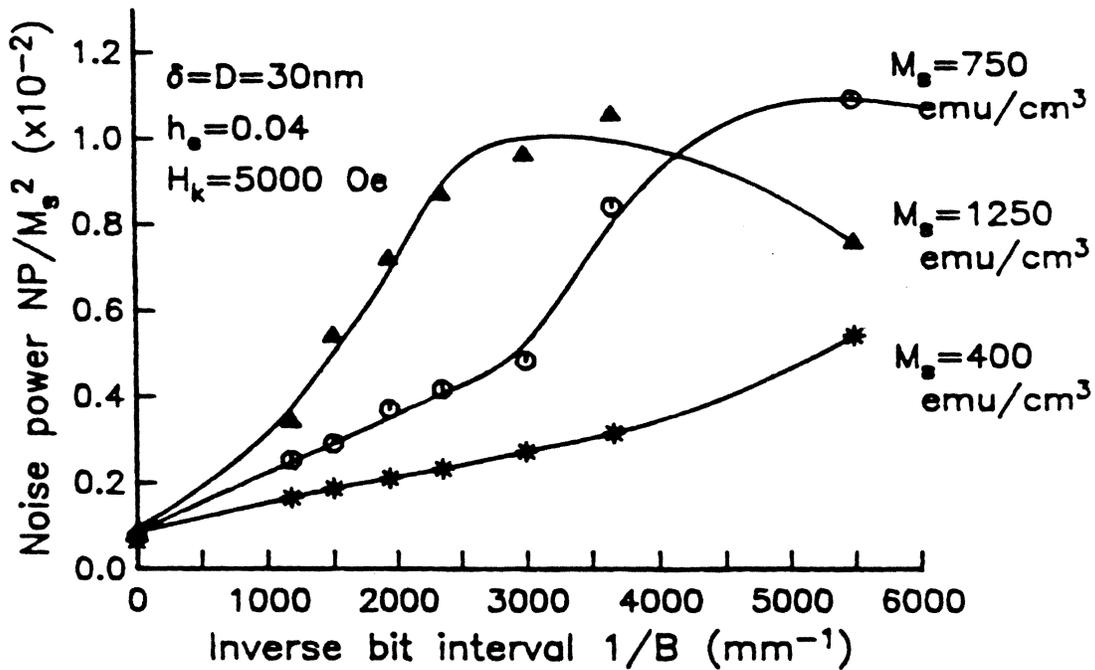
Calculated integrated noise power vs. recording density for three different film saturation magnetization values. The symbols are calculation results with the curves guiding the eye (*Zhu, 1993*).
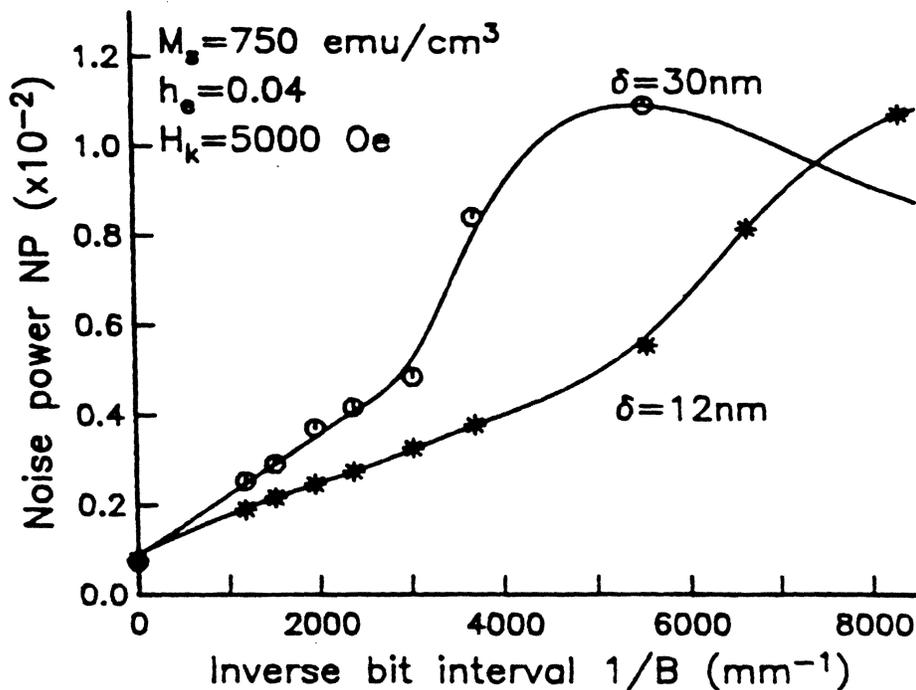
Calculated integrated noise power vs. recording density for two different film thicknesses (*Zhu, 1993*).

Measurement of Interactions

I) Coercive Squareness (S*)

S* can be measured staticly, using **VSM**.

Generally, noise decreases with decreasing value of S*:

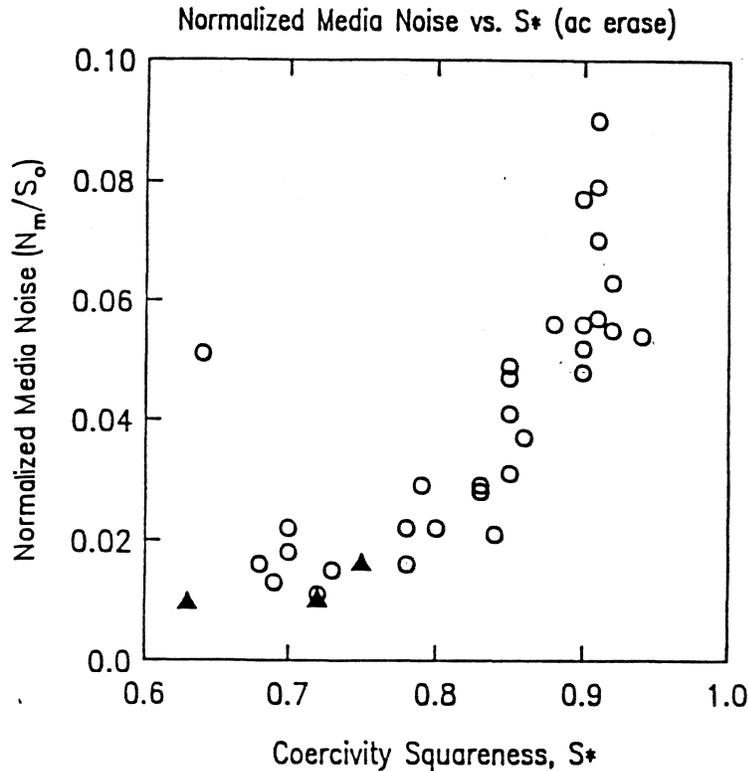Normalized Media Noise vs. S* (ac erase)

Figure 11. RMS media noise voltage N_m for ac erased media normalized to zero-to-peak isolated pulse amplitude S_0 vs. the coercivity squareness (Sanders et al., 1989).

The increase in noise with S* is **steep for S*=0.85-9**, implying the *initiation of exchange coupling leading to avalanche switching phenomenon*.
The above statement *is not always true*, since *S** is not only an indicator of coupling strength, but is also related to the direction of c-axis (e.g., for perp media, S* in planar direction is small, yet says nothing about the property of the medium.

It has been argued that films can be decoupled having low noise, but still have high *S** from **narrow distribution of anisotropy field (Hk)**.

(215.4)

125

4) Interlayer

Substantial reduction of all types of medium noise can be obtained for several Co alloys when multilayered.

The reduction is ~ **1/m** , where m = (number of magnetic layers) (E. S. Murdock et. al.)
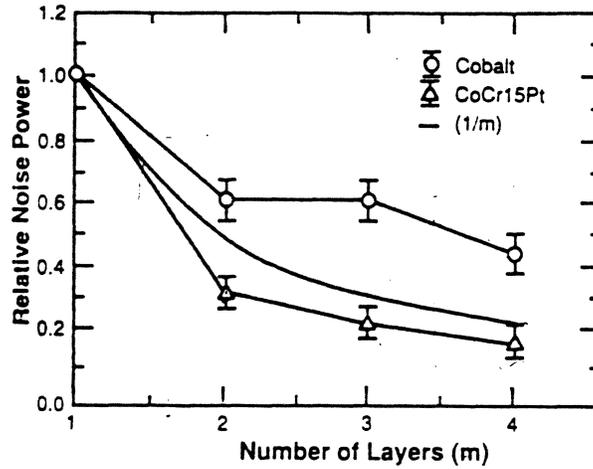
It is thought that by dividing a single recording layer into two or more, the number of isolated grains, and hence the noise sources, per unit volume of the medium is *increased*.

However, the vertically adjacent layers will no longer be exchange coupled, without significantly reducing the magnetostatic coupling . and hence their magnetization can be slightly or even totally different. Here, the magnetostatic interaction between layers would tend to reduce the medium noise because adjacent layers would then find it more favorable to be anti-parallel, reducing the flux variations detected by the head.

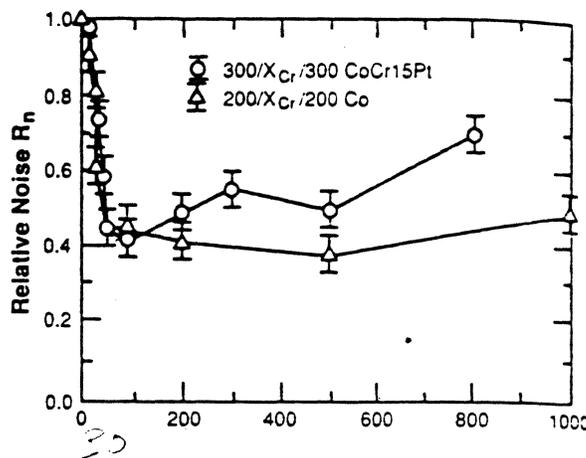∴ noise is reduced, and the epitaxy is maintained.

Figure shows the dependence of relative noise power of a symmetric bilayer media on isolation layer thickness (X_{cr}) .(E. S. Mudock et. al.). Correction has been made for *spacing losses.*

126

Media For MR Application

- MR heads are flux sensitive devices, therefore **more susceptible to noise**.

- Requires lower film thickness $(M_r t)$, $\therefore$ <u>more difficult to control properties</u>. On the good side, *easier to get higher coercivities*.

- MR device is *sensitive to electrostatic discharges*, $\therefore$ grounding of equipment and operators is important.

- Hard 'asperities' on the media can cause spikes in the output due to rapid thermal changes. This can be corrected with feedback amplifiers.

- <u>Multilayered media</u>:- equipment limited, also should be optimize for the No. of layers.

- Reduced track width and bit length place a <u>constraint on the allowable size of surface imperfection</u>. $\therefore$ reduce debris, handling etc.

- MR media more appropriate on alternative substrates (glass, 'canasite') since **they offer lower "glide height"**. However magnetic properties are not as good as Al/NiP due to Cr growth and heating differentials.
One solution is to **pre-coat the substrates**.

Media for MR Heads

For MR heads media noise is of prime importance, owing to *over 10 fold amplification*.
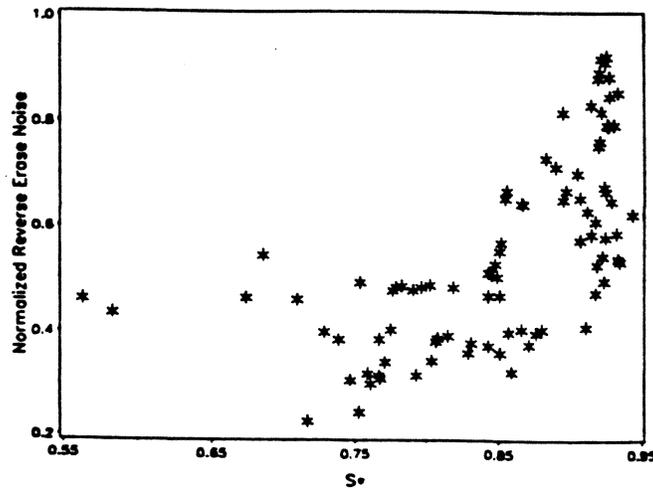
"What used to be appropriate for the 80s"
may no longer apply for 90s:-
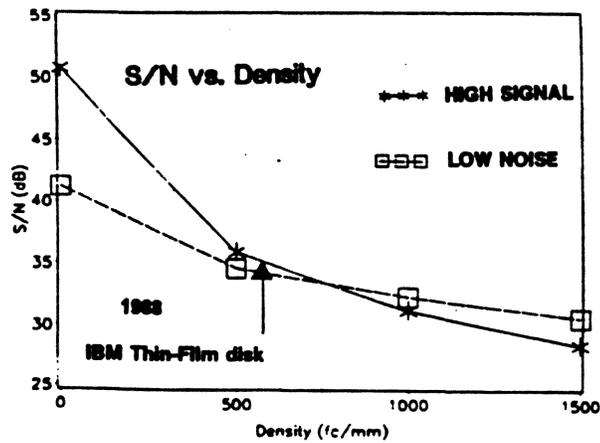
- **Transition noise.** This is the dominant noise source for thin film media.

I) Coercivity Squareness, S*.

The role of *macromagnetic properties*, such as **'S*'**, have to be reassessed.

Reverse erase noise vs S* for a variety of thin-film media.(R. M. White)

Of course, one would like high S* and low noise at the same time. One needs:

"uncoupled grains + tight distribution of anisotropy"

♦ <u>Cr segregation to needs to be promoted</u> to reduce S*.

♦ *Out of plane anisotropy* (K_P) helps reduce demagnetization fields (through providing alternative flux closure paths) *leading to narrower, zig-zag domain free transitions*. This is done by choosing the right Cr underlayer orientation.

II) Anisotropies.

a) Angle of incidence induced:-

♦ This can cause once around "**modulation**" problems.

This is less pronounced in circumferentially textured discs.

On the down side, it may lead to noisier media at small bit intervals, since texturizing will increase film stress:-
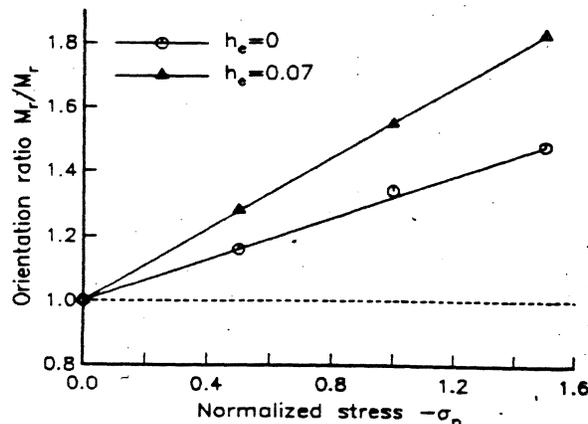

Figure 9. Calculated orientation ratio as a function of the compressive stress for a non-exchange coupled film: $h_e=0$ (circles) and an exchange coupled film: $h_e=0.07$ (triangles).

(J. G. Zhu)

Media Requirements for MR Heads

(continued)

- ## Low Mrt:

Good news!

- ### ◆ Lower transition noise.
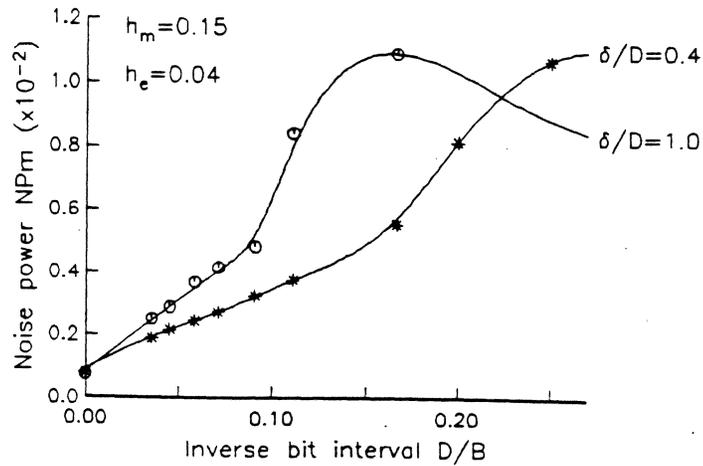

Figure 7. Integrated noise power for two different film thicknesses: $\delta/D = 0.4$ (stars) and $\delta/D=1.0$ (circles).

(J. G. Zhu)

This is because reducing film thickness *yields a sharper transition*.

- ◆ One can use more Cr in alloy to reduce noise.

- ◆ Higher coercivity attainable.

- ◆ Use of precious metals more practical.
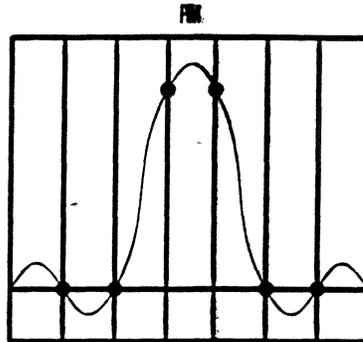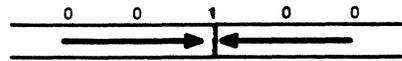
- ◆ Better target utilization.

Bad news!

   ◆ Smaller defects.

   ◆ Reduced asperity tolerance.

   ◆ Coercivity much more sensitive to film thickness, uniformity.

MR Head *Preamp* Requirement

- MR resistance variation.

- Preamp noise.

- MR bias current stability/optimization.

- Faster read as well as write channel (data rate).

- Power requirements should be minimized.

Partial Response

- **Use synchronous detection**, (i.e. synchronize the clock with the exact moments at which transitions may take place).

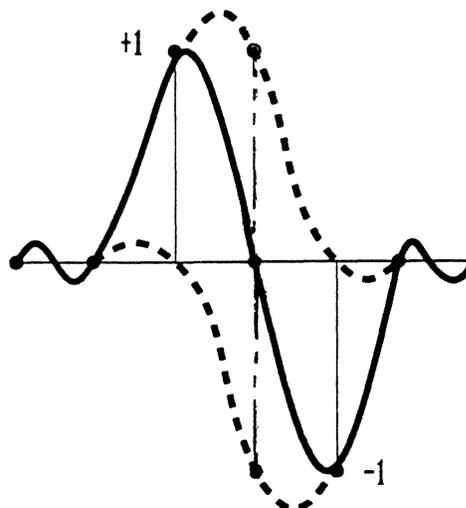- **Modify the pulse shape** (*equalize*) to get the following (for PR4 only!):

$$(1 + 0X1 - 0)$$

∴ the isolated pulse is defined by **sequence of samples {0,0,1,1,0,0,}**.
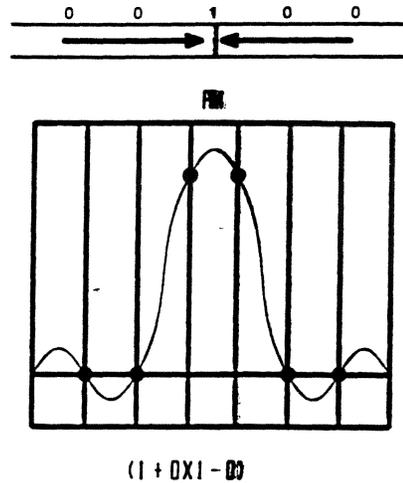
- Note that **this scheme allows more than one sample/pulse**, with each sample only containing part of the response (hence, *Partial Response*).

- Another transition leads to superposition, ie **ISI is allowed**:(Note: If we know the sample values, we **can reconstruct the written pattern on the disk**.)
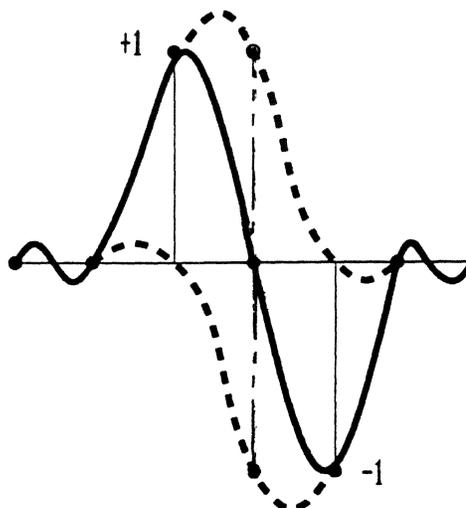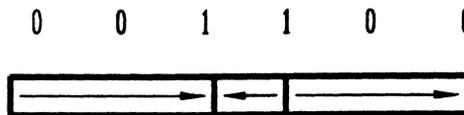
Partial Response

- **Use synchronous detection**, (i.e. synchronize the clock with the exact moments at which transitions may take place).

- **Modify the pulse shape (*equalize*)** to get the following (for PR4 only!):

$(1 + 0)(1 - 0)$

∴ the isolated pulse is defined by **sequence of samples {0,0,1,1,0,0,}.**

- Note that **this scheme allows more than one sample/pulse**, with each sample only containing part of the response (hence, *Partial Response*).

- Another transition leads to superposition, ie **ISI is allowed**:(Note: If we know the sample values, we **can reconstruct the written pattern on the disk**.)

Media For PRML

❑ **PRML uses *reduced transition spacing,*** since the bits are allowed to be closer together. With a minimum t.s. of ~ 280 nm**, one has to be concerned about NLTS**. The shift occurs when the demagnetization field from a freshly recorded transition adds to the field from the write head to produce a shift in the position of the immediately following transition.

❑ In **peak detection** NLTS tends to cancel the undesirable linear peak shift. **In PRML environment**, on the other hand, two transitions can be as close as one clocn period, and the sample values need to be rigth on the target.

❑ By applying proper amount of data dependent *precompensation* during writing **it can be arranged for the data to end up at the proper location even after NLTS**. However, precompensation can eliminate NLTS **for shifts upto B/4**, where **B** is the transition spacing. This is affected through delaying the second write current transition so that it gets written at the correct position in the presence of the field from the first transition. However, **when the ratio of transition spacing B over transition parameter, a**, (i.e. B/a) drops below 3.5, *'percolation'* begins to erase parts of the data patterns, an effect which cannot be undone by precompensation:


At high densities, the zigzags 'percolate'
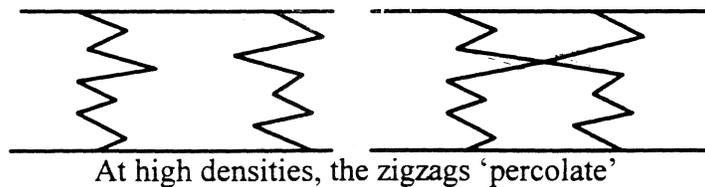
❑ The transition parameter, a, is given by:

$$a = \sqrt{(M_r \delta d_e \tau) / (\pi H_c Q)}$$

where Q and τ are numerical constant relating to the head field and the transition shape and are 0.8 and 0.69 respectively.

❑ Hence optimum Values for $M_r \delta$ and H_c can be adjusted so that B/a ratio remains above 3.5 value when using PRML. Reducing $M_r \delta$ helps reduce NLTS, but it also reduces signal amplitude.
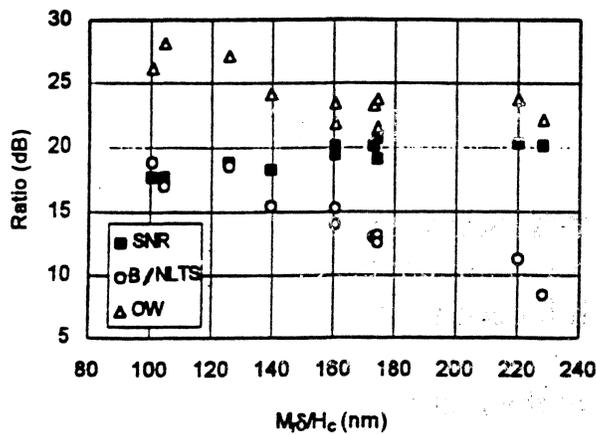
Transition shift, SNR and overwrite vs disk parameters (T.D. Howell, et al)

Head For PRML

☐ Excessive write current rise time, which is proportional to head inductance, causes increased NLTS.

☐ In MIG and MR heads the isolated transition response (ITR) is Lorentzian, and relatively easy to shape to the desired partial response. In thin film heads, however, the ITR has undershoots associated with finite pole length, causing oscillations on the roll-off curve. This can be mitigated by changing the heads' sharp outside edges.

149